

**NORMANDEAU
ASSOCIATES, INC.**

HYDRODYNAMIC AND DISPERSION PREDICTION MODEL
OF ENVIRONMENTAL IMPACTS
OF BREAKWATER CONSTRUCTION ON
BRISTOL HARBOR, RHODE ISLAND

VOLUME I

Prepared for

U. S. ARMY CORPS OF ENGINEERS
Waltham, Massachusetts

Contract No. DACW 33-78-C-0362
Gibb Chase, Contract Manager

Prepared by

NORMANDEAU ASSOCIATES, INC.
Bedford, New Hampshire

July 1980

ABSTRACT

The hydrodynamics and dispersion characteristics of Bristol Harbor, RI were studied using the depth-averaged finite-element models CAFE (Connor and Wang, 1974) and DISPER (Liemkuhler et al., 1975). Modeling techniques, critical assumptions within the models and their previous applications are highlighted. For this study, the circulation was simulated for mean and spring tidal conditions (amplitudes of 0.61 m and 0.76 m, respectively) for each of four cases: no breakwater and Plans A, D₁ and D₂. A comparison of existing tidal conditions with the breakwater¹ effects² shows a cyclic formation of several eddy-like circulation cells near the breakwaters in the upper harbor. Lower harbor circulation is unaffected by the structures. There is no difference in circulation patterns between mean and spring tidal conditions. The CAFE current results were utilized as the advective driving force in the DISPER model. The same conditions were used for both models. Three different source locations are utilized within the model: Walker Cove sewage treatment plant outfall, Bristol industrial area adjacent to the Town Pier, and the Bristol Yacht Club. Results from the models confirm our intuitive understanding of the effects of breakwaters on circulation and dispersion: the more restricted the areas of flow are, the more these patterns deviate from the existing patterns. Several analytical techniques are highlighted concerning wind-induced circulation. Winter winds should enhance harbor flushing. Summer winds, although retarding flushing, are weaker and should not dominate circulation. Strong wind events should significantly disrupt the basic patterns, but the effects are only temporary. The effect of a culvert through the short breakwater of Plan D₂ is analyzed with Manning's formula using the tidal height differential across the breakwater as the driving force. Results from the CAFE model indicate that this may not be a reliable source since the differentials do not appear cyclic with respect to the tide. Comparing the magnitude of the culvert flow rate with the inter-breakwater (main channel) rates indicate the former are two-to-three orders smaller than the latter. To eliminate entrapment, detachment is recommended rather than including the culvert. Plan D₁ is recommended on the basis of good flushing and adequate protection from wind waves generated along a southwest fetch. Plan D₂ should be considered only if there has previously been wave 'damage'² to the yacht club. The trade off for increased protection is restricted flushing which may have an effect on the biota. Plan A is not considered due to a question of adequate protection from wind waves.

TABLE OF CONTENTS

	PAGE
1.0 INTRODUCTION	1
1.1 PROJECT SUMMARY	5
2.0 STUDY AREA	7
3.0 MODELS	9
3.1 HYDRODYNAMIC MODEL	9
3.2 DISPERSION MODEL	12
3.3 PREVIOUS APPLICATIONS	13
3.4 INITIALIZATION	15
3.4.1 Finite Element Grids	15
3.4.2 Model Conditions	18
3.4.3 Calibration	19
4.0 MODEL RESULTS	21
4.1 SIMULATED HARBOR CIRCULATION	21
4.1.1 Existing Tidal Effects	21
4.1.2 Breakwater Effects	28
4.2 SIMULATED HARBOR DISPERSION	42
4.2.1 Existing Dispersion Pattern	42
4.2.2 Breakwater Effects on Dispersion Patterns	48
5.0 WIND EFFECTS	63
5.1 WIND DRIVEN CIRCULATION	63
5.1.1 Classical Model	63
5.1.2 Analytical Model	65
5.1.3 Velocity Profiles	70
5.1.4 Influence of Wind on Current Patterns in Harbor under Existing Conditions	72
5.1.5 Influence of Various Breakwater Configurations on Non-tidal Circulation Effects	73

	PAGE
5.2 WAVE EFFECTS.	74
5.2.1 Limited Fetch.	74
5.2.2 Wave-Breakwater Interaction.	75
6.0 CULVERT EFFECTS.	76
6.1 CULVERT FLOW.	76
6.1.1 The Manning Formula.	76
6.1.2 Culvert Application.	77
6.1.3 Culvert Results.	77
7.0 CONCLUSIONS AND RECOMMENDATIONS.	81
8.0 REFERENCES	84

LIST OF FIGURES

	PAGE
1. Proposed offshore breakwater, Plan A.	2
2. Proposed offshore breakwater, Plan D ₁	3
3. Proposed rock breakwater, Plan D ₂	4
4. Grid A showing source nodes and Plan A breakwater locations	16
5. Grid D showing source nodes and Plan D ₂ breakwater locations	17
6a. Tidal currents at mid-ebb for mean tide (no breakwater) . .	24
7a. Tidal currents at low-slack for mean tide (no breakwater) .	25
8a. Tidal currents at mid-flood for mean tide (no breakwater) .	26
9a. Tidal currents at high-slack for mean tide (no breakwater).	27
6b. Tidal currents at mid-ebb for mean tide (Plan A).	29
6c. Tidal currents at mid-ebb for mean tide (Plan D ₁)	30
6d. Tidal currents at mid-ebb for mean tide (Plan D ₂)	31
7b. Tidal currents at low-slack for mean tide (Plan A).	32
7c. Tidal currents at low-slack for mean tide (Plan D ₁)	33
7d. Tidal currents at low-slack for mean tide (Plan D ₂)	34
8b. Tidal currents at mid-flood for mean tide (Plan A).	36
8c. Tidal currents at mid-flood for mean tide (Plan D ₁)	37
8d. Tidal currents at mid-flood for mean tide (Plan D ₂)	38
9b. Tidal currents at high-slack for mean tide (Plan A)	39
9c. Tidal currents at high-slack for mean tide (Plan D ₁).	40
9d. Tidal currents at high-slack for mean tide (Plan D ₂).	41
10a. Concentrations at mid-ebb for mean tide (no breakwater) . .	44
11a. Concentrations at low-slack for mean tide (no breakwater) .	45
12a. Concentrations at mid-flood for mean tide (no breakwater) .	46
13a. Concentrations at high-slack for mean tide (no breakwater).	47
10b. Concentrations at mid-ebb for mean tide (Plan A).	49
10c. Concentrations at mid-ebb for mean tide (Plan D ₁)	50
10d. Concentrations at mid-ebb for mean tide (Plan D ₂)	51
11b. Concentrations at low-slack for mean tide (Plan A).	52
11c. Concentrations at low-slack for mean tide (Plan D ₁)	53

	PAGE
11d. Concentrations at low-slack for mean tide (Plan D ₂)	54
12b. Concentrations at mid-flood for mean tide (Plan A).	56
12c. Concentrations at mid-flood for mean tide (Plan D ₁)	57
12d. Concentrations at mid-flood for mean tide (Plan D ₂)	58
13b. Concentrations at high-slack for mean tide (Plan A)	59
13c. Concentrations at high-slack for mean tide (Plan D ₁).	60
13d. Concentrations at high-slack for mean tide (Plan D ₂).	61
14. Normalized plot of current velocity vs depth.	68

LIST OF TABLES

	PAGE
1. Conversion Table: Centimeters per second to knots.	22
2. Maximum wind driven currents and flushing times for basin lengths of 1 and 2 nautical miles at various wind speeds	69
3. Comparative flow rates for two tidal cases across the Culvert, the eastern side channel, and the main central channel.	79

HYDRODYNAMIC AND DISPERSION PREDICTION MODEL
OF ENVIRONMENTAL IMPACTS
OF BREAKWATER CONSTRUCTION ON
BRISTOL HARBOR, RHODE ISLAND

1.0 INTRODUCTION

The proposed navigational improvement project for Bristol Harbor, Rhode Island, is authorized under the River and Harbor Act of 13 August 1968. Three alternative plans are proposed for rock breakwater construction in Bristol Harbor, located on the upper reaches of eastern Narragansett Bay. In order to investigate the effects of each plan on the circulation and the flushing of the harbor, numerical models are used to simulate this behavior. From these results, the topics of culvert flows through the breakwater and the influence of wind stress on circulation patterns can also be addressed. Finally, from the total set of results, a series of conclusions and recommendations can be made concerning the effect of each breakwater design on the harbor.

The primary construction plan, Plan A (Figure 1) consists of a 1600-ft (488 m) rock breakwater across the entrance to Bristol Harbor with a 400-ft (122 m) wide entrance on the west passage and a 1300-ft (396 m) wide entrance on the east passage. The second alternative, Plan D_1 (Figure 2) a 1700-ft (518 m) dog-leg breakwater separated from the Coast Guard Pier by 100 feet (30 m), and a west passage entrance of 1700 feet (518 m). The third alternative, Plan D_2 (Figure 3), is the same as D_1 with the addition of a 700-foot (213 m) breakwater attached to the western shore which leaves a harbor entrance of 1000 feet (305 m). There are provisions for installing a 6-foot by 6-foot (1.8 m by 1.8 m) gated-culvert in the short, western breakwater in Plan D_2 . (The original alternatives, Plans B and C had the dog-leg breakwaters attached to the Coast Guard Pier, also with provisions for a gated-culvert).

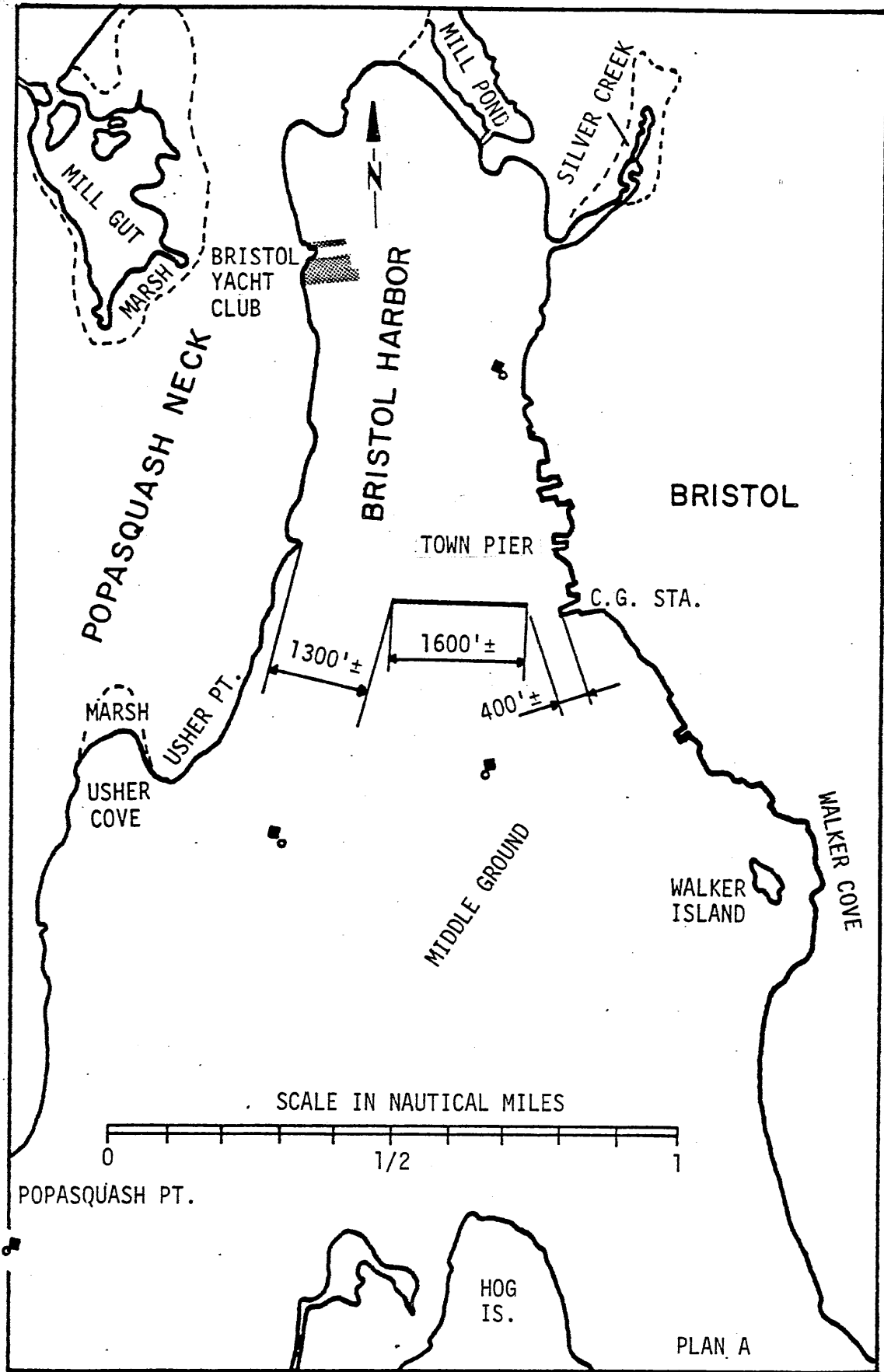


Figure 1. Plan A: Proposed offshore breakwater. Bristol Harbor, Rhode Island.

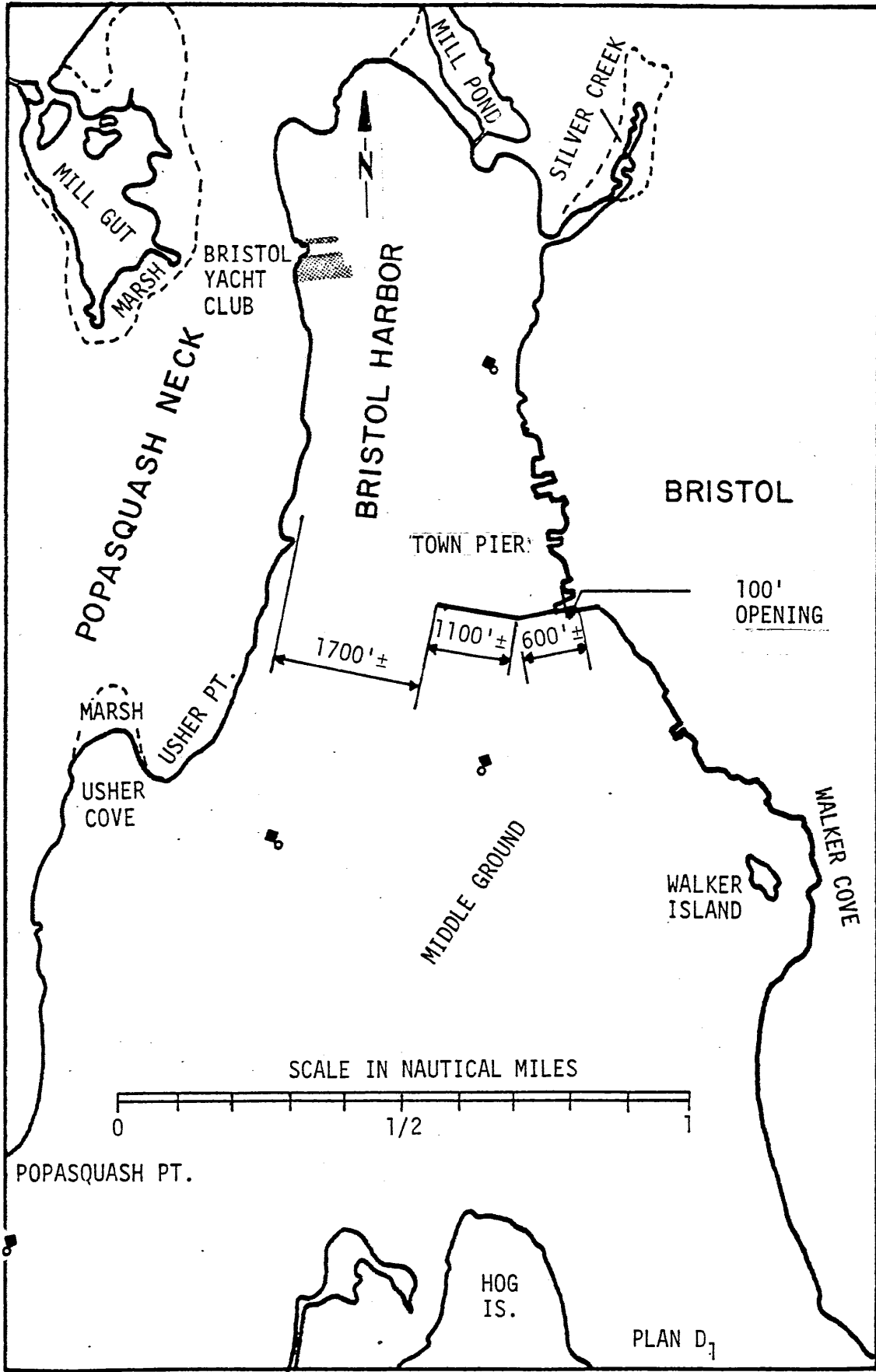


Figure 2. Plan D₁: Proposed offshore breakwater. Bristol Harbor, Rhode Island.

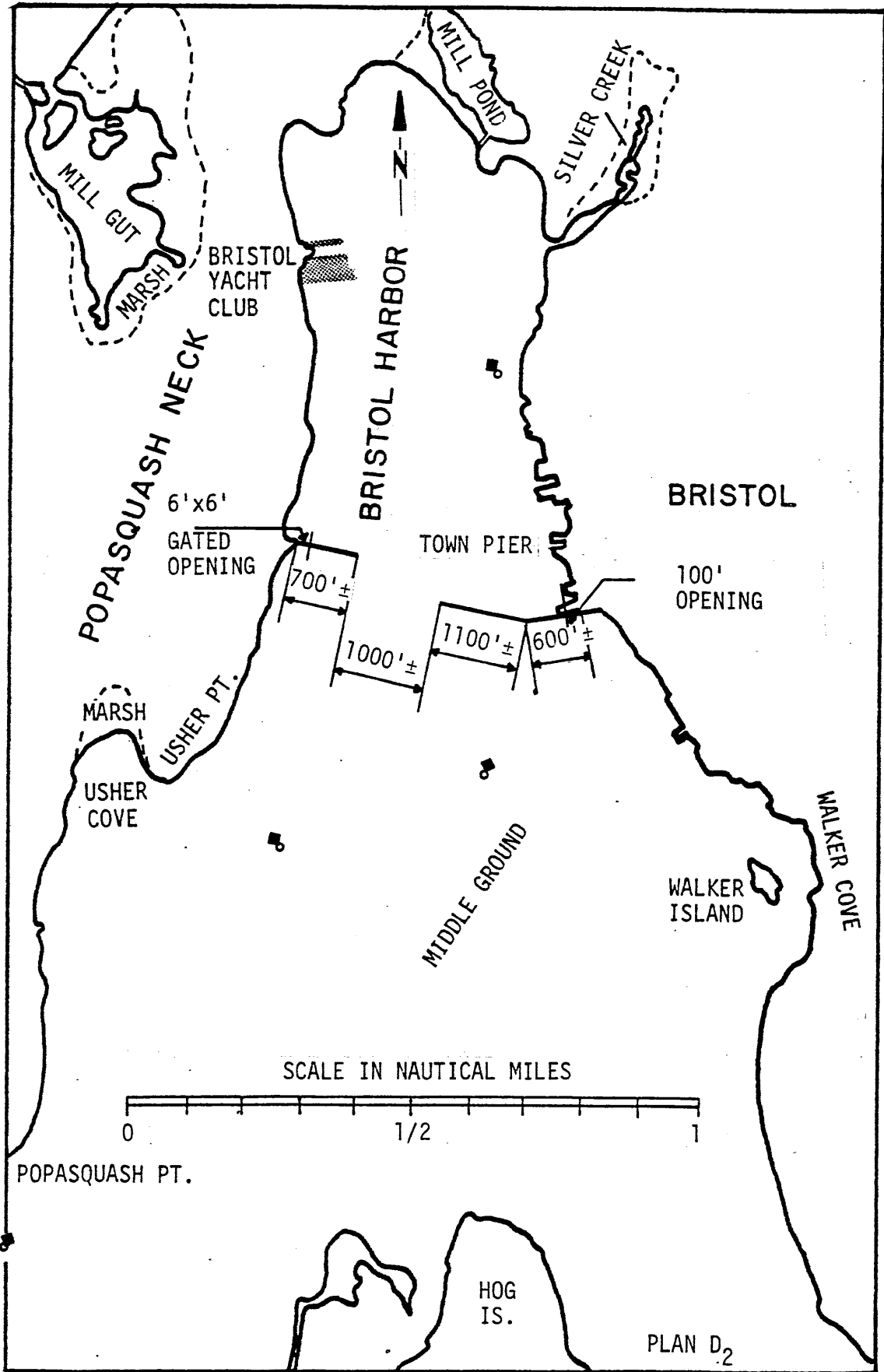


Figure 3. Plan D₂: Proposed rock breakwater. Bristol Harbor, Rhode Island.

In order to understand the present conditions existing in Bristol Harbor with respect to tidal circulation, a two-dimensional numerical, hydrodynamic model is applied to the study area for mean and spring tidal ranges. These circulation results are subsequently used as input for a two-dimensional numerical, dispersion model for the purpose of simulating pollutant dispersion and flushing. Once the existing conditions of flow and transport are known, the effects of each breakwater plan on circulation and dispersion can be measured by comparison. The primary concern of this modeling effort focuses on the prediction of the impact each breakwater will have on harbor flushing.

From the results of these numerical models two other topics can be addressed using analytical procedures. The first analysis concerns the effects of wind stress on the predicted tidal circulation and flushing in Bristol Harbor with and without breakwaters. The second analysis concerns the effect of installing a 6-foot by 6-foot culvert within the 700-foot western breakwater of Plan D₂. From the previous numerical and subsequent analytical results recommendations are made for the various breakwater configurations.

1.1 PROJECT SUMMARY

General Scope - Development of a Hydrodynamic and Dispersion Numerical Model for the analysis of tidal currents, flushing patterns, culvert flows, wind influences and tidal circulation patterns within Bristol Harbor with and without the construction of the proposed three alternative rock breakwaters.

Work Element I. HYDRODYNAMIC AND DISPERSION MODELING IN BRISTOL HARBOR, RI

Task 1 - Application of a two-dimensional numerical, hydrodynamic model to determine normal tidal circulation and elevation patterns under present conditions (Mean and Spring Tide Ranges).

Task 2 - Case studies using the computer model to predict the impact of three (3) proposed breakwater plans on circulation within the harbor and to optimize the length, orientation, and configuration of the breakwater(s) with respect to flushing action.

Task 3 - Case study using the computer model to predict the dispersion and flushing of pollutants to accompany each of the three proposed structures and compare with conditions forecasted to exist in their absence.

Task 4 - Specific analysis will be performed using the computer model to predict the effects of winds on the tidal dynamics within the harbor with and without these structures and also with the possible construction of culverts (6' x 6' gated opening) built into the breakwater(s).

Task 5 - Report - discussion of methodology and findings including graphics, conclusions and recommendations.

2.0 STUDY AREA

Bristol Harbor is located in Bristol, Rhode Island between Popasquash and Bristol Necks on the upper portion of Narragansett Bay. This harbor with a surface area of 10.8 square miles (28 km^2) has no appreciable source of fresh water inflow. However, two small bodies of water, Mill Pond and Silver Creek, are located at the northern end of the harbor.

Bristol Harbor connects with Narragansett Bay by two passages, one on each side of Hog Island. Tides in the Bay as well as the harbor are dominated by the M_2 or lunar, semi-diurnal tidal component. The harbor is a small embayment which behaves within the context of the larger, overall behavior of Narragansett Bay.

The town of Bristol, located 16 miles (25.7 km) southeast of Providence, dominates the eastern shore of the harbor. This small but growing community had a population density of 1751 per square mile ($676/\text{km}^2$) as of 1970 within an area of 10.2 square miles (26.4 km^2). This community with its rich and colorful history dates back to 1681, and has always had a maritime tradition which included ship-building between the Civil War and post-World War II. Like many other coastal New England towns, Bristol's economy changed from an agriculture basis to manufacturing during the course of the Industrial Revolution and remains so today.

The town of Bristol generates harbor pollutants from three main sources. About 2.5 million gallons per day (110 liters/second) of treated effluent are discharged into the lower harbor west of Walker Island from the local primary sewage treatment plant. Manufacturing and docking facilities occupy about an 800 yard (732 meter) stretch of shore along the upper harbor and constitute a second source of pollution. Lacking any specific data from this area, the figures are generally considered to be of the order of one-tenth that of the sewage treatment effluent. A third source of pollution in the harbor is expected to be the Bristol Yacht Club. Again, for lack of data this source is generally

considered to be of the order of one-hundredth that of the sewage treatment discharge. The fact that the dispersion characteristics of the harbor will be altered by the breakwater construction, especially when considering these pollution discharge points, is the primary concern of this investigation.

Very little actual hydrographic data exists for Bristol Harbor. The National Ocean Survey (NOS) has produced tables for tidal currents (NOS, 1980a) and tidal heights (1980b) in or near the study area. Currents at the Mount Hope Bridge which connects Bristol Point to Aquidneck Island average 1.1 knots (0.6 m/s) at 47° True at maximum flood and 1.4 knots (0.7 m/s) at 230° True at maximum ebb. The minimum before both flood and ebb is zero indicating the currents here are bidirectional. The range of the mean and spring tides at Bristol Point, where the Mount Hope Bridge connects to Bristol Neck, is 4.0 feet (1.2 m) and 5.0 ft (1.5 m) respectively. At the town of Bristol, the mean and spring tide ranges are 4.1 feet (1.2 m) and 5.1 feet (1.6 m) respectively.

3.0 MODELS

3.1 HYDRODYNAMIC MODEL

A hydrodynamic numerical model is used to predict the tidal height and current vectors within the marine environment. The body of water is approximated by an appropriate gridwork of points. By specifying the initial and boundary conditions of the problem, a series of results are simulated. Breakwaters are handled as simply changes in the boundary conditions. Usually a hydrographic data set is required to calibrate and verify the model simulation.

The basis of the hydrodynamic, numerical model are the Eulerian equations of motion for a viscous Newtonian flow, or the Navier-Stokes equations consisting of the momentum equations in three dimensions and the ensemble-averaged continuity equation (Neumann and Pierson, 1966). A general, analytical solution does not exist for the hydrodynamic equations due to the closure problem, that is, there are more variables to solve for than equations. A number of simplifying assumptions must be made to achieve closure which renders the equations of motions solvable by particular techniques. The equations are initially simplified by assuming incompressible fluid flow, constant density, constant eddy viscosity and that the second derivative of each velocity component with respect to perpendicular coordinates is small enough to be considered negligible. Applying a Reynolds decomposition, which represents each variable as the sum of its ensemble average and a fluctuation about that average, to the equations of motion produces an averaged set of equations whose stochastic processes are smoothed or filtered while retaining deterministic processes (Schlichting, 1968). However, this process produces several extra terms which are the components of the Reynolds stress tensor (the product of the density and the ensemble average of the product of the component velocity fluctuations about their means). These terms are simplified in a subsequent step. Without a loss of meaning, the three-dimensional equations of motion can be reduced to a set of two-dimensional equations by integrating over the total depth assuming vertical variations of variables are negligibly small and by

applying Leibnitz's rule (Connor and Wang, 1974). The vertical momentum equation simply reduces to the hydrostatic balance relation as expected. The sum of the Reynolds stress and the internal stress forms the total stress. The Boussinesq approximation replaces the momentum flux terms resulting from the vertical integration of total stress components with velocity gradient terms whose constants of proportionality are the kinematic eddy viscosity coefficients (Neumann and Pierson, 1966). Bottom shear stress is approximated by a quadratic function of depth-integrated fluid velocity whose proportionality constant is a dimensionless friction factor. Similarly surface shear stress, if present, is approximated by a quadratic function of the wind velocity (usually measured at 10-meters) whose proportionality constant is a different dimensionless friction factor. (For simplicity these friction factors are considered constants, but several function relationships with respective velocities have been presented in the literature). The result is a two-dimensional momentum balance. The temporal and convection acceleration terms are balanced primarily by the surface slope and bottom friction terms and secondarily by the Coriolis and eddy viscosity terms. Thus the driving force of the surface slope is primarily resisted by bottom friction with the remaining energy producing the velocity vector field.

The problem is completed by specifying the boundary conditions which is the value of a flow component or of the surface elevation along a boundary. Normal flow on land boundaries are zero, and along river boundaries, if present, are equal to the river flow rates. Along open ocean boundaries, the values of the surface elevation are specified. The system of equations, while still too complex for analytical techniques to solve, can be solved using one of several numerical techniques. (Analytical methods arrive at exact solutions to specific problems. When an analytic solution does not exist, or is overly complex, then solutions can be approximated using numerical methods).

A variety of numerical methods exist to solve partial differential equations (Ames, 1977) of which the two-dimensional, vertically-averaged, hydrodynamic equations are an important subset (Roache, 1976).

Two general techniques are used to obtain solutions: finite-differences and finite-elements. The finite difference (FD) method, the simpler of the two, has two different types of techniques for the advancement of the equations in time: explicit and implicit. Explicit-time FD-equations are advanced through time for each time-step using previous values. Implicit-time FD-equations, step through time by solving systems of simultaneous equations, which is a time-consuming process since each step requires a matrix inversion or an equivalent technique. The finite-element (FE) method approximates a solution by optimizing a precise linear interpolating function which also requires a series of matrix inversions or equivalent since it is also an implicit method. Each method has its particular advantages and drawbacks (Thacker, 1978a,b)..

In comparing the methods, let us first consider the stability criterion. The Courant number γ represents a dimensionless measure of the time step as

$$\gamma = c \Delta t / \Delta x$$

where c is the celerity or wave velocity ($c = \sqrt{gD}$, where g is the acceleration due to gravity equal to 9.81 m/sec^2 or 32.2 ft/sec^2 and D is the total water depth), Δt the time increment and Δx the grid spacing. Implicit-time FD methods are unconditionally stable, at least for incompressible flows, whereas the stability criterion for the explicit-time FD-methods is given by $\gamma \leq 1$ (Roache, 1976). The FE-method has the stability criterion of $\gamma \leq 1/\sqrt{2} \approx 0.707$ (Connor and Wang, 1974). Thus the stability criterion requires the FE-method take 30% more time than the time-explicit FD-method which affects the computational economy of this method.

FD-methods have the advantage of being easily understood and applied especially in the case of an explicit-time step. Irregular grids for FD-equations are possible but tend to make the application more difficult. FE-methods were specifically devised for irregular grids which makes them very attractive in coastal modeling applications. For this reason, we use the two-dimensional FE-solution technique of

Connor and Wang (1974) presented in Circulation Analysis by Finite Elements or CAFE model (Celikkol and Reichard, 1976). Let us examine this method more closely.

The finite element method approximates the solution of a boundary value problem with a function of piece-wise continuous polynomials. This involves discretization of the continuum into an equivalent system of finite elements. Connor and Wang selected the simplest configuration, triangles with nodes at the vertices. The values of the variables within the element are assumed to be a linear function of the values at the nodes. The equations are transformed for application to an element using this linear polynomial representation. Treatment of the entire continuum is accomplished through summation of the contributions of each element. Each nodal value influences all of the elements containing that node, and each element value influences the three nodes of the element. Depth is selected at each node point, while bottom friction and eddy viscosity are selected for each element.

3.2 DISPERSION MODEL

A dispersion numerical model is used to predict the concentrations of material within a fluid body. This material is transported by three processes: advection by currents, turbulent diffusion by eddies and molecular diffusions by Brownian motion (which is essentially small enough to ignore when compared to the first two processes). Thus the solution of the dispersion model depends on results from the hydrodynamic model to calculate advection.

The basis of the dispersion, numerical model is the Eulerian equation for the conservation of mass of the dispersant (Sayre, 1975). A number of simplifying assumptions are necessary to achieve closure. By assuming an incompressible flow as in the hydrodynamic model case, this relationship reduces to the Eulerian diffusion equation in a convective flow field. By applying a Reynolds decomposition to this

diffusion equation, additional terms (the negative of the ensemble average of the product of the component velocity fluctuations and the concentration fluctuation about the mean) are produced analogous to the components of the Reynolds stress tensor (Sayre, 1975). Again, without a loss of meaning, the resultant equation is integrated over depth (Liemkuhler et al., 1975). The Boussinesq approximation replaces the mass flux terms resulting the vertical integration of diffusion components with mean concentration gradient terms whose constants of proportionality are the turbulent diffusion coefficients. The molecular diffusion coefficients are generally several orders of magnitude smaller than the turbulent diffusion coefficients which can be absorbed by the turbulence parameters or simply ignored as being negligible. The similarity between this development and that for the hydrodynamic equations makes them compatible. Consistency is required since the advection terms in the diffusion equation come from the hydrodynamic equations. The problem is completed by specifying the initial and boundary conditions, the source and sink parameters, decay coefficients for any non-conservative constituents and settling velocities in the case of suspended sediments.

The same numerical methods available for the hydrodynamic equations are applicable to the dispersion equation. For reasons previously stated at the end of Section 3.1, a FE-technique is used. The companion to the CAFE model is the two-dimensional, FE, vertically-integrated dispersion model of Liemkuhler et al. (1975) known as DISPER. By properly specifying the various input parameters to the program such as grid spacing, sources, sinks, and the associated coefficients, the model can determine the simulated behavior of constituent concentrations with respect to a simulated flow field.

3.3 PREVIOUS APPLICATIONS

Both the CAFE and DISPER models have been previously applied in several studies. The CAFE model was originally applied to a model of Massachusetts Bay by Connor and Wang (1973). CAFE solutions compare

favorably with the analytical solutions for the simple case when analytical solutions can be found by linearizing the equations of motion. CAFE solution for the general case of non-linear equations of motion describe what is intuitatively believed to be the general circulation of the Bay. Sufficient field data did not exist to compare the model with.

The CAFE model has also been applied to the Great Bay Estuarine System (Celikkol and Reichard, 1976), Sakonnet Harbor, Rhode Island (NAI, 1979a), New Haven Harbor, Connecticut (NAI, 1979b), the Piscataqua River, New Hampshire (NAI, 1980) and Portsmouth Harbor, New Hampshire (Parsons *et al.*, 1976). For each study, the model results compared favorably with the field results from current meter surveys when the field conditions approximated the model assumptions (Reichard and Celikkol, 1978; NAI, 1979a, 1979b, 1980; Parsons *et al.*, 1976). The dispersion model DISPER was used in conjunction with the CAFE model for two of these studies. In Portsmouth Harbor, DISPER was utilized to predict the extent of suspended sediment dispersion over varying tidal conditions (Parsons *et al.*, 1976). In the second case, for New Haven Harbor, DISPER predicted the dispersal of sewage effluent by tidal currents (NAI, 1979b). The predicted effluent dispersion patterns compared favorably with a companion dye study when field conditions approximated the model assumptions. In conclusion, both the CAFE and DISPER models have been successfully applied to several different study areas. Their results compare well with either the intuitive understanding of the study area dynamics, the analytical results from the linearized set of equations, or field measurements taken for model validation. Because of these previous successes, we assume these models adequately simulate the behavior of Bristol Harbor within the context of assumptions of the derivations.

3.4 INITIALIZATION

3.4.1 Finite Element Grids

The first task necessary in applying either a FE- or a FD-model is the specification of the grid which represents the space in which solutions are to be found. Irregular grid spacing in either case can not be too irregular since numerical instabilities could subsequently develop (Thacker, 1978b). As a rule of thumb for the triangular elements of the FE-method, the areas of adjacent triangles should not differ more than 20% and the interior angles should be greater than 30 and less than 90 degrees. Referring to each triangle as an "element" of the grid, and the vertices as "nodes", an important consideration in grid construction is that an element may not have more than two of its three nodes on a land boundary. Finally, as few nodes as possible should be utilized to adequately describe the given problem to minimize computer time and required memory space.

The grid for Bristol Harbor is based on NOAA Chart No. 13224 (old number 278) for the Providence River and the Head of Narragansett Bay. The gridwork is superimposed on an outline of the harbor. The dominant feature of this grid is that Hog Island is included on the open-ocean boundary which splits the boundary into two passages. At each node, the depth in meters is specified from the chart along with the nodal coordinates based on the state coordinate system.

Two different sets of grids have to be constructed because of the geometric differences between breakwater Plan A and Plans D₁ and D₂. The grids will be referred to as A and D respectively. Grid A (Figure 4) consists of 233 nodes with 390 elements and Grid D (see Figure 5) 232 nodes with 388 elements. Both models use the same grid when working on a particular case.

16

Figure 4. Grid A showing source nodes and Plan A breakwater locations. Bristol Harbor, Rhode Island.

BRISTOL
YACHT
CLUB



BRISTOL
INDUSTRIAL
AREA

WALKER
ISLAND

HOG ISLAND

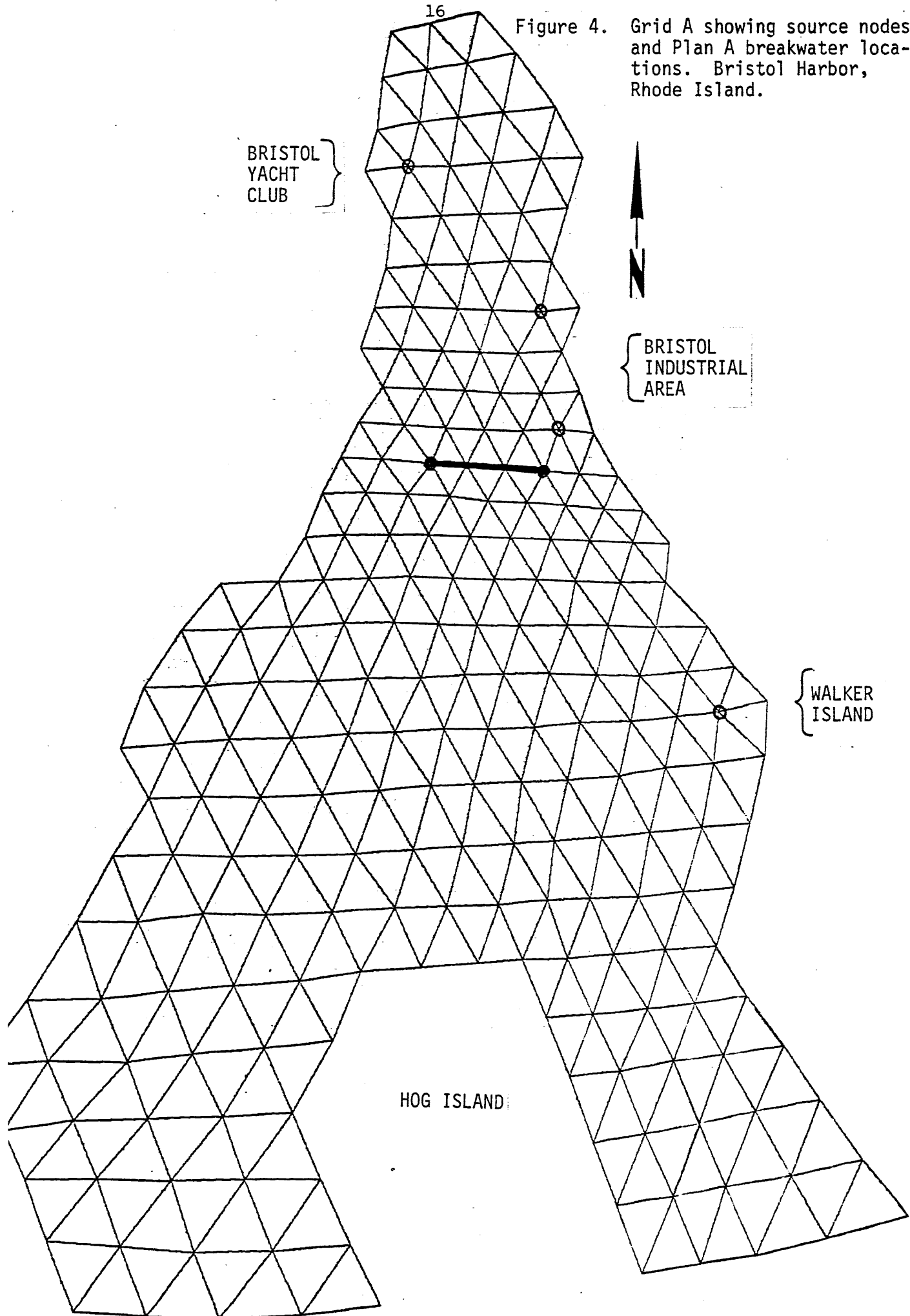
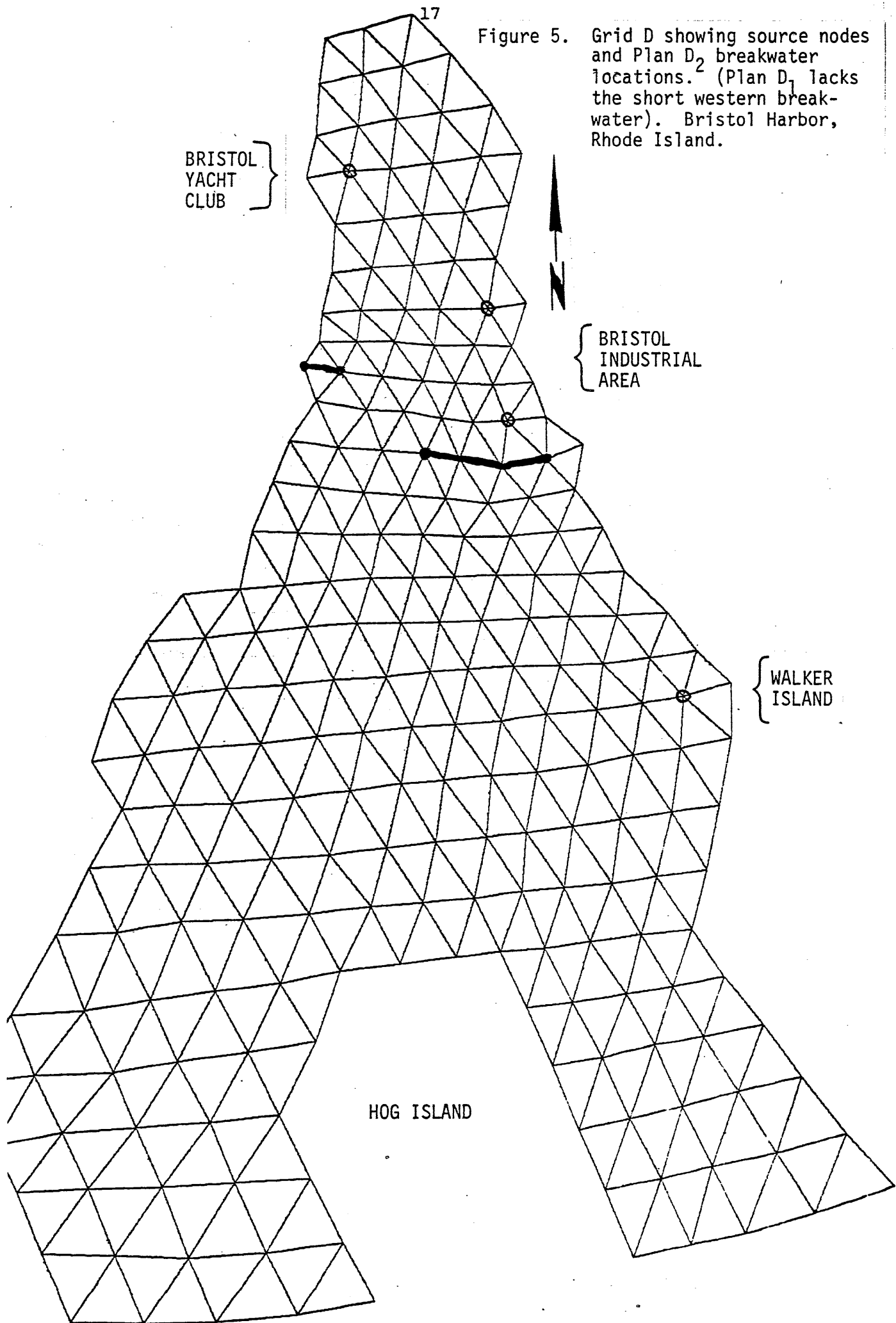


Figure 5. Grid D showing source nodes and Plan D₂ breakwater locations. (Plan D₁ lacks the short western breakwater). Bristol Harbor, Rhode Island.



3.4.2 Model Conditions

The CAFE model runs are separated into two groups based on tidal amplitude. According to NOS (1980b), at Bristol Point which is the eastern end of the harbor opening, the mean tidal amplitude is 2.0 feet (0.61 m) and the spring tidal amplitude is 2.5 feet (0.76 m). These are the boundary conditions for the open ocean boundary. The driving force is assumed to be the M_2 tide with a period of 12.42 hours. (For simplicity, model output time is incremented on the basis of a 62 minute lunar hour.) Modeling of tides and currents in Narragansett Bay by Swanson and Spaulding (1977) shows a phase difference between the east and west passages of Bristol Harbor (Spaulding and Swanson, 1974). This model uses a phase lag of 180 seconds between the east and west passages to account for this difference. Along the land boundaries, zero normal flow is imposed. For Plan D₂, there is zero flow at the node where the short western breakwater intersects the land boundary. The initial conditions, typical for this kind of model, are to start it from rest (all velocities equal to zero) at high water (tidal amplitude at maximum height on ocean boundary) at time $t=0$.

The other input parameters include a time step Δt of 12 seconds, zero eddy viscosities ($v_{xx} = v_{yy} = v_{xy} = 0$) and a bottom friction coefficient of 0.020. The time step was chosen to be stable according to the criterion at the end of Section 3.1. The eddy viscosities are ignored since there is no field data to adjust them by. Because the eddy viscosities are second-order terms, this assumption is valid in the context of this model (Briggs and Madsen, 1974). The bottom friction coefficient is adjusted so that the velocity conditions match those given by Spaulding and Swanson (1974). This value has the same order of magnitude used in the studies of the Great Bay Estuary (Celikkol and Reichard, 1976), Sakonnet Harbor (NAI, 1979a), New Haven Harbor (NAI, 1979b), the Piscataqua River (NAI, 1980) and Portsmouth Harbor (Parsons et al., 1976). This value of the friction coefficient is an order of magnitude larger than that used in studies for Massachusetts Bay (Connor and Wang, 1974 and Briggs and Madsen, 1974). This difference appears to

be related to the influence of friction within the respective study areas. Finally the velocity results are saved every five minutes for input to the DISPER model and printed every lunar hour (62 minutes) with plots.

The associated DISPER model also has its required initial conditions, boundary conditions and parameters. The initial conditions require that the concentration at each node be initially specified, in this case, as zero for every node. Boundary conditions require the location, duration and magnitude at prescribed concentration nodes including source/sink nodes. This model prescribes a concentration of zero on the ocean boundary since a conservative mixing process is assumed. Source terms are defined as follows for a simulated dye release study: 1) a source rate of 7.5 mg/sec at Walker Island, 2) two sources at the pier and adjacent industrial area of 0.75 gm/sec, and 3) a source of 0.075 gm/sec at the Bristol Yacht Club. There are no sink nodes in conservative mixing. The required parameters are the dispersion coefficients, decay rates, and the time step. For lack of field data, the same dispersion coefficients used in the New Haven Harbor dispersion study (NAI, 1979b) are used here ($D_{xx} = D_{yy} = 25 \text{ m}^2/\text{s}$, $D_{xy} = 0$). Conservative mixing does not allow for a decay coefficient so its value is set to zero. Finally the same time step of 12 seconds used in the CAFE model is also used in DISPER.

3.4.3 Calibration

Due to the lack of field data, the tidal model is calibrated using the results for Bristol Harbor from the Narragansett Bay model of Spaulding and Swanson (1974). The phase difference between the east and west passage was adjusted to 180 seconds which develops similar circulation patterns around Hog Island and within the upper harbor. The bottom friction coefficient was adjusted to 0.020 so that equivalent current vectors had the same magnitude and direction. The lack of current meter data also does not allow adjustment to be made on the eddy viscosities.

Since these are second order terms, the simplest approach sets them equal to zero. Dispersion coefficients, normally estimated from field studies, were taken from a similar study that had an associated field program (NAI, 1979b).

4.0 MODEL RESULTS

4.1 SIMULATED HARBOR CIRCULATION

The CAFE model was run for two conditions in Bristol Harbor, spring tide and mean tide, for each of the four cases; present conditions, Plan A, Plan D₁ and Plan D₂. The required initial conditions, boundary conditions and input parameters were discussed in a prior section. The time step was 12 seconds. Every five minutes the velocity results were stored for later use as input to drive the advection in DISPER. Printed and plotted output were produced every lunar hour (62 minutes or 3,720 seconds). By convention, the model was started at time $t = 11,160$ seconds, corresponding to high slack water. The results presented which are also the results saved as input for the DISPER model span from time $t = 22,320$ seconds to $t = 66,960$ seconds, a complete cycle from mid-ebb to the next mid-ebb. The currents are specified at each element of the grid. Current speeds are given in units of centimeters per second. Table 1 is a conversion table for cm/sec into knots.

4.1.1 Existing Tidal Effects

The circulation within Bristol Harbor is generated by the M_2 tide via communications with Narragansett Bay. These currents are bidirectional which means that their magnitudes reduce to zero at slack water unlike rotary currents. Current speeds within the upper harbor are weak, whereas speeds within the lower harbor in the circulation around Hog Island are much stronger. This circum-island circulation is driven by a tidal phase difference between the east and west passages entering into the harbor (Spaulding and Swanson, 1974). The general circulation pattern within the study area appears to behave as follows with no discernible differences between the mean and spring tides:

Ebb Tide ($t = 22,320$ sec)

Water enters the lower harbor through the east passage and exists via the west passage. The strongest flows

TABLE 1. CONVERSION TABLE: CENTIMETERS PER SECOND TO KNOTS.
BRISTOL HARBOR, RHODE ISLAND.

cm/sec	knots	knots	cm/sec
1	0.19	0.05	2.
2	0.039	0.10	5.1
3	0.058	0.15	7.7
4	0.078	0.20	10.3
5	0.097	0.25	12.9
6	0.117	0.30	15.4
7	0.136	0.35	18.0
8	0.155	0.40	20.6
9	0.175	0.45	23.2
10	0.194	0.50	25.7
11	0.214	0.55	28.3
12	0.233	0.60	30.9
13	0.253	0.65	33.5
14	0.272	0.70	36.0
15	0.291	0.75	38.6
16	0.311	0.80	41.2
17	0.330	0.85	43.8
18	0.350	0.90	46.3
19	0.369	0.95	48.9
20	0.389	1.00	51.5
21	0.408		
22	0.427		
23	0.447		
24	0.466		
25	0.486		
26	0.505		
27	0.525		
28	0.544		
29	0.563		
30	0.583		

range between 8 and 13 cm/sec (9-15 cm/sec for spring tides). Water in the upper harbor flows south at about 3 cm/sec (mean and spring tides). Water flow in the middle harbor reflects a merging of upper and lower harbor circulation (Figure 6a).

Low Slack Water (t = 33,480 sec)

Theoretically at low slack water, the velocities vanish simultaneously for bidirectional currents in a standing tidal wave (as opposed to a traveling tidal wave). In actuality, there is always some water movement somewhere in the harbor. In the lower harbor flow is still entering through the east passage and exiting via the west passage which changes within one lunar hour after low tide. Speed in the lower harbor ranges between 4 to 6 cm/sec (5 to 7 cm/sec during spring tides). Currents in the upper harbor have speeds of the order of 1 cm/sec or less and variable directions (Figure 7a).

Flood Tide (t = 44,640 seconds)

After the tide turns, water enters the lower harbor through the west passage and leaves through the east passage. Peak speeds range between 7 and 12 cm/sec (8 to 15 cm/sec during spring tides). Water is entering the upper harbor flowing north at about 2 to 3 cm/sec for both mean and spring tidal conditions (Figure 8a).

High Slack Water (t = 55,800 seconds)

A flow still persists west-to-east around Hog Island of about 5 to 7 cm/sec (6 to 8 cm/sec during spring tide). The flow reverses within one lunar hour after high tide. In the upper harbor, flows have small magnitudes (\lesssim 1 cm/sec) and variable directions (Figure 9a).

Lower harbor circulation patterns remain essentially the same for each different breakwater plan.

Figure 6a. Tidal Currents at mid-ebb for mean tide (no breakwater). Bristol Harbor, Rhode Island.

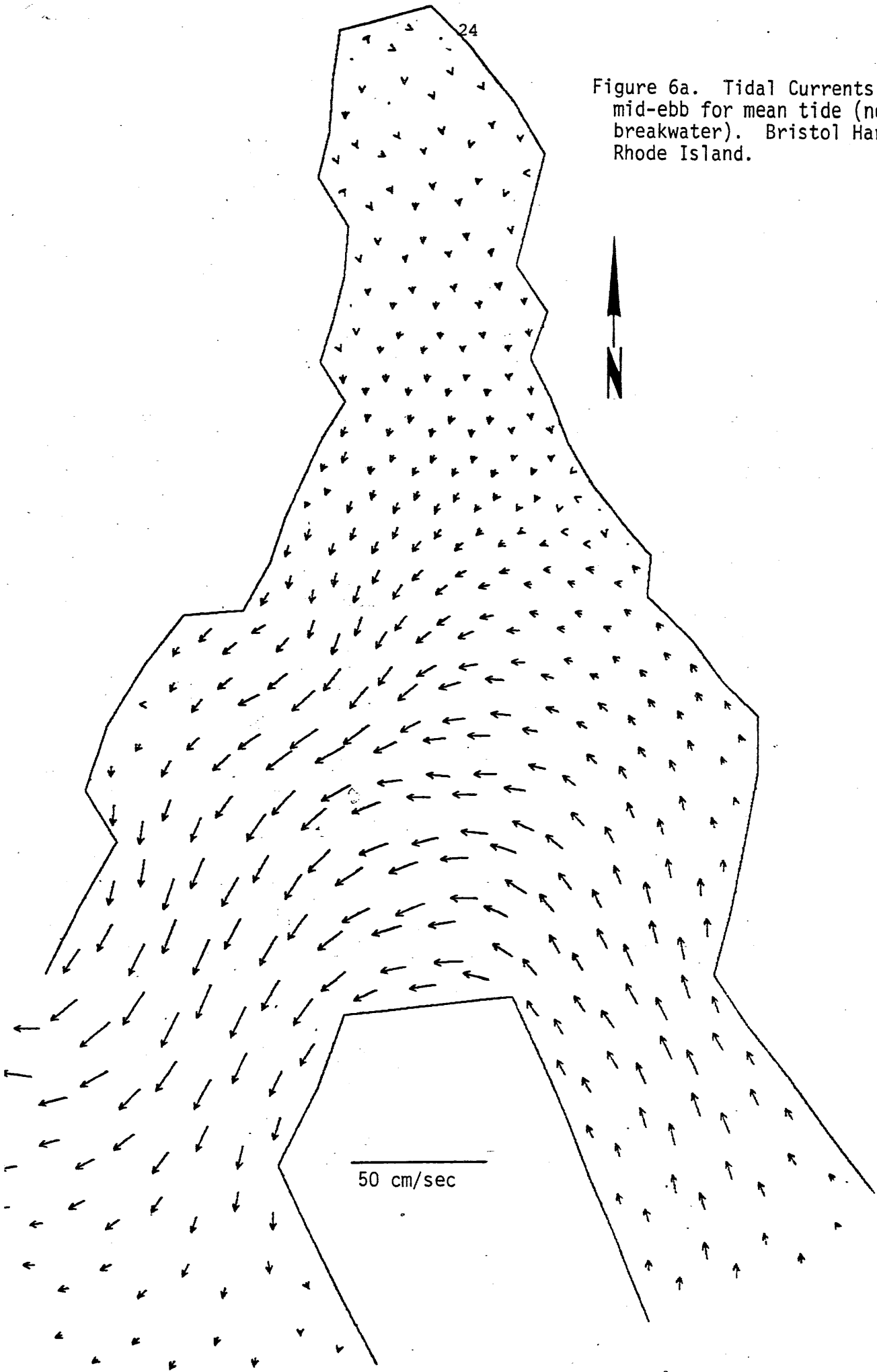


Figure 7a. Tidal Currents at low-slack for mean tide (no breakwater).
Bristol Harbor, Rhode Island.

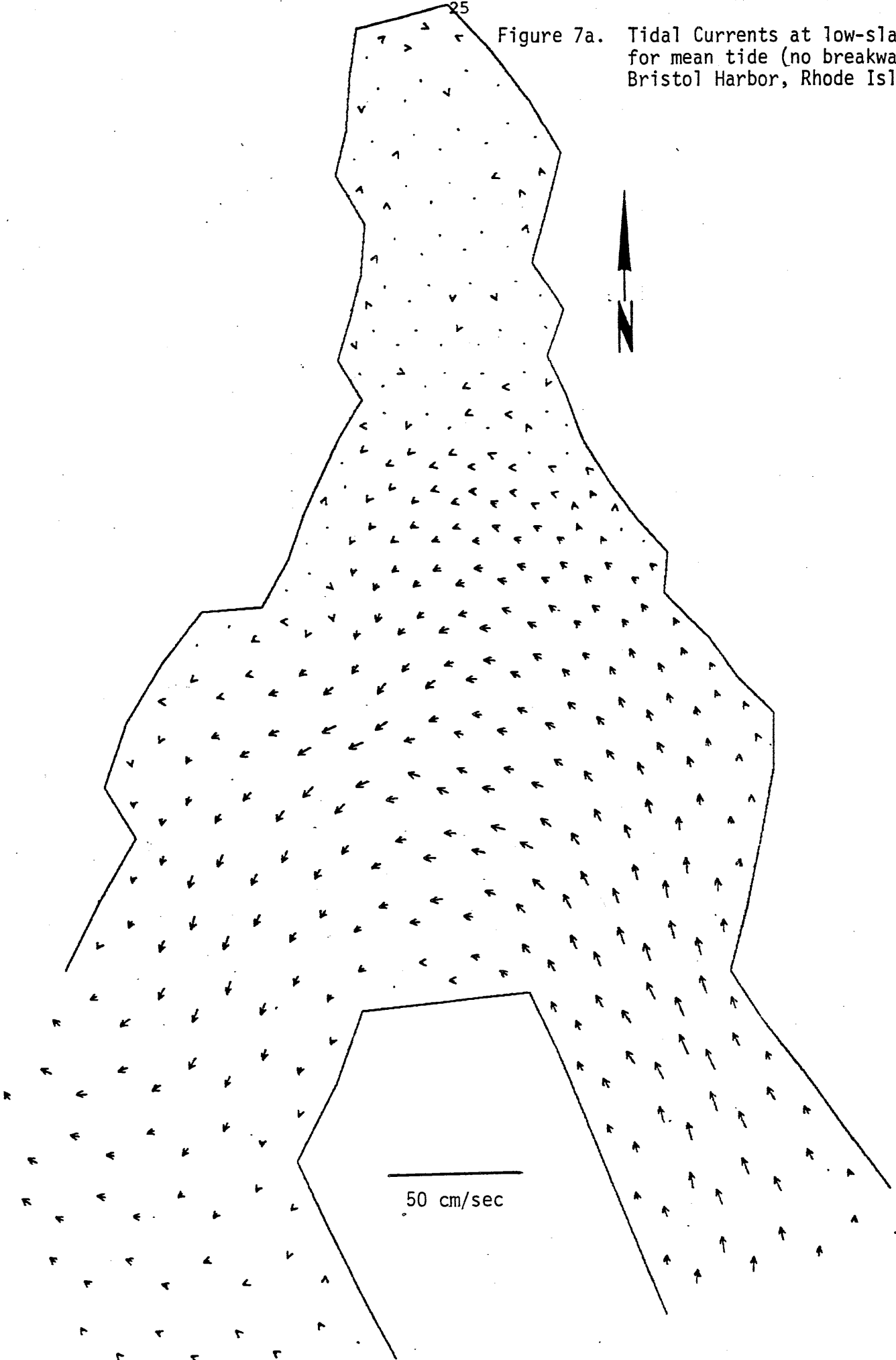


Figure 8a. Tidal Currents at mid-flood for mean tide (no breakwater).
Bristol Harbor, Rhode Island.

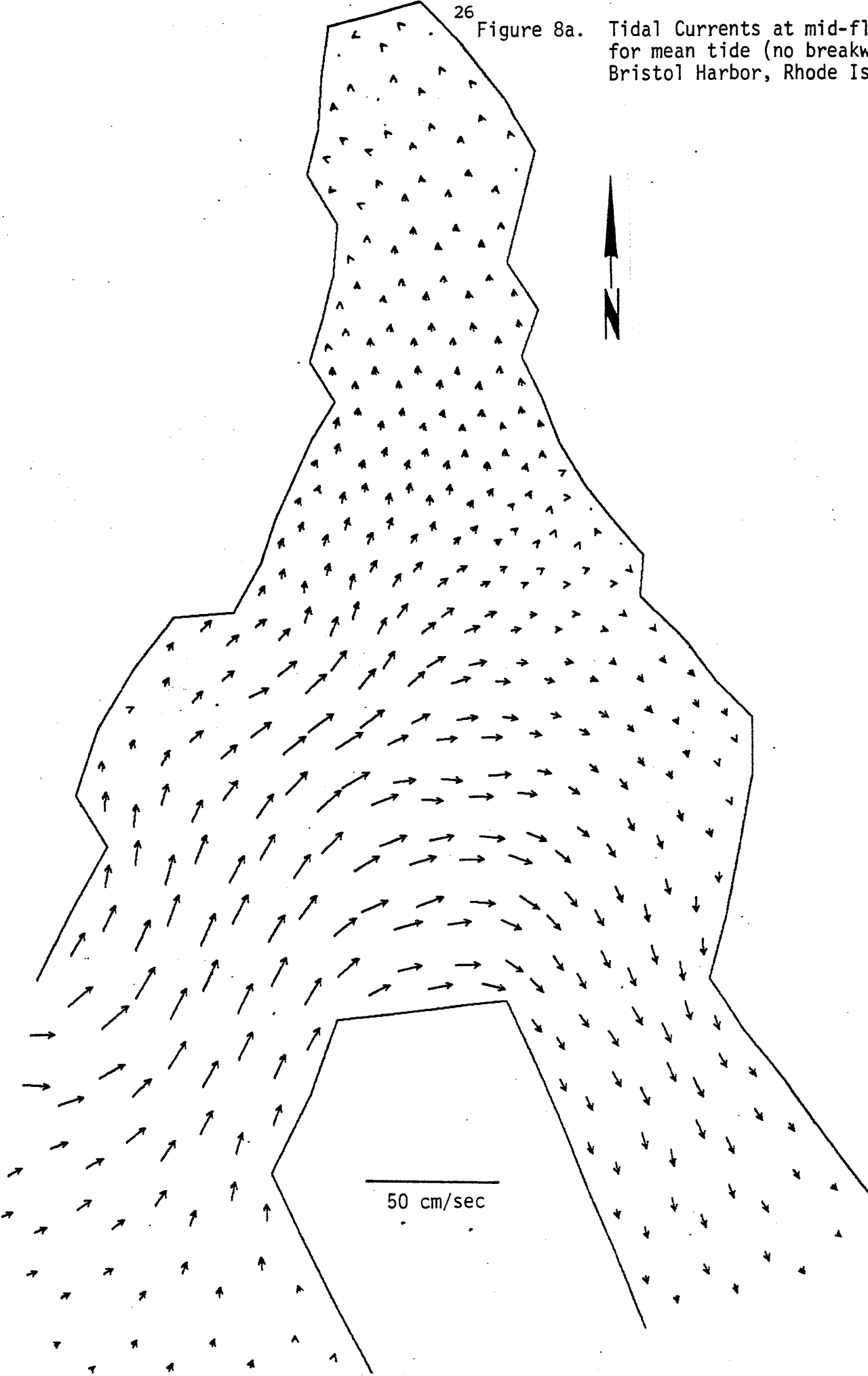
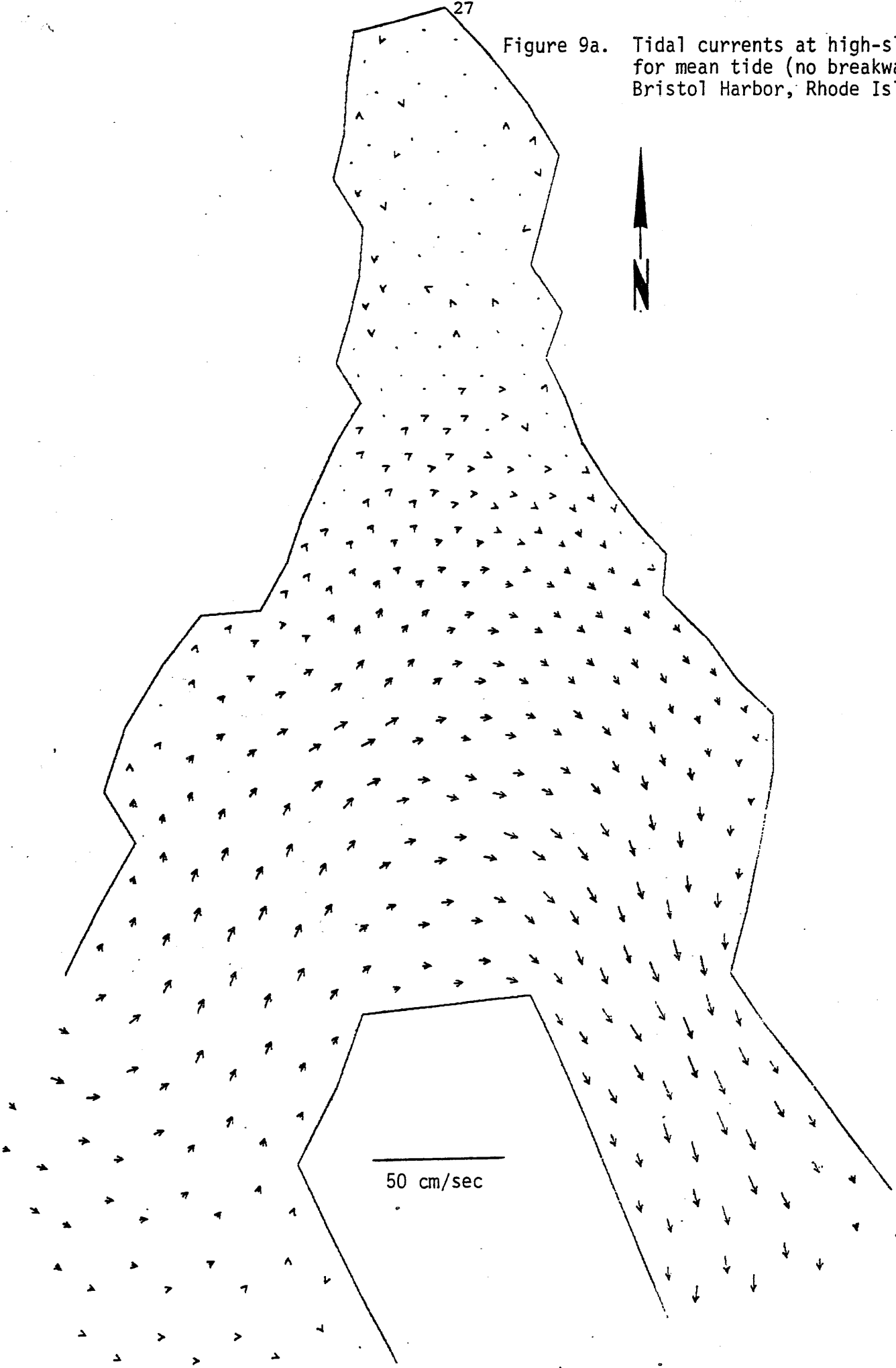


Figure 9a. Tidal currents at high-slack for mean tide (no breakwater).
Bristol Harbor, Rhode Island.



4.1.2 Breakwater Effects

The different breakwater configurations cause the upper harbor circulation pattern to change radically compared to present conditions. Current speeds tend to increase in the regions around the breakwater which is not unexpected. Intuitively if a volume of water V has an amount of time t (at a rate $Q = V/t$) to move through a cross-sectional area A , then the velocity U must increase when the area is decreased since the rate $Q = UA$ must be the same in both cases. In addition the breakwaters also cause eddies to develop which is also not an unexpected result. Consider the following effects on the circulation patterns in the upper harbor due to the presence of each different breakwater configuration:

Ebb Tide ($t = 22,320$ seconds)

During the mid ebb phase of the tidal cycle, eddy motion north and south of the breakwater is not well organized. No substantial differences are evident in comparing spring and average tide plots for this current phase. Typical speeds are 6 to 8 cm/sec around breakwater A, 6 to 9 cm/sec around D_1 and D_2 (Figure 6b, c, d). As ebbing continues, the eddies organize and intensify. Peak speeds of about 16 m/sec are found in the eddies adjacent to breakwater A, and about 23 cm/sec in eddies adjacent to D_1 and D_2 .

Low Slack Water ($t = 33,480$ seconds)

During this tidal phase, the eddies around breakwater A are still organized but the speeds have decreased to maximum values of 8 or 9 cm/sec. The same behavior is true about D_1 and D_2 where the peak velocities have dropped to about 14 cm/sec (Figure 7b, c, d). After the tide turns, the eddies strengthen and intensify with peak speeds of 19 cm/sec near A, and of 25 cm/sec near D_1 and D_2 .

Figure 6b. Tidal Currents at mid-ebb
for mean tide (Plan A).
Bristol Harbor, Rhode Island.

PLAN A

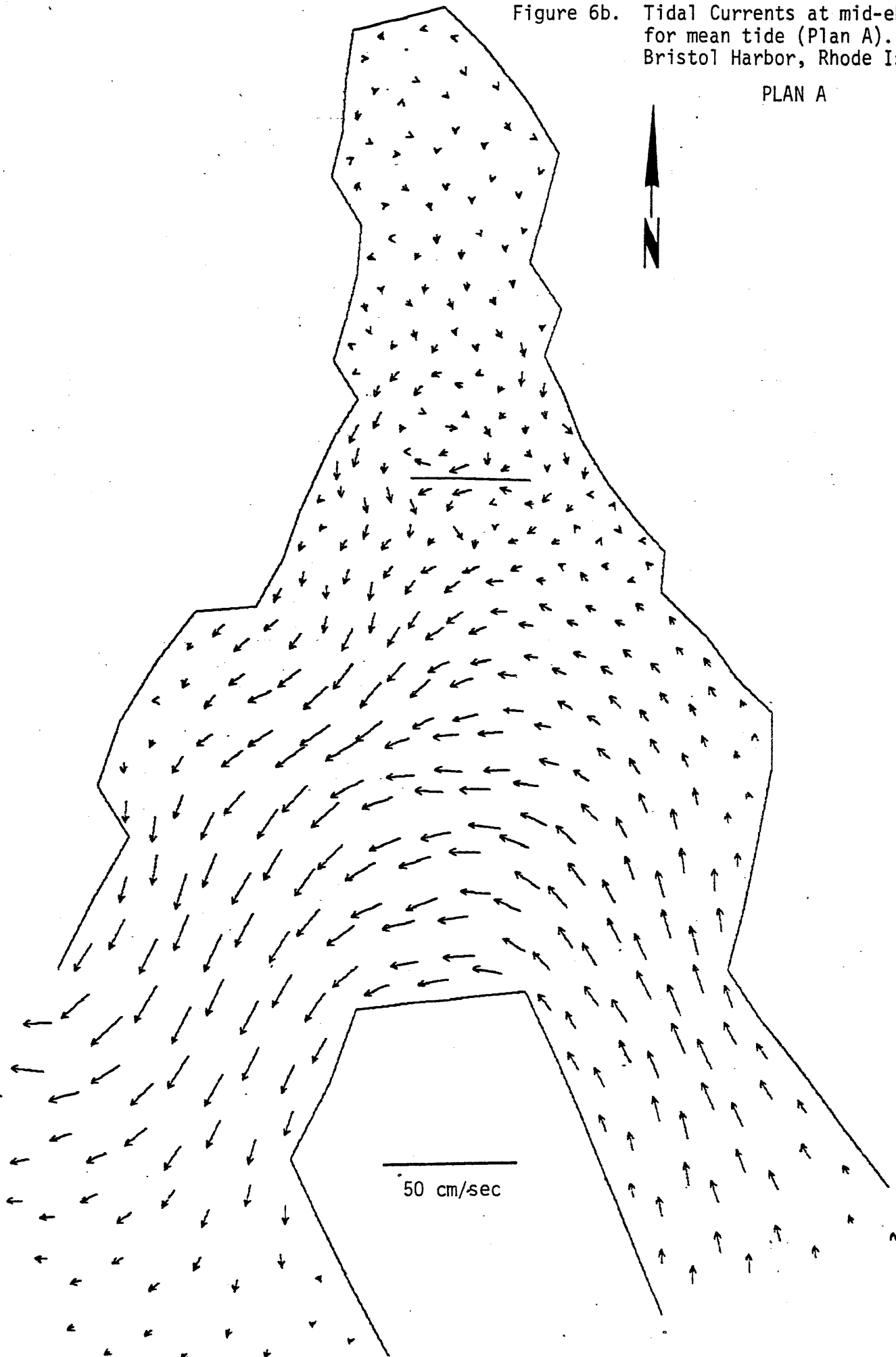


Figure 6c. Tidal Currents at mid-ebb for mean tide (Plan D₁).
Bristol Harbor, Rhode Island.

PLAN D₁

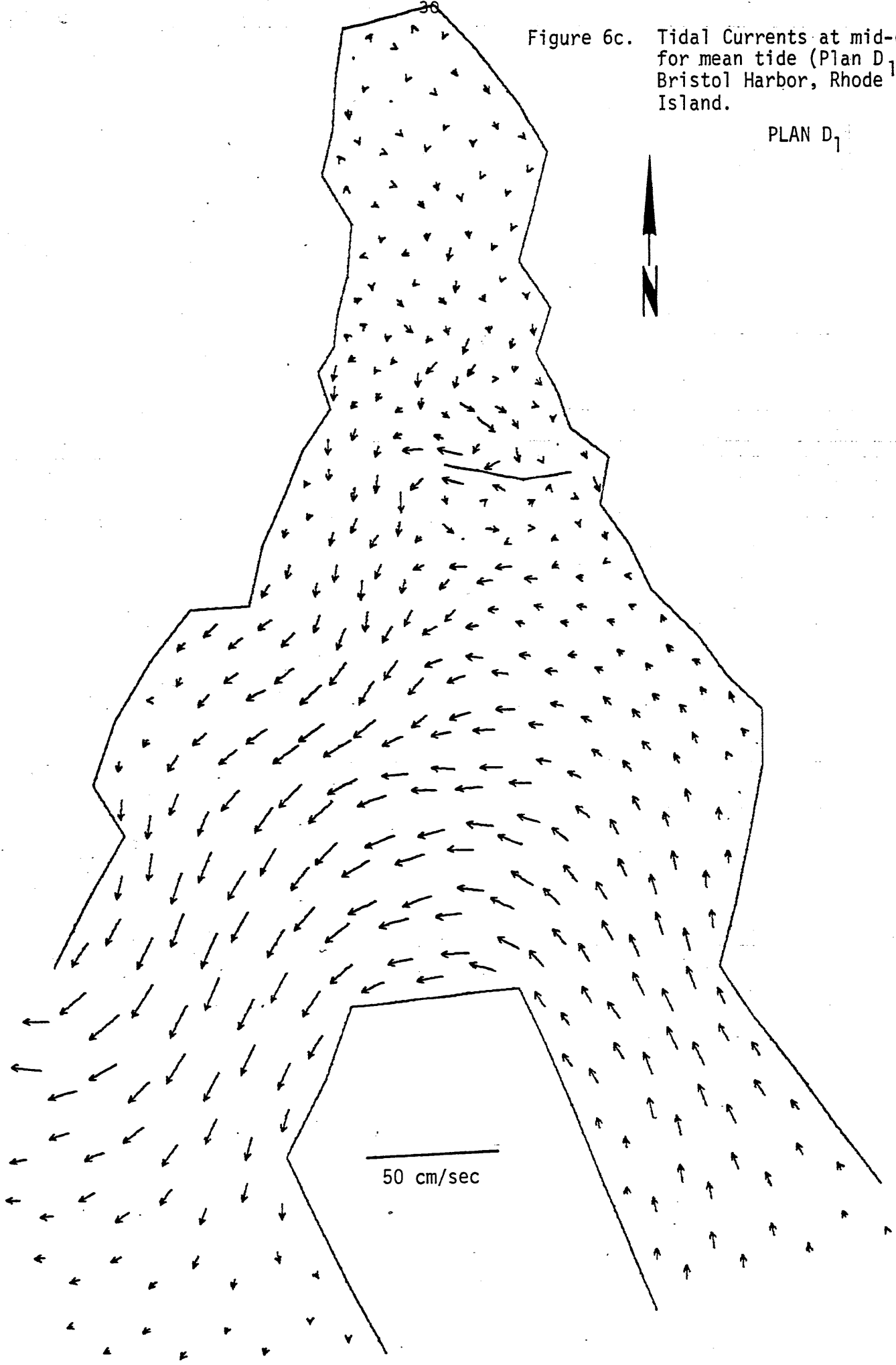


Figure 6d. Tidal Currents at mid-ebb
for mean tide (Plan D₂).
Bristol Harbor, Rhode Island.

PLAN D₂

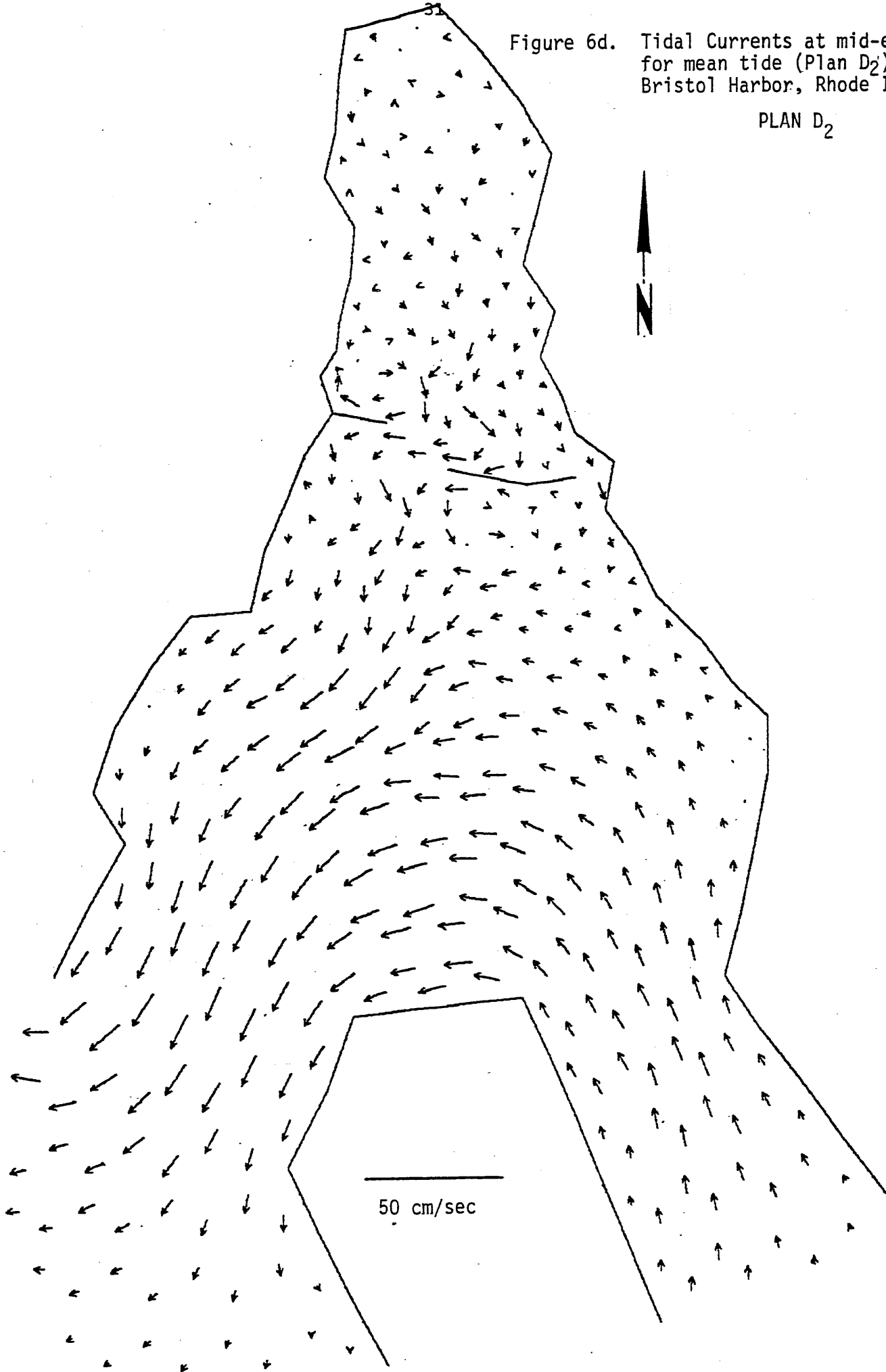
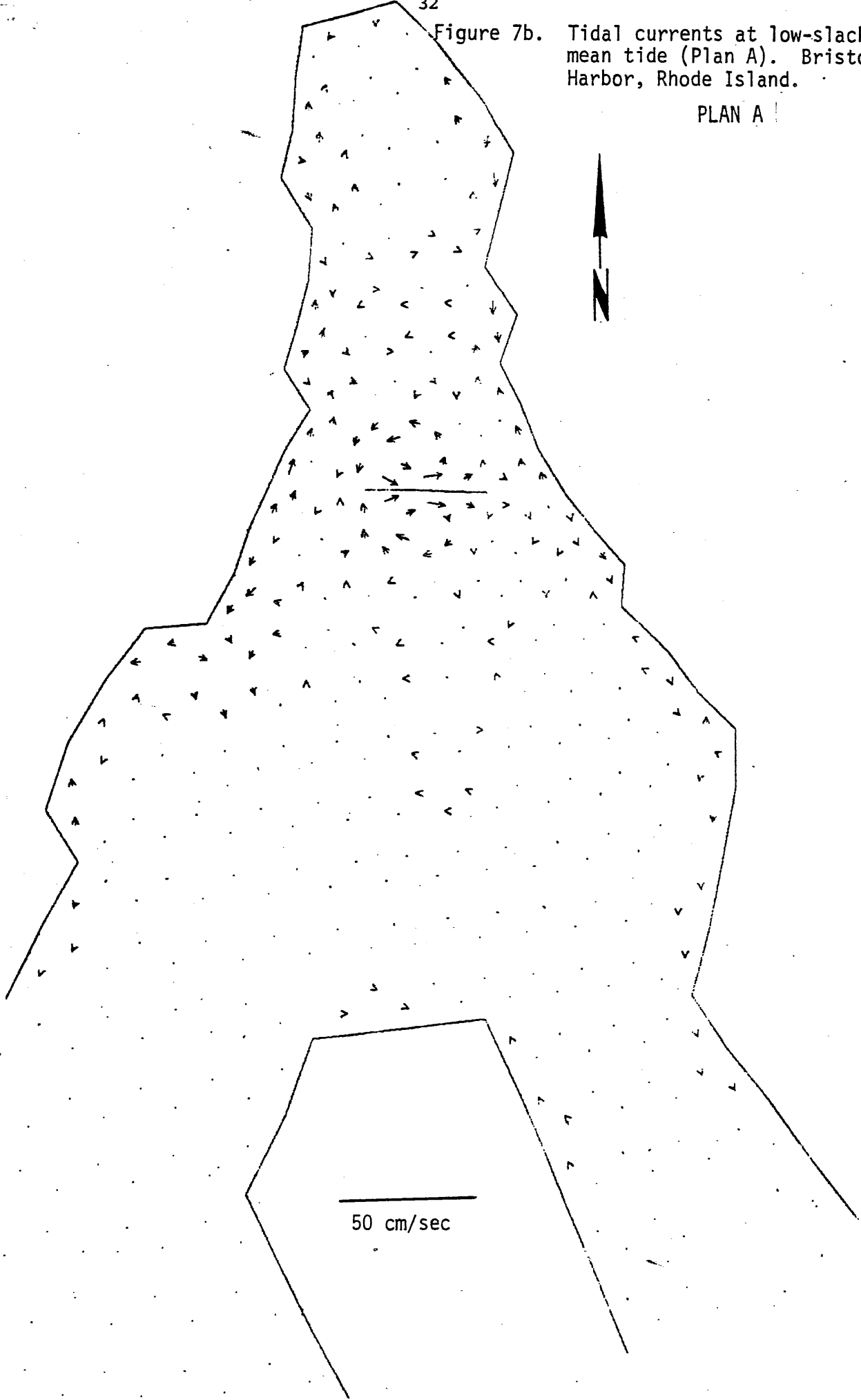


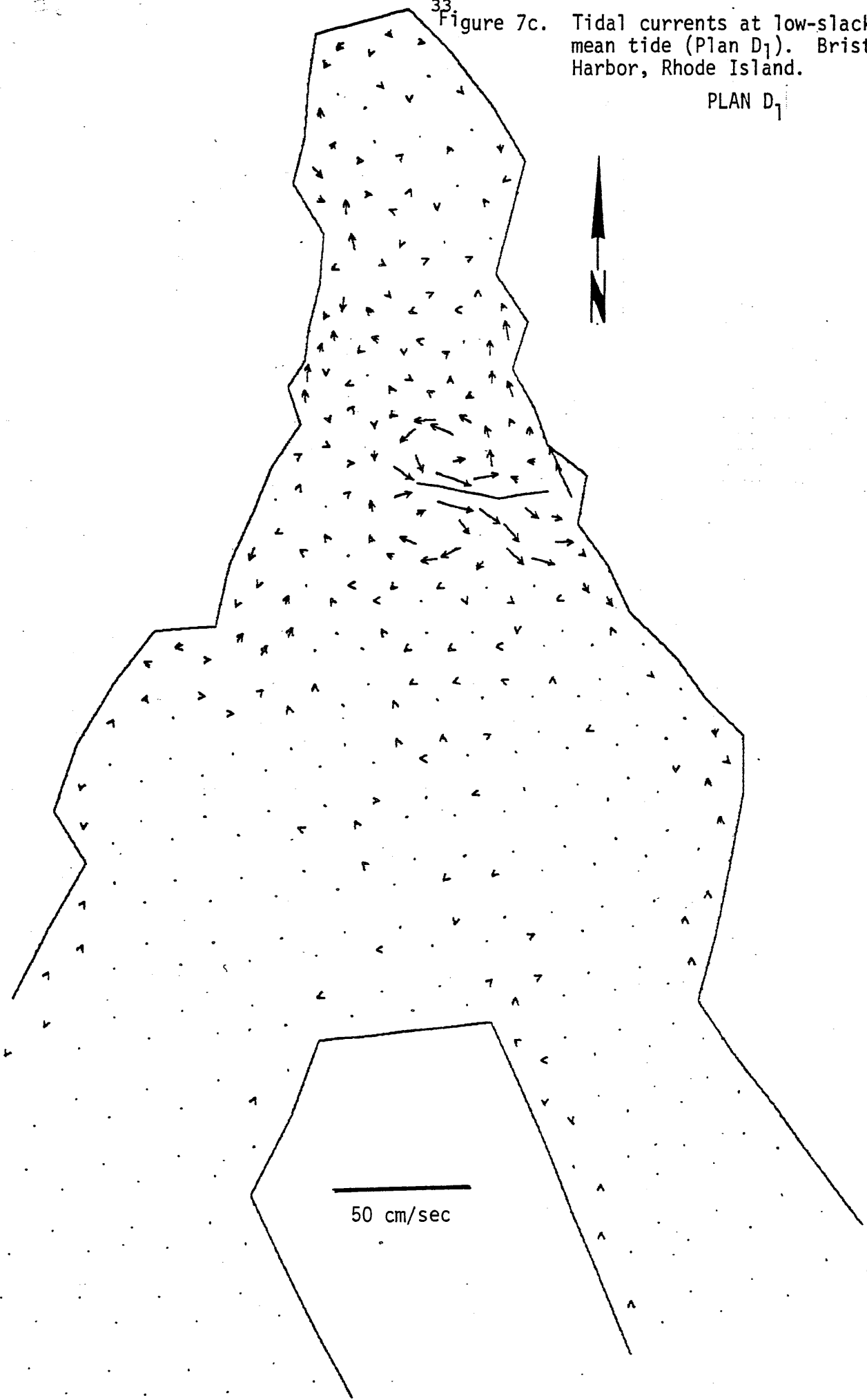
Figure 7b. Tidal currents at low-slack for mean tide (Plan A). Bristol Harbor, Rhode Island.

PLAN A



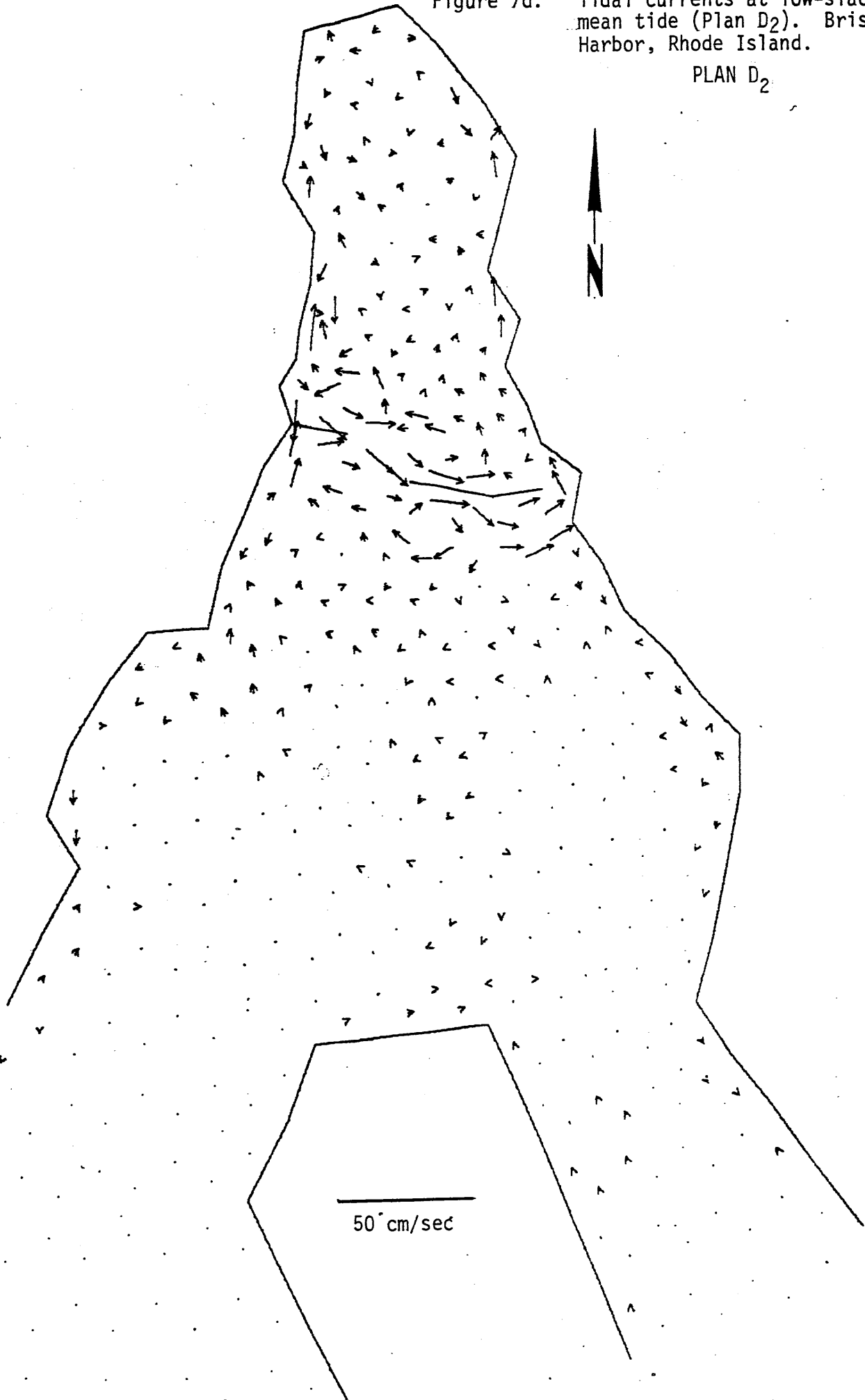
33. Figure 7c. Tidal currents at low-slack for mean tide (Plan D₁). Bristol Harbor, Rhode Island.

PLAN D₁



34 Figure 7d. Tidal currents at low-slack for mean tide (Plan D₂). Bristol Harbor, Rhode Island.

PLAN D₂



Flood Tide (t = 44,640 seconds)

As the time of the mid-flood tidal phase draws near, the eddies again begin to lose both speed and organization (Figure 8b, c, d). Peak speeds during mid-flood are comparable to those during mid-ebb. As flooding continues, the eddies reorganize, reversing in their direction of rotation from the first half of the flood phase and increase in speed.

High Slack Water (t = 66,800 seconds)

The largest eddy speeds occur an hour before and after slack water. As before during low slack water, the eddies remain organized but decrease somewhat in speed (Figure 9b, c, d). After the tide turns they grow in strength until mid-ebb again approaches. The eddies will again become disorganized. After mid-ebb they will reorganize and intensify, having again changed rotation direction.

Each breakwater has the same general effect on upper harbor circulation although the current speeds and the number of eddies formed vary. Maximum eddy velocities occur about an hour before and after slack water. During slack water the eddies remain organized but currents decrease in speed somewhat. During the mid-ebb and mid-flood the eddies become disorganized and have minimum current speeds. The eddy rotation directions reverse as they reorganize after the midpoint is passed. A complete set of tidal height and tidal current figures have been included as Appendices I and II, respectively.

Breakwater A, which provides for the widest openings into the upper harbor, has peak currents in each passage of only about 11 cm/sec. Breakwater D₁ with its constricted east passage can develop peak speeds in both passages of about 11 to 13 cm/sec. Breakwater D₂, which restricts flow into the inner harbor the most of all three designs also exhibits speeds in the eastern passage of 11 to 13 cm/sec, but in the western passage between the two breakwaters, speeds peak at 20 to 25 cm/sec.

Figure 8b. Tidal Currents at mid-flood for mean tide (Plan A).
Bristol Harbor, Rhode Island.

PLAN A

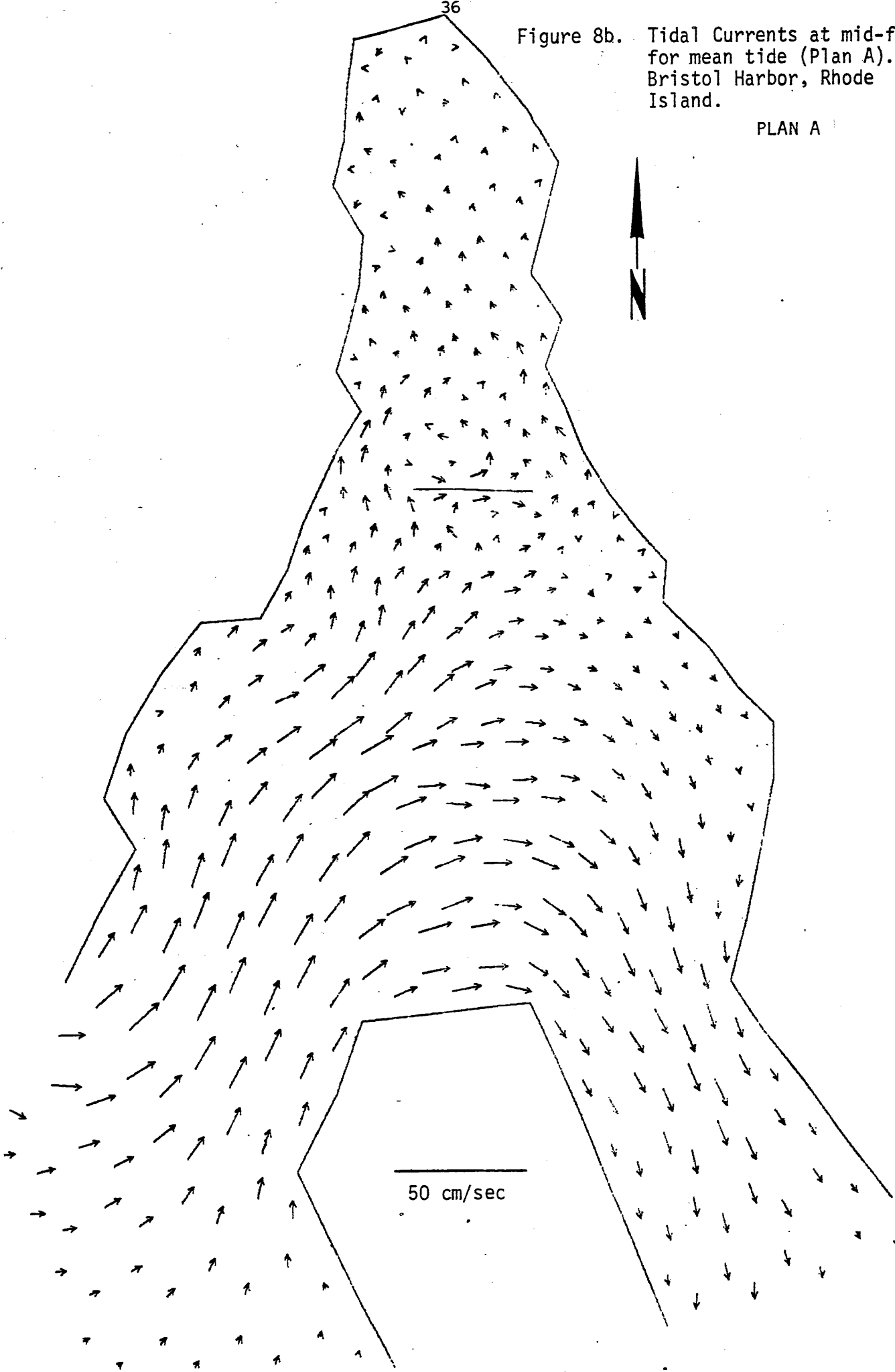


Figure 8c. Tidal currents at mid-flood for mean tide (Plan D₁).
Bristol Harbor, Rhode Island.

PLAN D₁

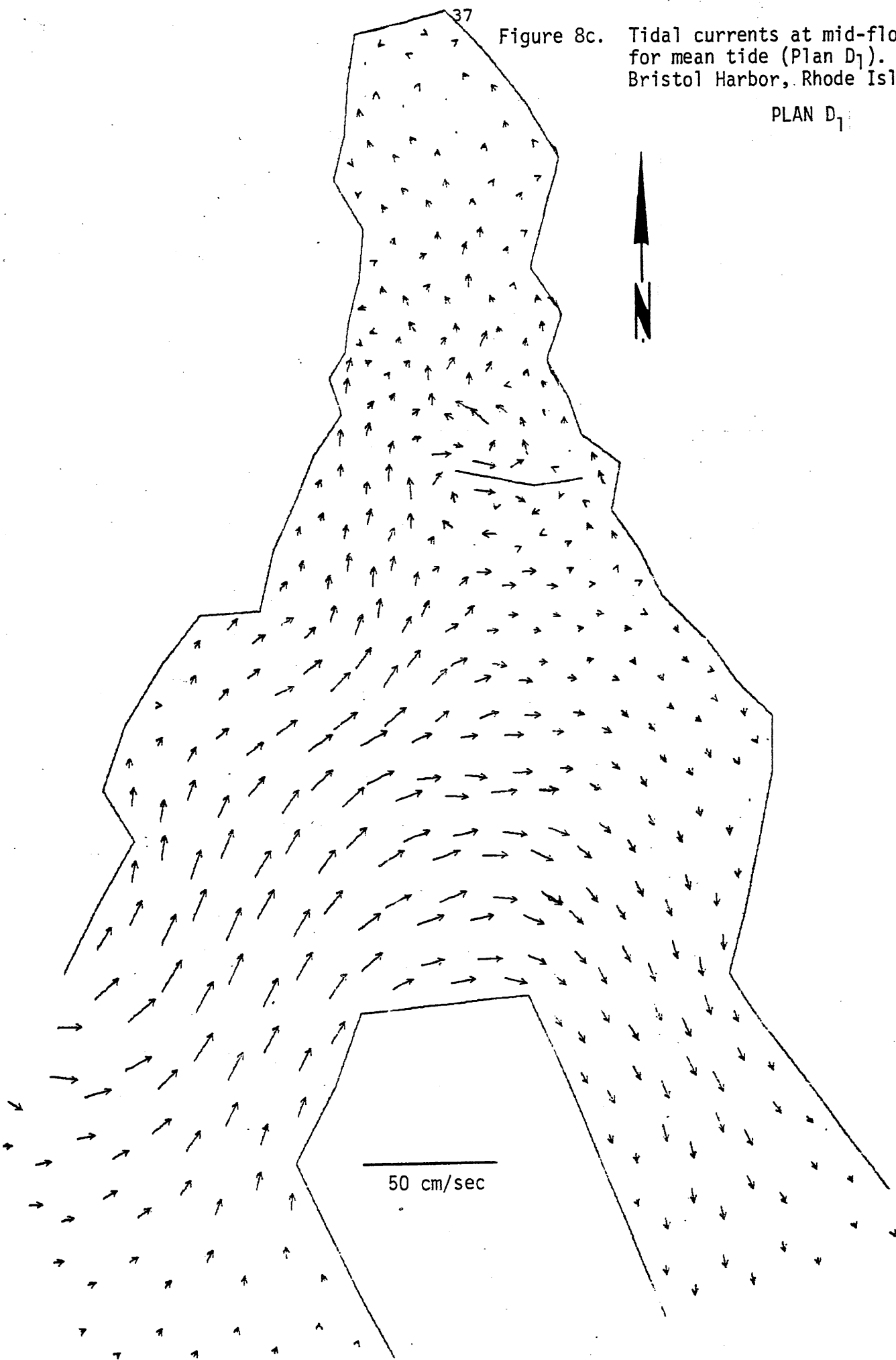


Figure 8d. Tidal currents at mid-flood for mean tide (Plan D₂).
Bristol Harbor, Rhode Island.

PLAN D₂

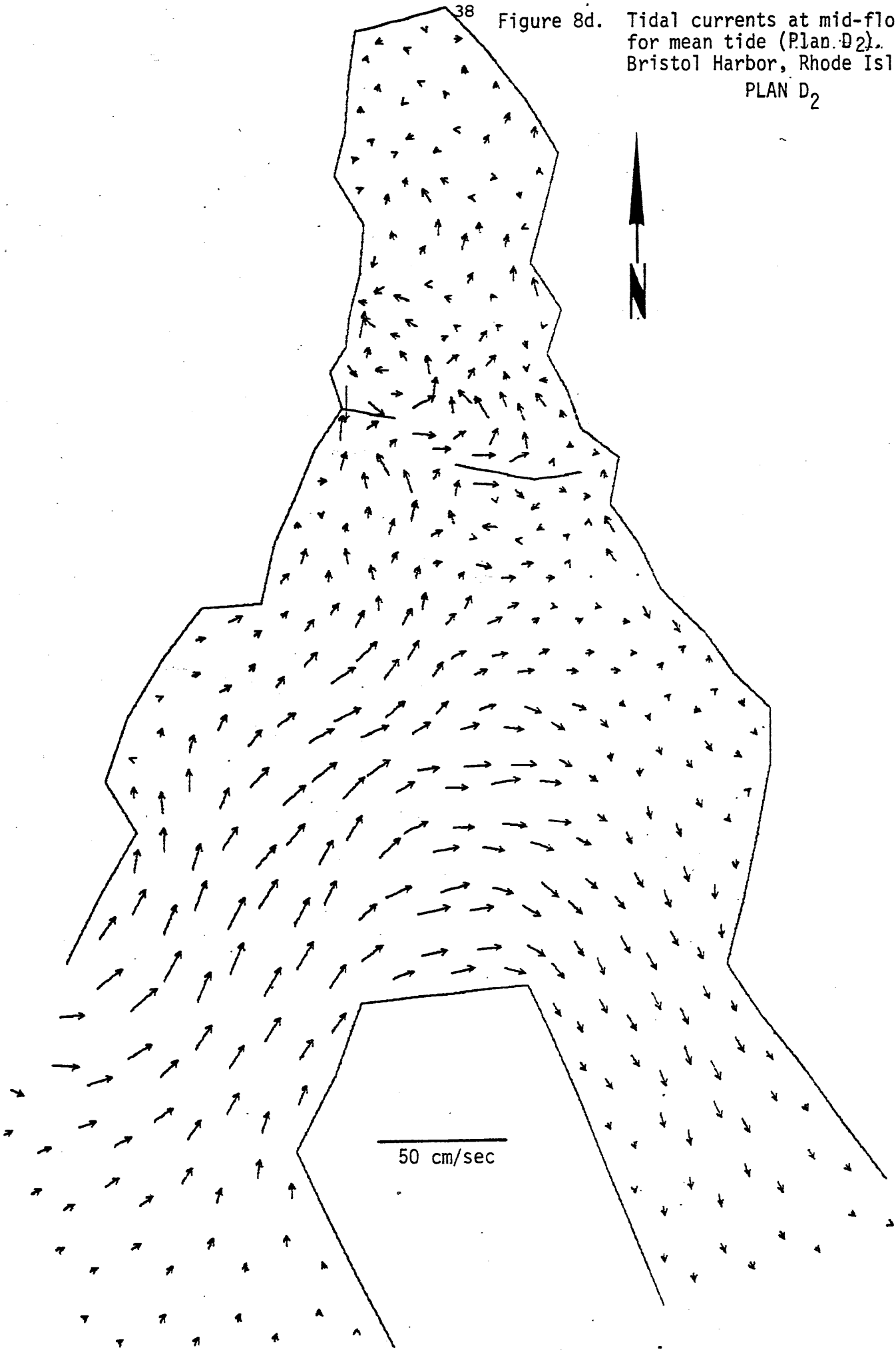


Figure 9b. Tidal currents at high-slack for mean tide (Plan A).
Bristol Harbor, Rhode Island.

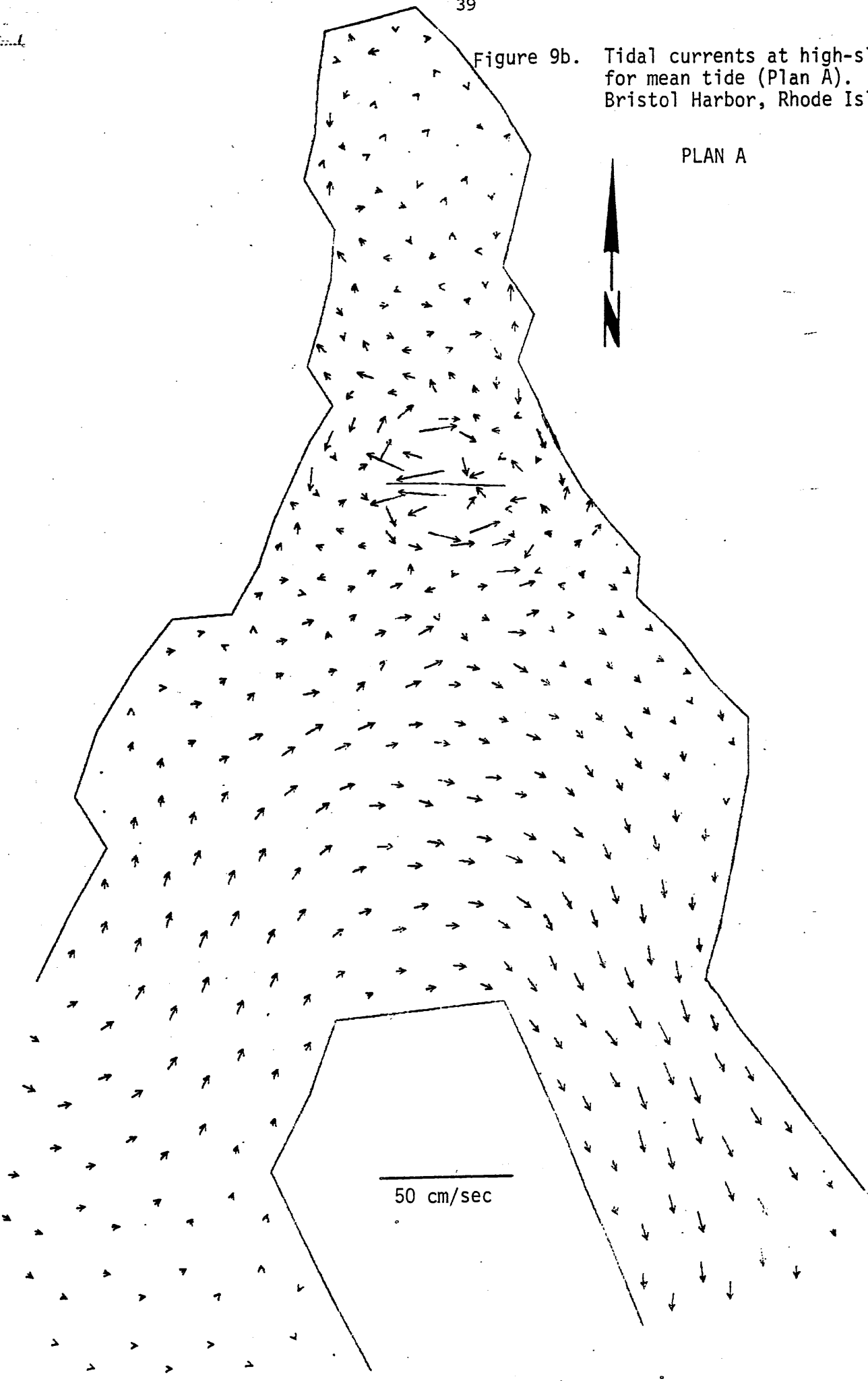


Figure 9c. Tidal currents at high-slack for mean tide (Plan D1).
Bristol Harbor, Rhode Island.

PLAN D₁



50 cm/sec

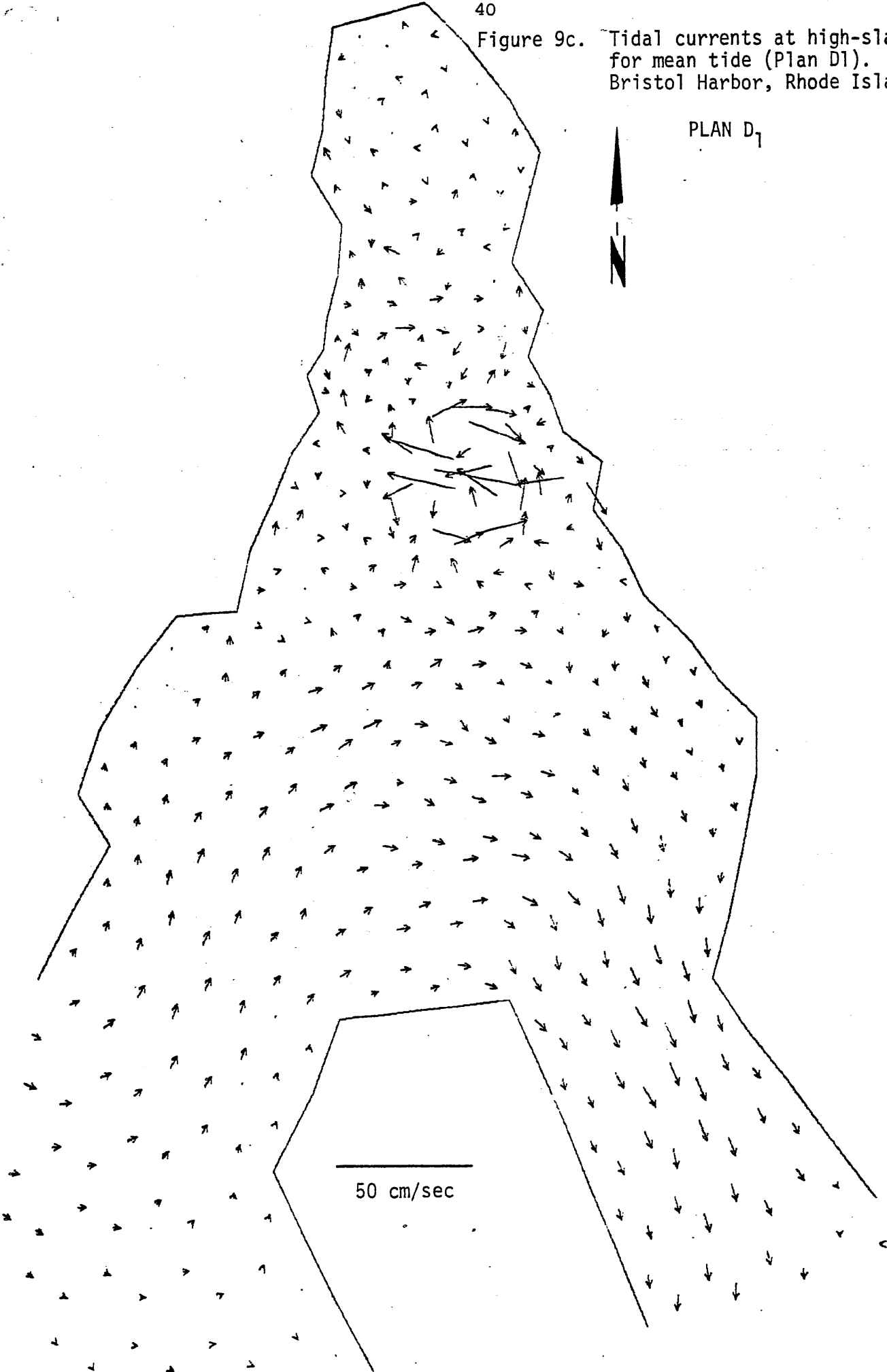
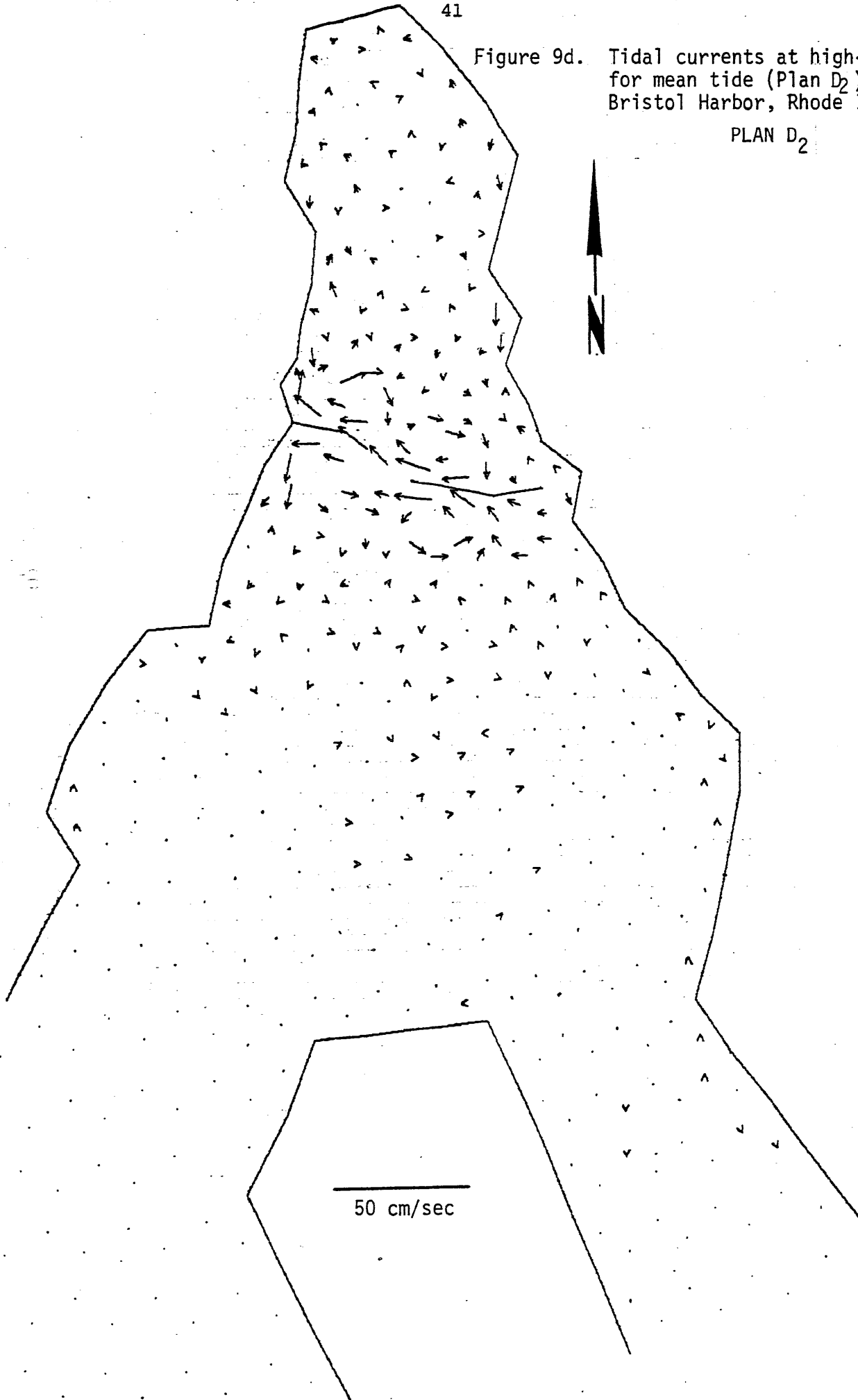


Figure 9d. Tidal currents at high-slack for mean tide (Plan D₂).
Bristol Harbor, Rhode Island.

PLAN D₂



4.2 SIMULATED HARBOR DISPERSION

The DISPER model was also run for two conditions in Bristol Harbor, spring tide and mean tide, for each of four cases: present conditions, Plan A, Plan D₁ and Plan D₂. The required initial conditions, boundary conditions and input parameters were discussed in a prior section. The time step was again 12 seconds. Required velocity input values were obtained from stored results from the CAFE model.

The program was run for six tidal cycles (t = 22,320 sec to t = 290,160 sec) to allow a quasi-steady state to develop. Results over the first four tidal cycles (t = 22,320 sec to t = 200,800 sec) were printed and plotted every three hours. Using the final results at initial conditions, one program was run for an additional two tidal cycles (t = 22,320 sec to t = 111,600 sec) to yield hourly printouts and plots of results. Concentration units are mass per unit volume which is grams per cubic meter in the metric system. Since the numbers are of the order of 10⁻¹, plotted values were scaled up by a factor of 10⁴. The unit on the plot values were therefore 10⁻⁴ gm/m³. For the sake of convenience, no units will be explicitly used within the discussion with the understanding that the above unit of measure is implied. In addition, the plotted concentration values have been reduced to a series of contour plots for ease of comparison. Only the mean tidal concentrations have been contoured for each of the four tidal cycle phases used in the discussion of currents. Like the current patterns, there is little discernable difference between dispersion during the mean tide and during the spring tide for each configuration.

4.2.1 Existing Dispersion Pattern

The primary force moving suspended and dissolved material with Bristol Harbor are the tidal currents generated by the M₂ tides. Several sources have been identified and simulated within the dispersion model. The primary source, the sewage treatment plant discharge into Walker Cove, is a constant feature over all tidal phases and all configura-

tions. This can be identified by the area within the 700-contour in the accompanying figures. This is the maximum size contour used, since any higher valued-contours would be within this one. Central values in this area range from about 850 to 1100. Contours were arranged in increments of 100 from 0 to 700. Source points are marked by X's.

The following description of existing dispersion patterns is primarily confined to upper harbor where we expect breakwater effects to be the greatest.

Mid-ebb (t = 66,960 seconds)

Most of the area of the upper harbor is contained within the 400-contour at mid-ebb. A smaller percentage is within the 300-contour (Figure 10a).

Low-slack (t = 78,120 seconds)

The upper harbor concentrations change proportions during low-slack water. Most of the area contained within the 300-contour. The area of the 400-contour has shrunk and lies along a portion of the eastern shore. The small pocket of water enclosed by the 400-contour and the leading edge of the larger area likewise enclosed mark the industrial source locations (Figure 11a).

Mid-flood (t = 44,640 seconds)

A portion of the water within the 300-contour remains within the upper harbor (marked as <400) at mid-flood. However, water with the 400-contour is again beginning to dominate the upper harbor area (Figure 12a).

High-slack (t = 55,800 seconds)

The effects of the local industrial sources appear to dominate upper harbor concentrations during high-slack. The area is dominated by the 500-contour which encloses all three upper harbor sources. Proportionally smaller areas are enclosed by the 400- and 300-contours (Figure 13a).

Figure 10a. Concentrations at mid-ebb for mean tide (no break-water). Bristol Harbor, Rhode Island.

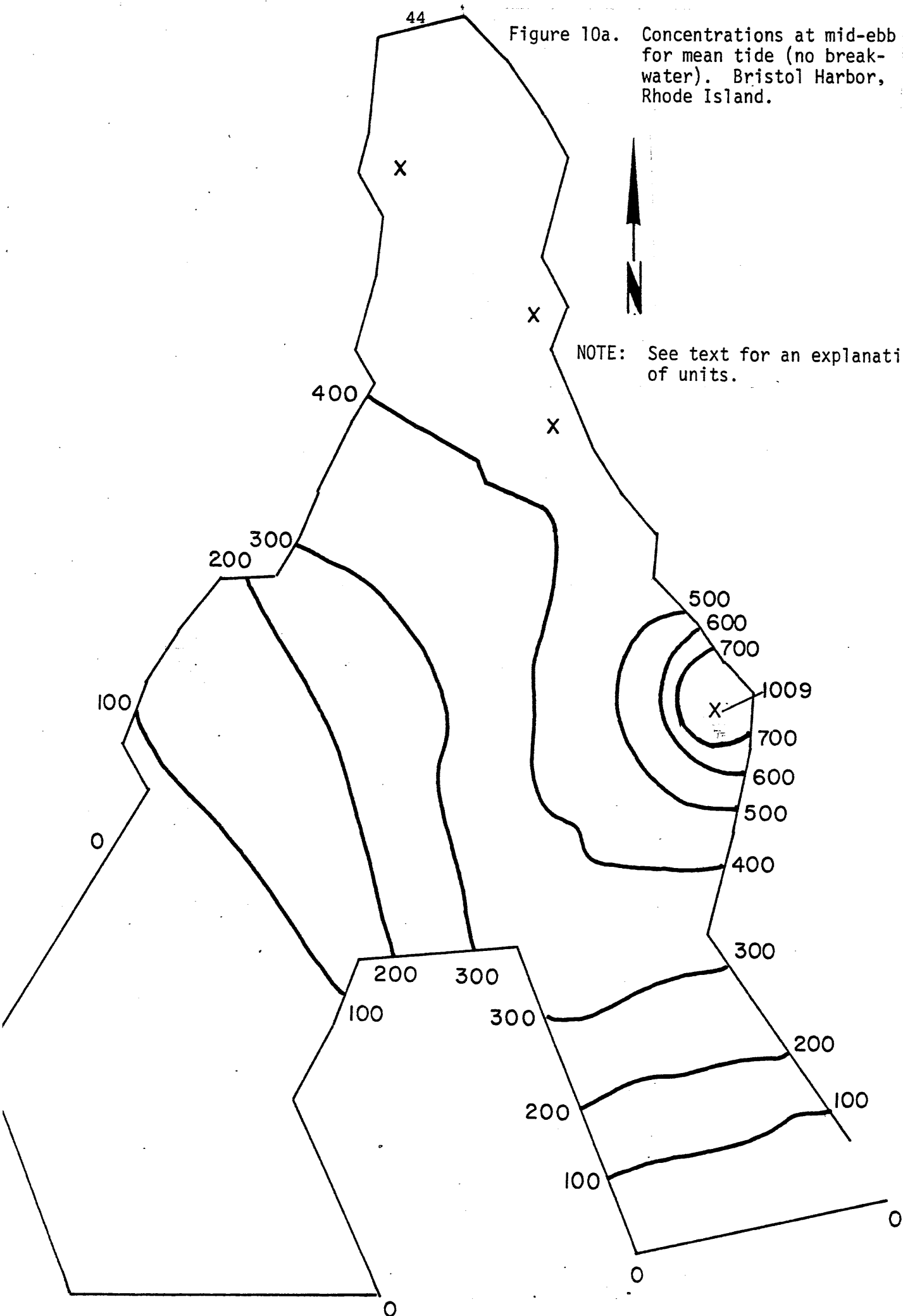


Figure 11a. Concentrations at low-slack for mean tide (no break-water). Bristol Harbor, Rhode Island.

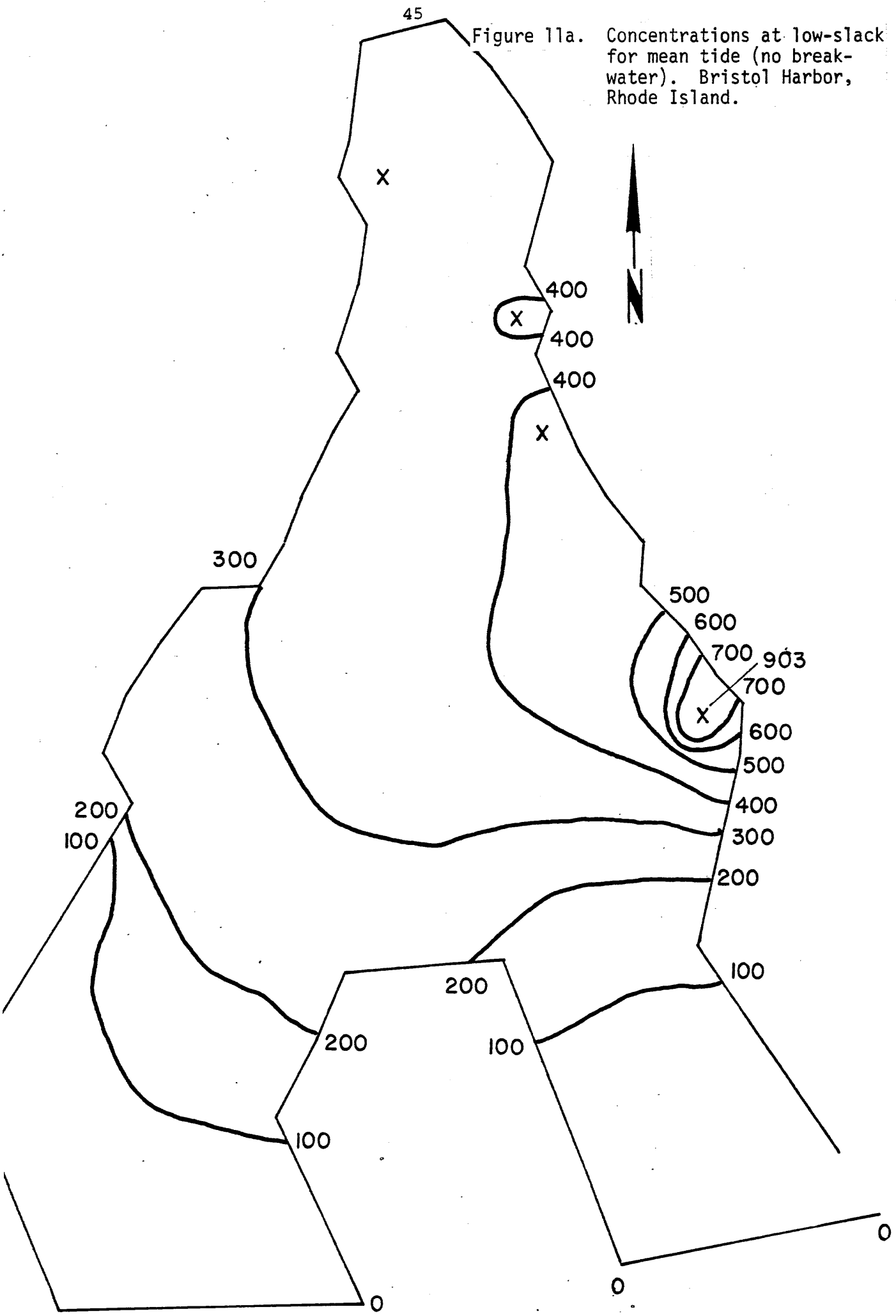


Figure 12a. Concentrations at mid-flood for mean tide (no break-water). Bristol Harbor, Rhode Island.

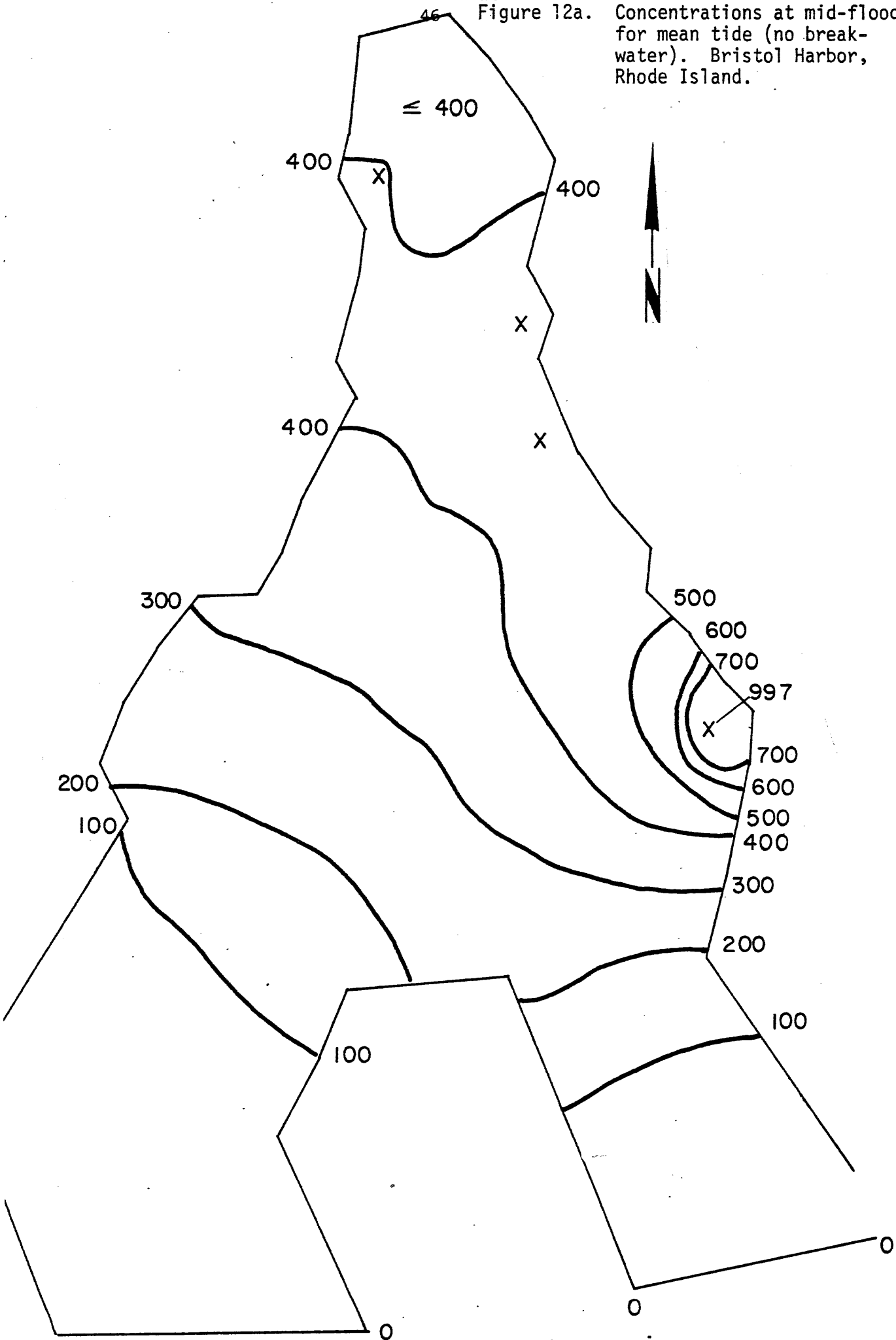
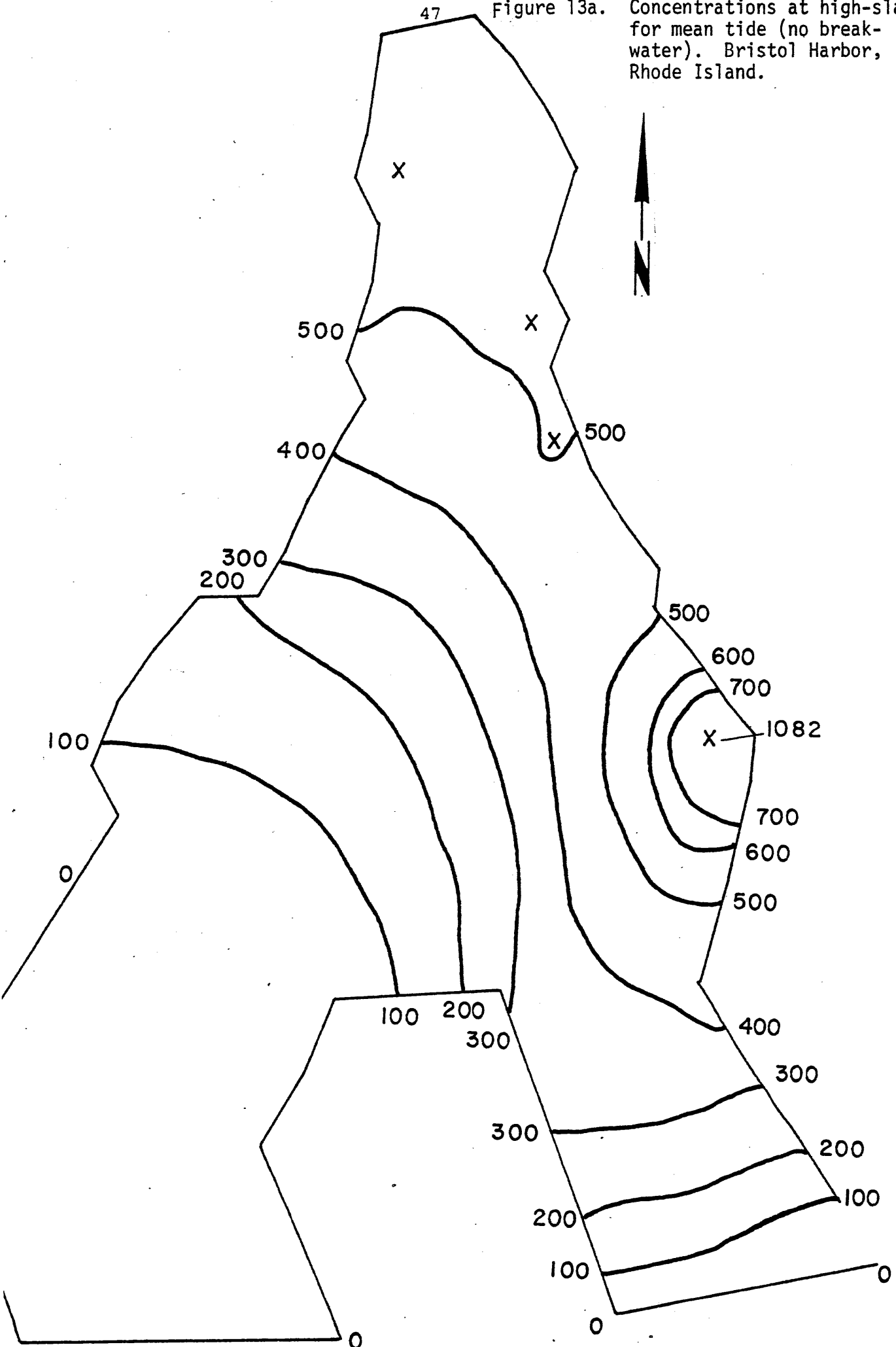


Figure 13a. Concentrations at high-slack for mean tide (no break-water). Bristol Harbor, Rhode Island.



After the tide changes, the area with the 500-contour is gradually reduced so that again by mid-ebb (Figure 10a), that area has disappeared.

An interesting pattern emerges here. The highest overall concentrations occur during highslack water in the upper harbor, and the lowest during low slack. The major source located in Walker Cove dominates the dispersing pattern of the entire harbor. The effects of the secondary sources become very evident during slack water periods.

4.2.2 Breakwater Effects on Dispersion Patterns

The breakwaters appear to have a significantly discernible effect on the dispersion patterns which is not surprising in light of the breakwater effect on the circulation patterns. The simulated effects during each phase of the tidal cycle are discussed below.

Mid-ebb (t = 66,960 seconds)

The circulation patterns (Figure 10b, c, d) during this phase superficially resemble those for no breakwater (Figure 10a). For all three designs, the largest area is enclosed by the 400-contour, followed by the 300-contour as a poor second. Interesting features to note are small pockets enclosed by the 500-contour north of the dog-leg breakwater in Plans D₁ and D₂ (Figure 10c, d).

Low-slack (t = 78,120 seconds)

Plan A and D₁ patterns (Figure 11b, c) better resemble existing conditions in the upper harbor during low slack water. Most of the area is enclosed by the 300-contour, with an isolated patch enclosed by the 400-contour adjacent to the industrial shore area. Dispersion in Plan D₂ (Figure 11d) shows much larger areas enclosed by 400-contour. A small patch of water within the 400-contour with values from 300 to less than 400 dominates the small opening

Figure 10b.

Concentrations at mid-ebb
for mean tide (Plan A).
Bristol Harbor, Rhode Island.

PLAN A

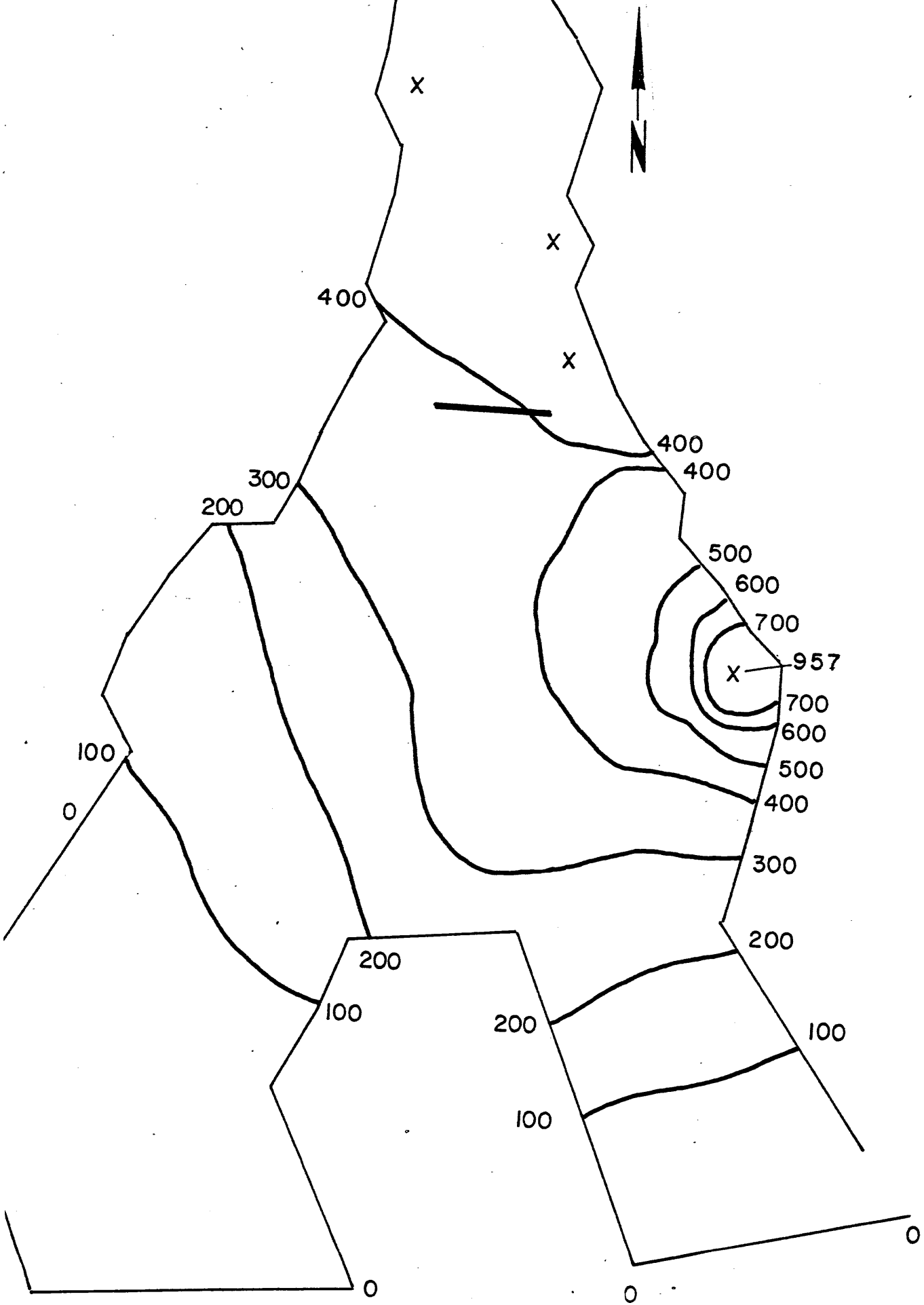
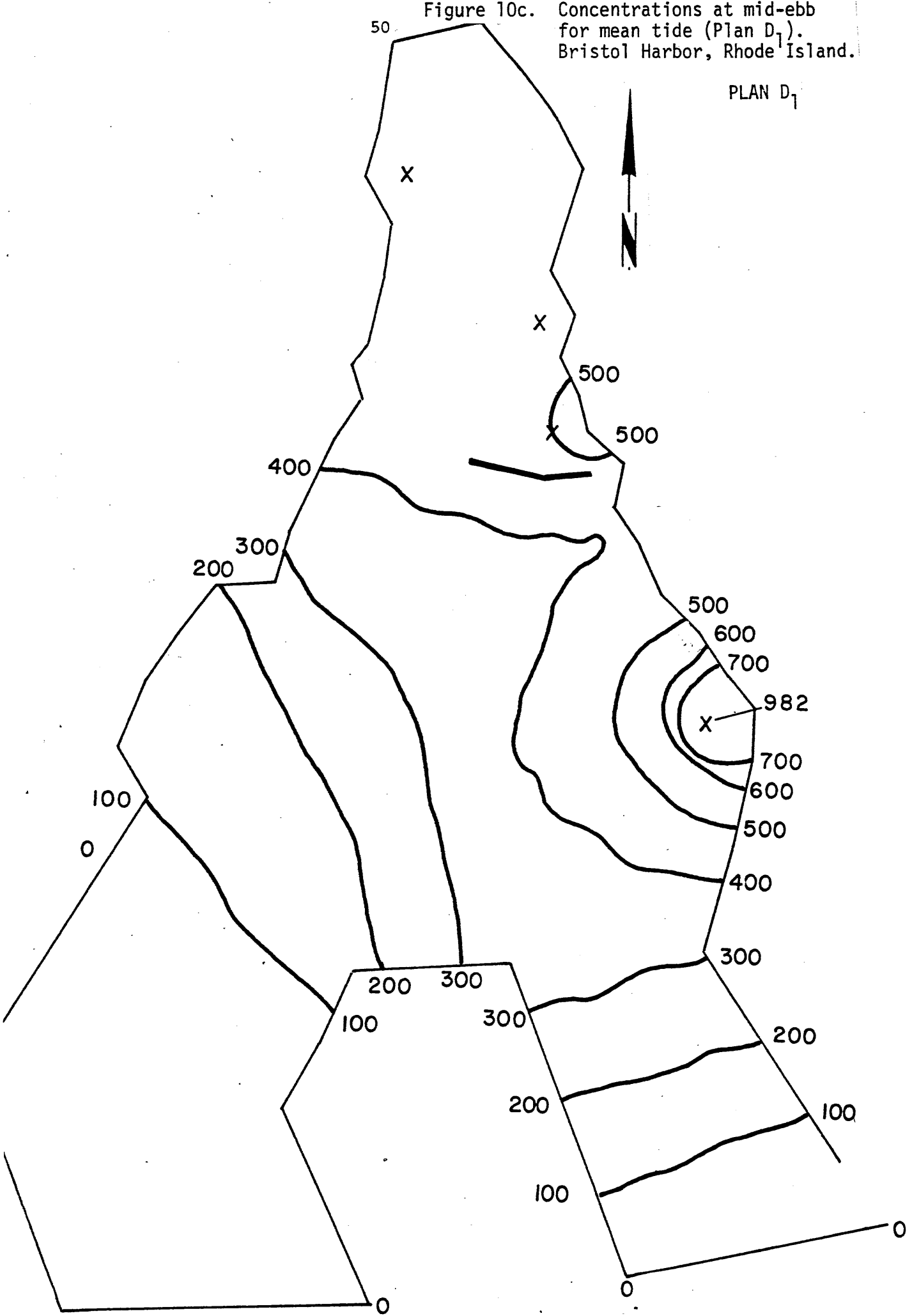


Figure 10c. Concentrations at mid-ebb for mean tide (Plan D₁).
Bristol Harbor, Rhode Island.



51

Figure 10d.

Concentrations at mid-ebb
for mean tide (Plan D₂).
Bristol Harbor, Rhode Island.

PLAN D₂

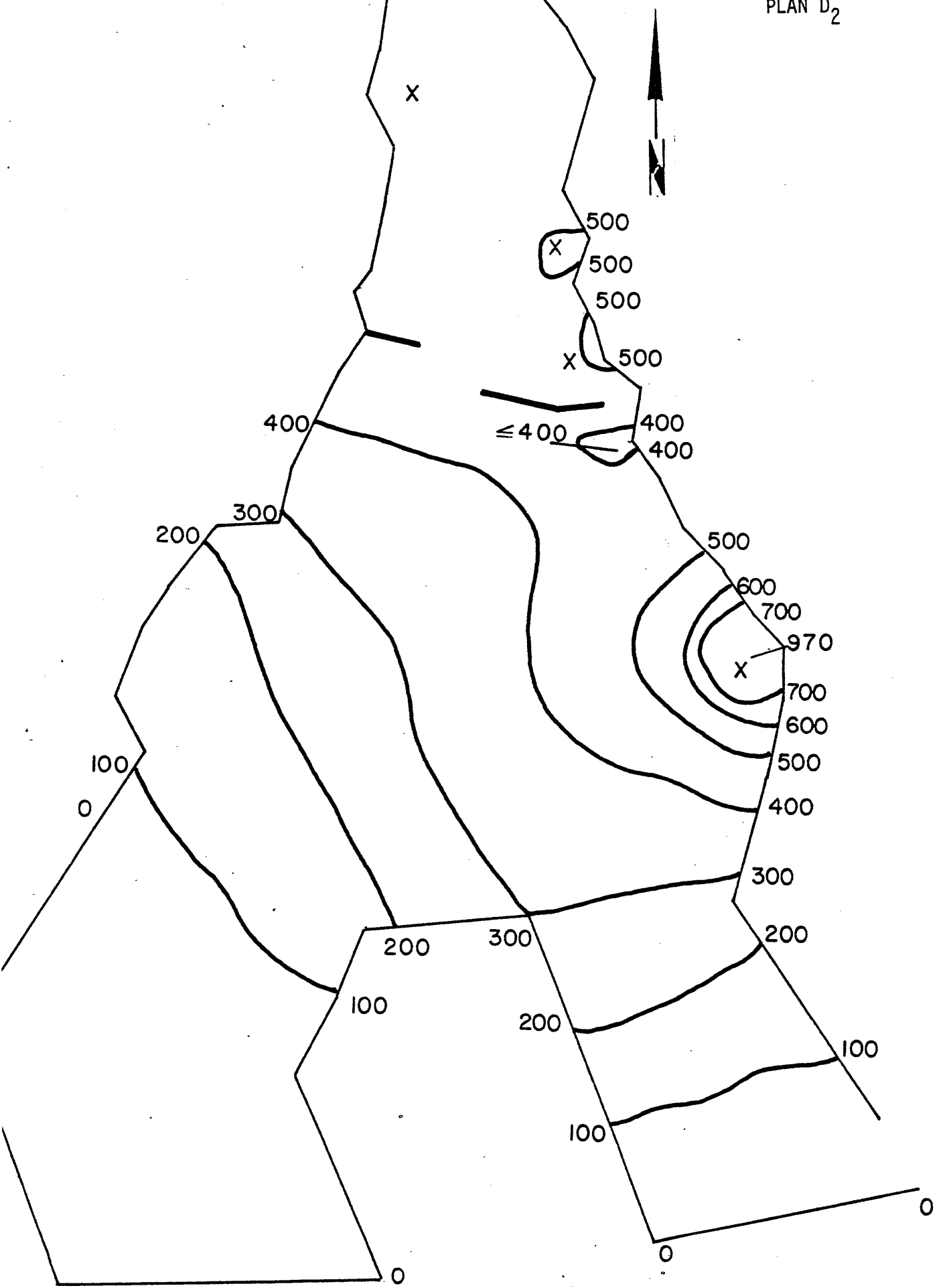


Figure 11b. Concentrations at low-slack for mean tide (Plan A).
Bristol Harbor, Rhode Island.

PLAN A

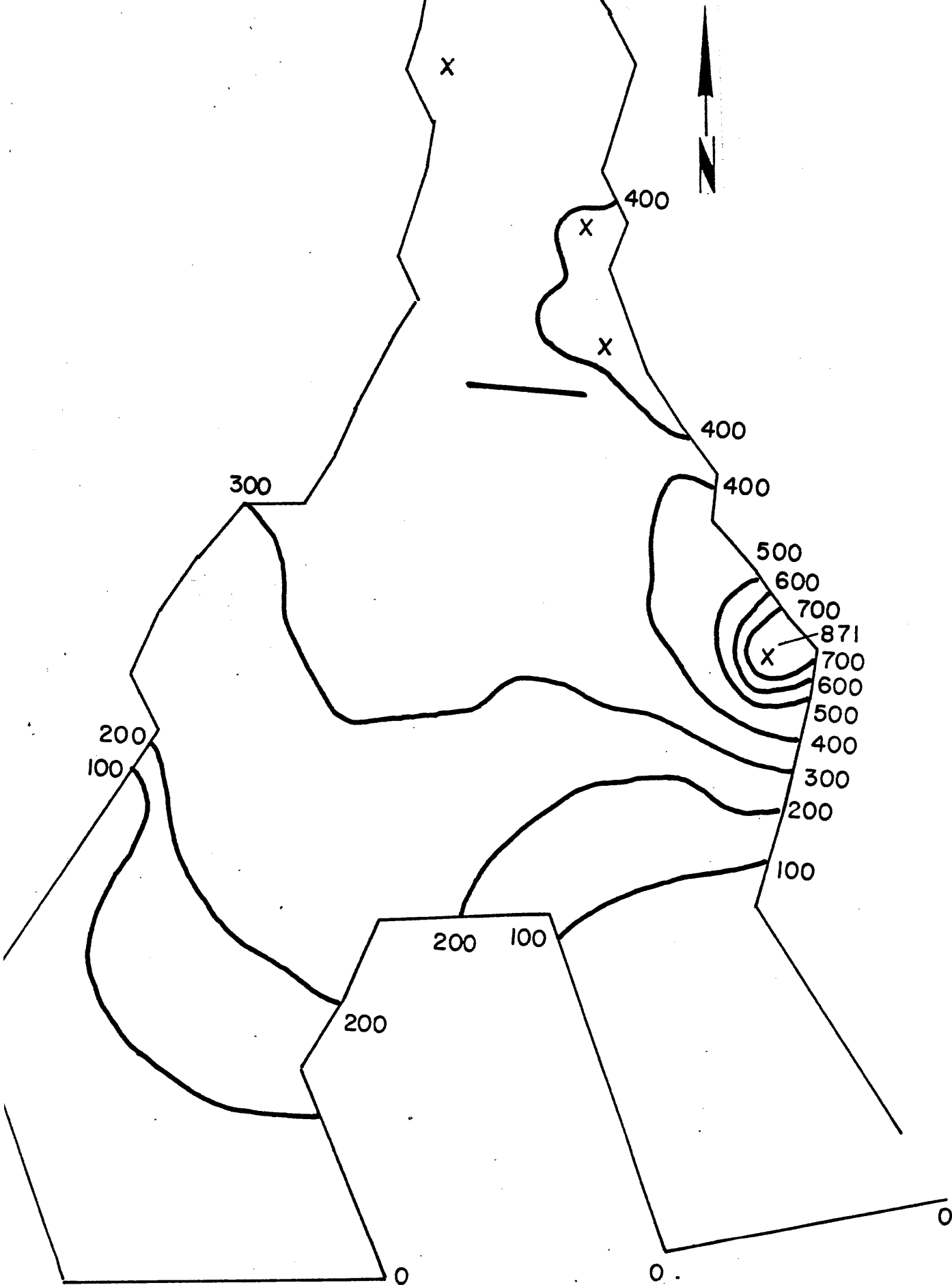


Figure 11c. Concentrations at low-slack for mean tide (Plan D₁).
Bristol Harbor, Rhode Island.

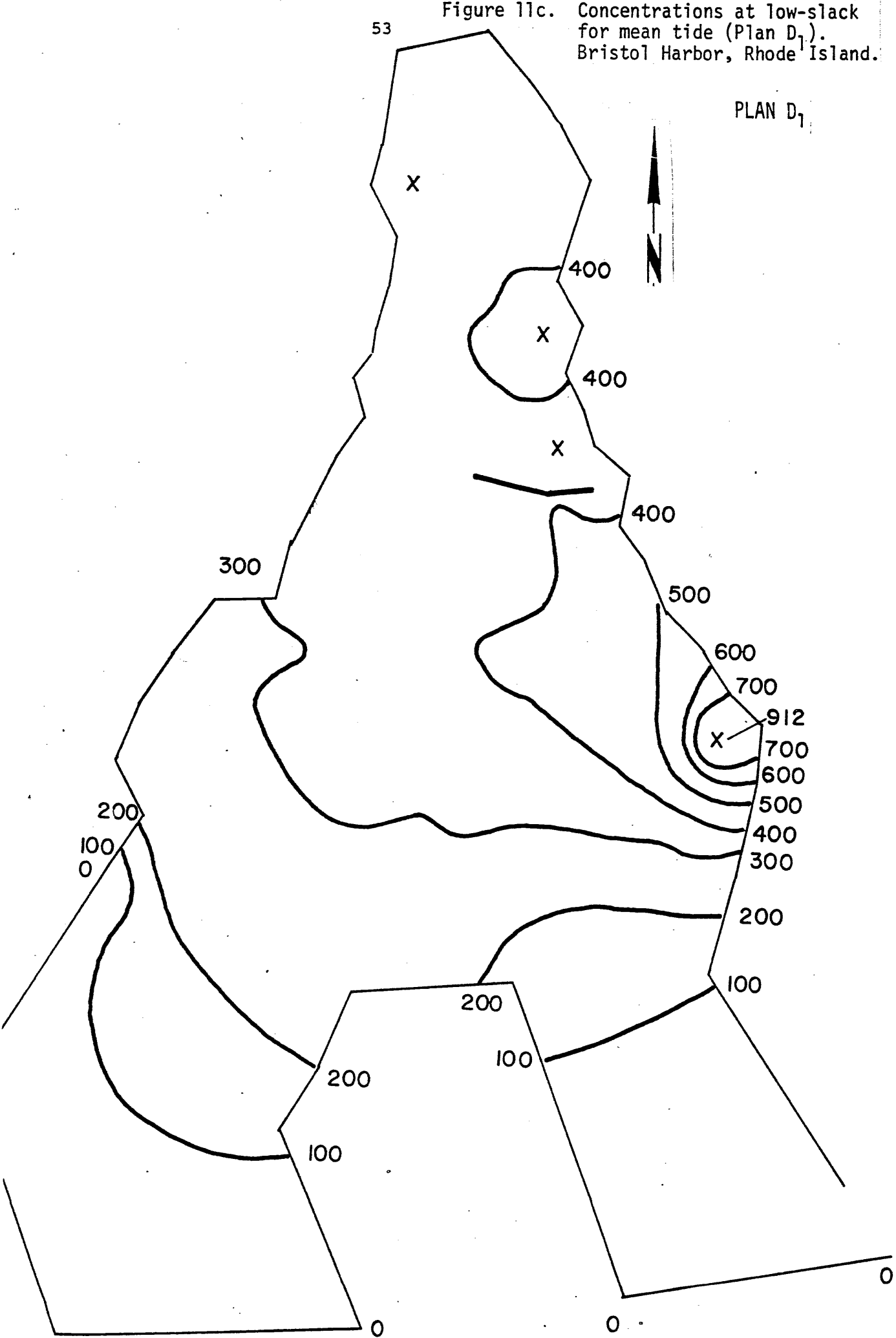
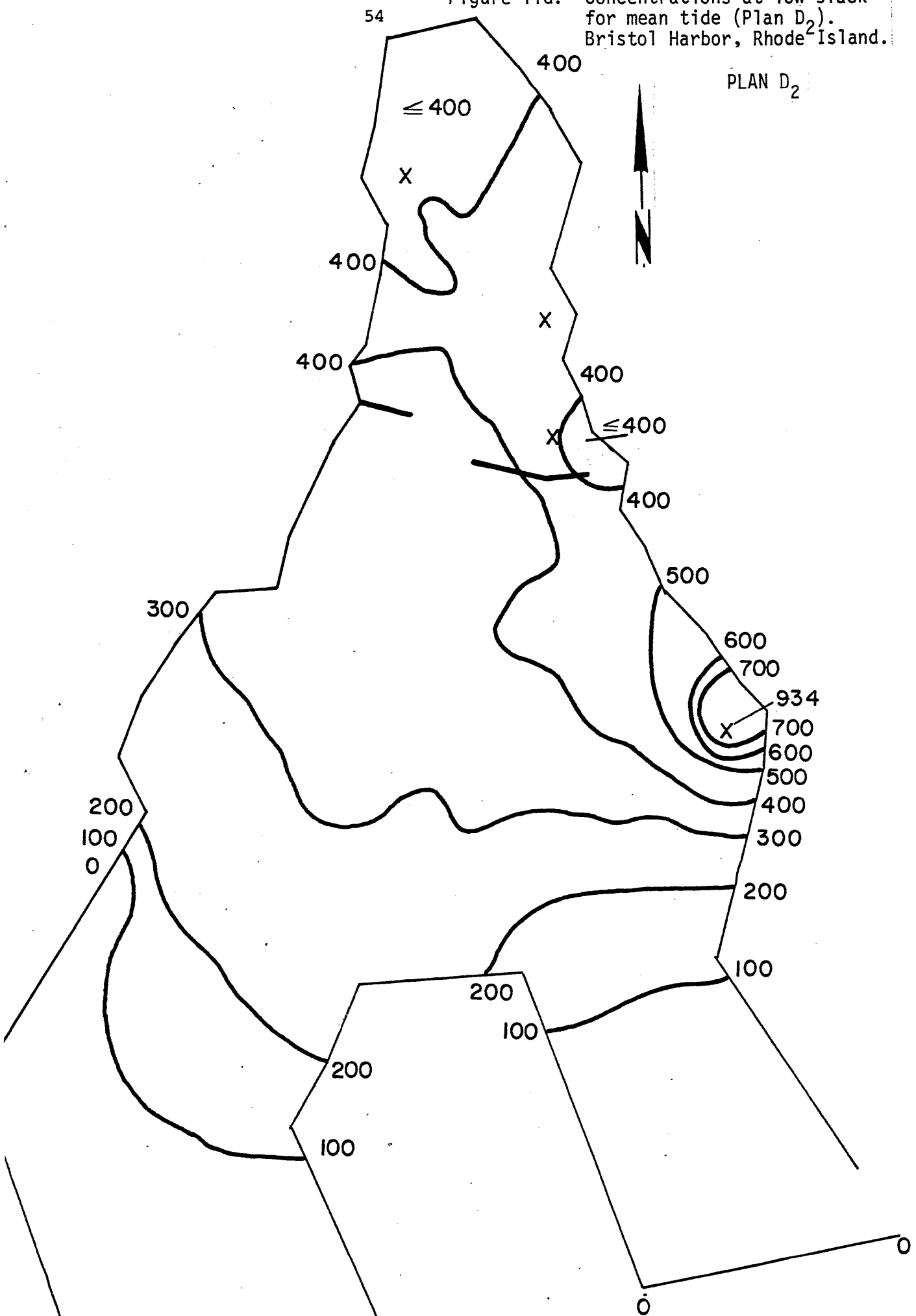


Figure 11d. Concentrations at low-slack for mean tide (Plan D₂).
Bristol Harbor, Rhode² Island.



between the dog-leg breakwater and the shore while a larger patch dominates the northern portion of the upper harbor. This development of isolated water masses appears to be due to the eddy circulation and the location of the industrial sources.

Mid-flood (t = 44,640 seconds)

Comparatively speaking, patterns during mid-flood least resemble each other except that the upper harbor is dominated by an area within the 400-contour. Small patches enclosed by the 500-contour and by the 400-contour of less than 400 appear in the dispersion of Plans A and D₁ (Figure 12b, c). Dispersion in Plan D₂ exhibits no patches, but a simple overall dominance of area within the 400-contour in the upper harbor (Figure 12d).

High-slack (t = 55,800 seconds)

Dispersion patterns of Plans A and D₁ (Figure 13b, c) again more closely resemble that of present conditions (Figure 13a). Concentration areas are dominated by the 500-contour followed by the 400-contour. Again the dispersion of Plan D₂ (Figure 13d) exhibits the least similarity with existing conditions. A small but rather noticeable patch of water enclosed by the 600-contour

appears along the northern shore of the upper harbor. And a smaller patch enclosed by the 500-contour of less than 500 has formed to the north of the short breakwater connected to the western shore. This small feature appears to be associated with the eddy-like circulation generated in this area.

Unlike the circulation patterns, the dispersion patterns for the various configurations show a greater similarity to the existing patterns. To

PLAN A

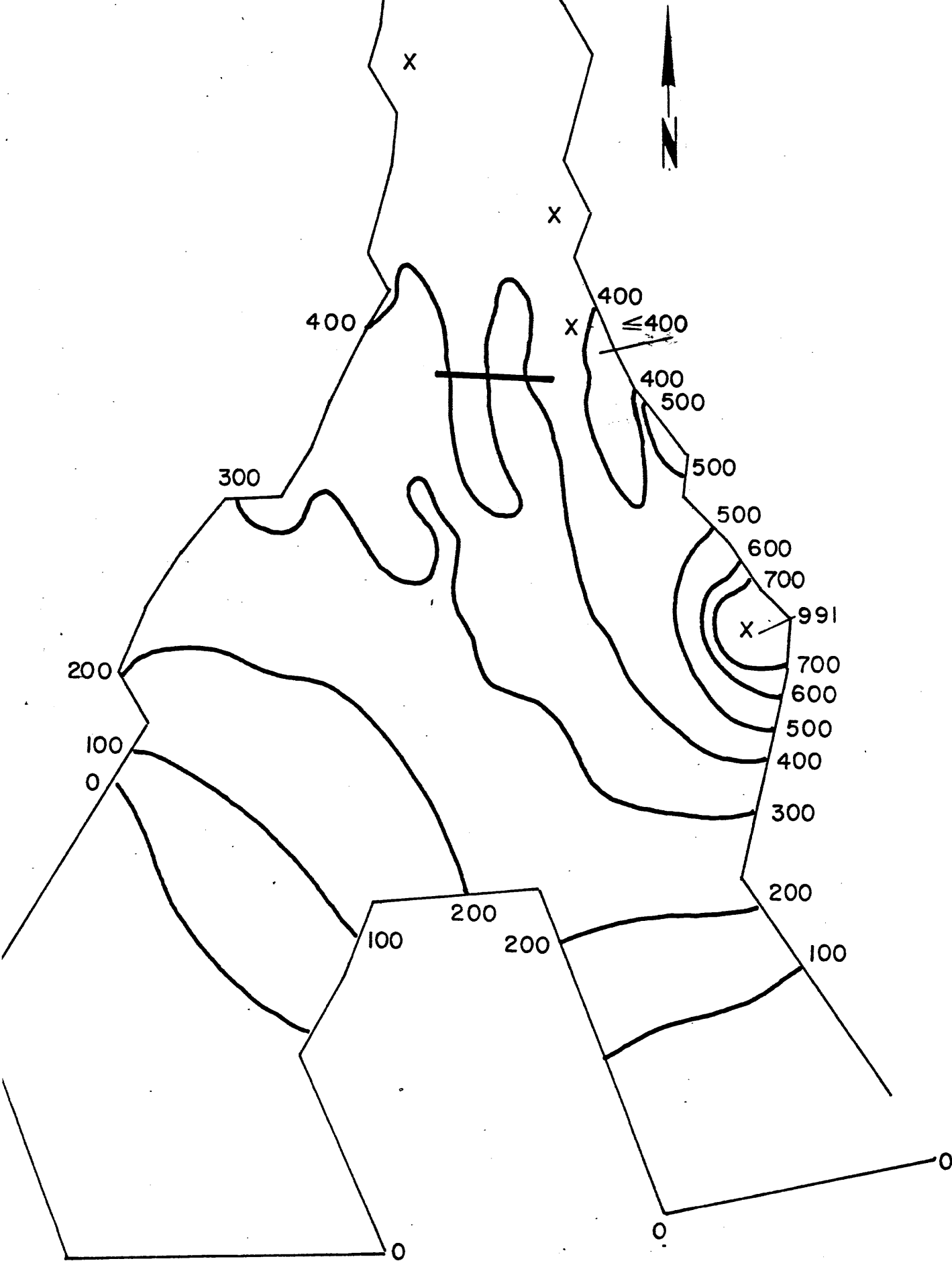


Figure 12c. Concentrations at mid-flood for mean tide (Plan D₁), Bristol Harbor, Rhode Island.

PLAN D₁

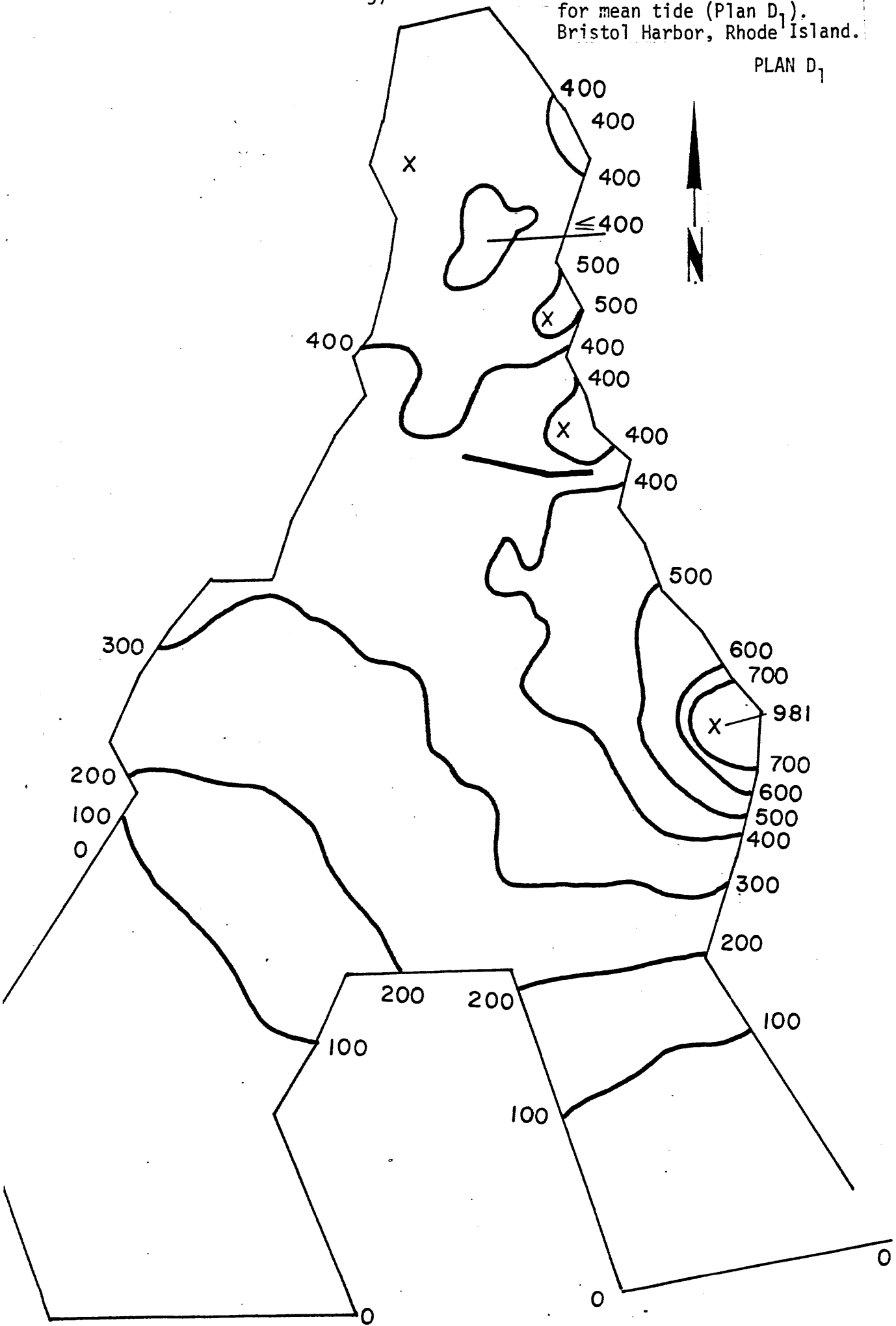


Figure 12d.

Concentrations at mid-flood
for mean tide (Plan D₂).
Bristol Harbor, Rhode² Island.

PLAN D₂

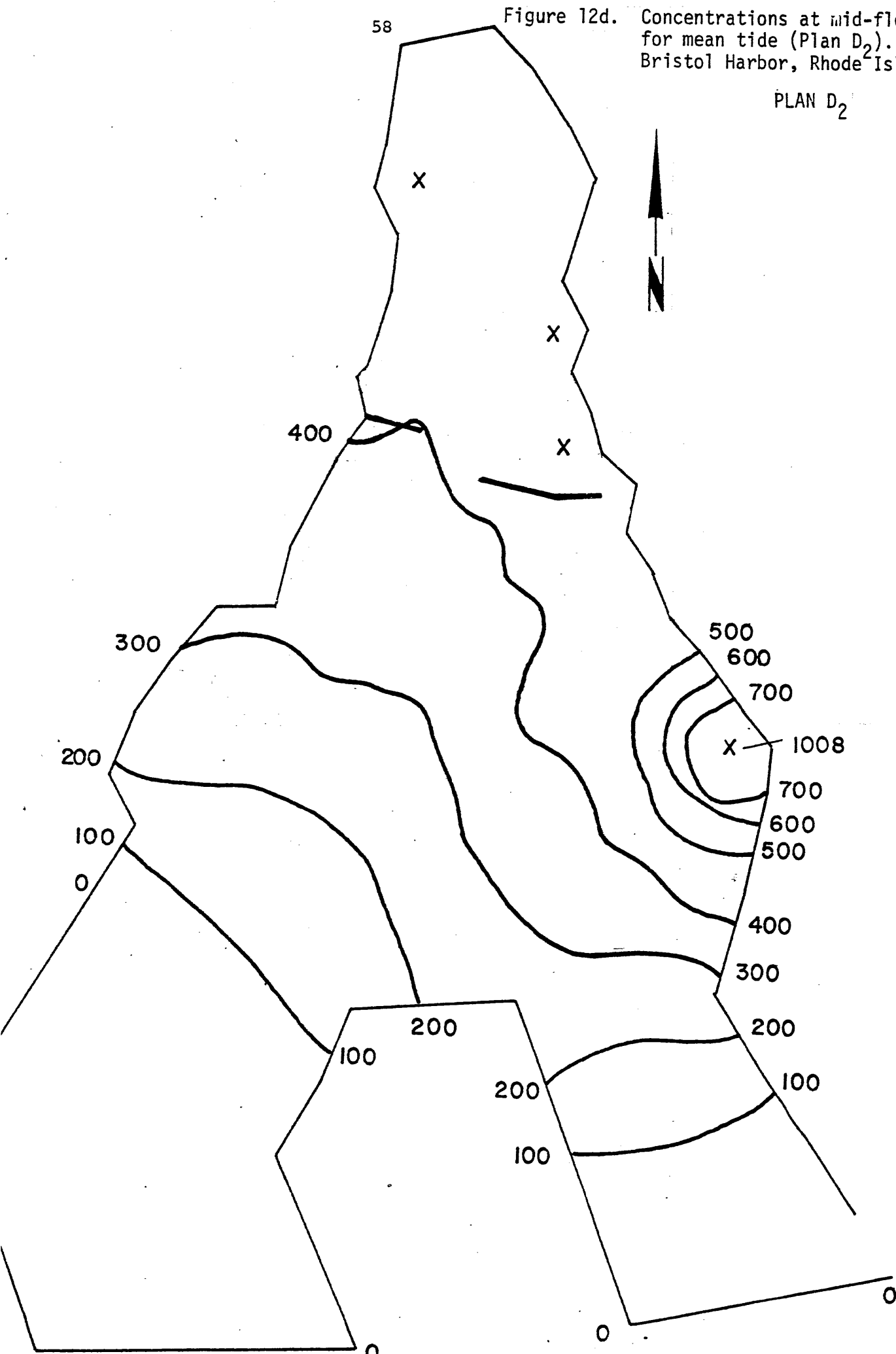


Figure 13b. Concentrations at high-slack for mean tide (Plan A).
Bristol Harbor, Rhode Island.

PLAN A

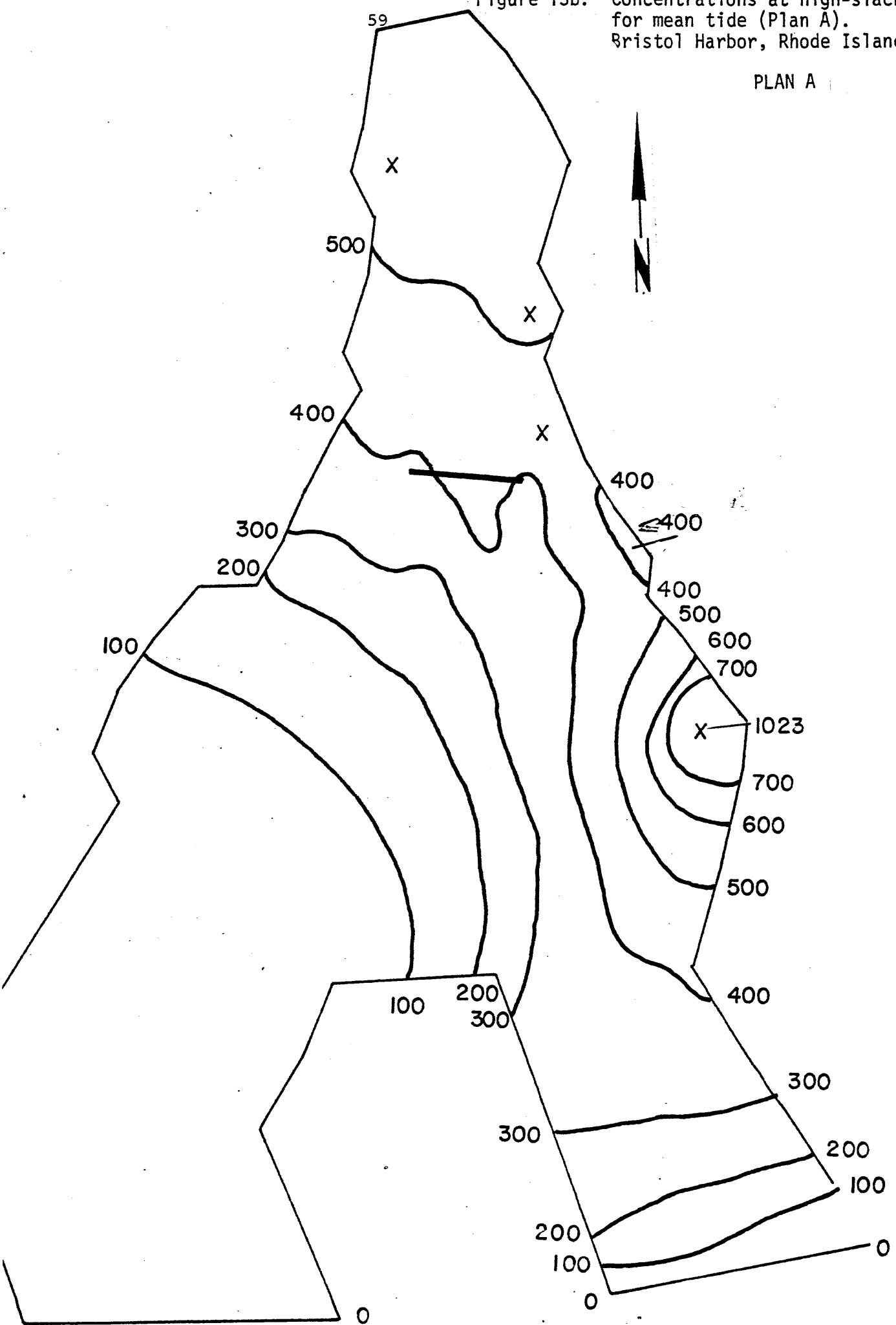


Figure 13c. Concentrations at high-slack for mean tide (Plan D₁).
Bristol Harbor, Rhode Island.

PLAN D₁

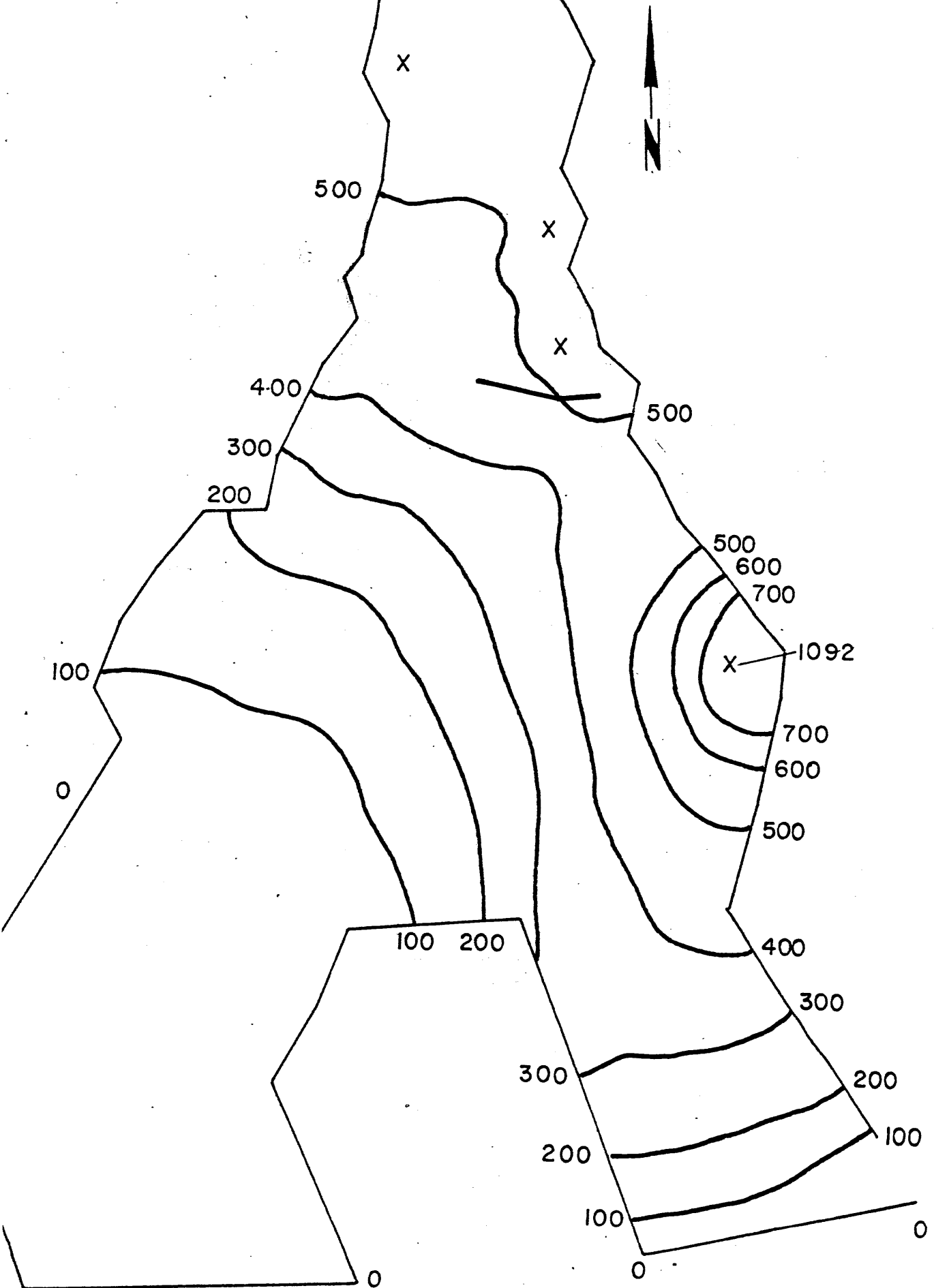
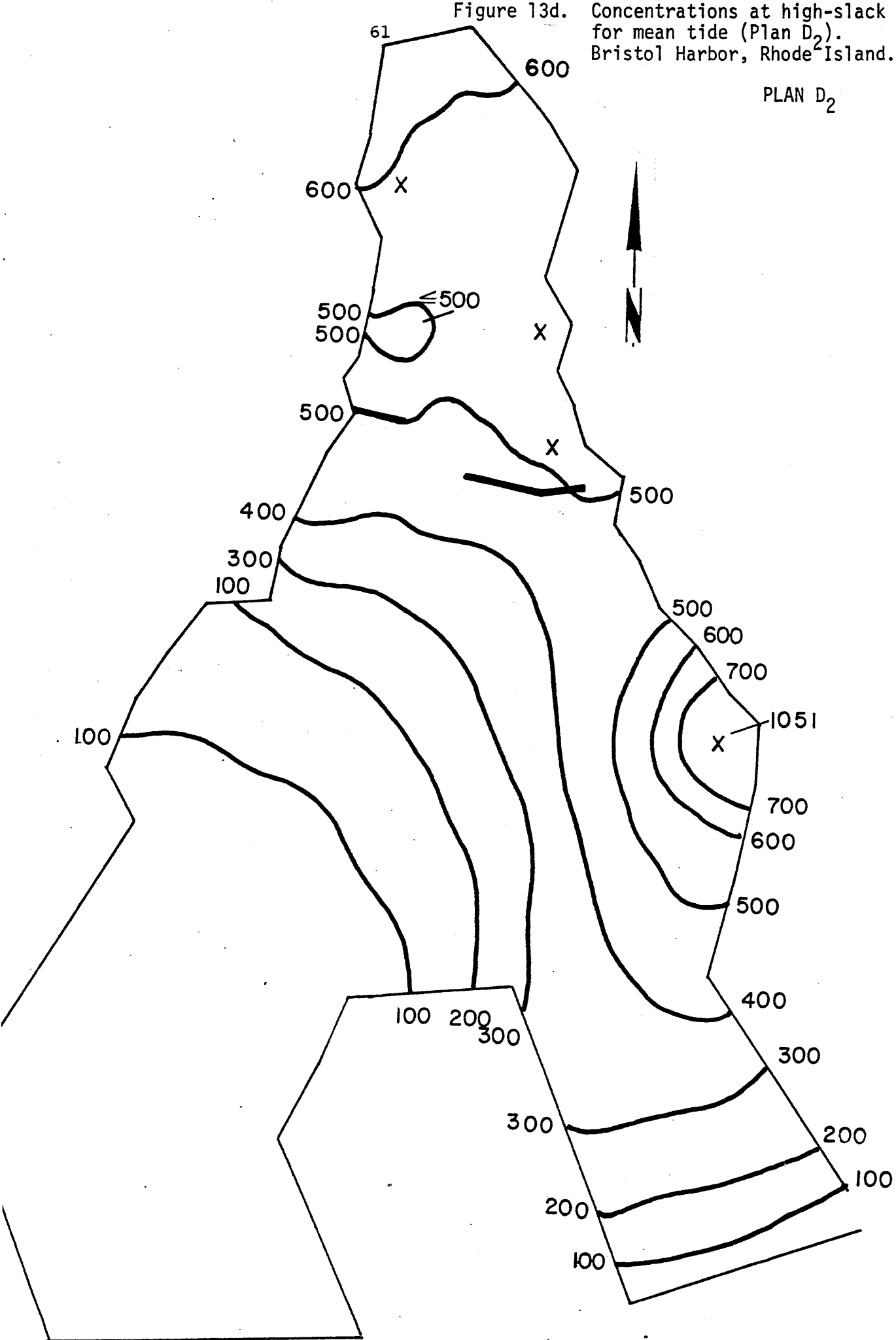


Figure 13d.

Concentrations at high-slack
for mean tide (Plan D₂).
Bristol Harbor, Rhode²Island.

PLAN D₂



be sure there are individual variations, but it appears that Plan D₂ would have the most profound effect on harbor dispersion and circulation with respect to present patterns. In terms of the better design for dispersion either Plans A or D₁ should be used. A complete set of dispersion figures is included as Appendix III.

Flushing is important when considering the effect of pollution on benthic organisms in the upper harbor. Plans A and D₁ have dispersion patterns similar to those without a breakwater. Therefore, the impact of either Plan A or D₁ is expected to be minimal with respect to the biota since the flushing is adequate. On the other hand, Plan D₂ appears to allow a higher concentration water mass to remain in the upper harbor during a portion of the tidal cycle. This entrapment indicates a less efficient flushing of the upper harbor, and that the biota is exposed to a more polluted water mass. On the basis of flushing, either Plan A or D₁ would maintain the present water quality within the upper harbor.

5.0 WIND EFFECTS

5.1 WIND DRIVEN CIRCULATION

The three-dimensional movements of water in an estuary or harbor are governed by the Navier-Stokes and continuity equations. When the equations governing a system are known, it is generally assumed that the response of the system can be accurately modeled. This is not the case with estuaries and harbors, as the equations are non-linear, and represent both deterministic and stochastic processes, which range in scale from fractions of a centimeter per second, to hundreds of kilometers and weeks or months. In addition, the forcing functions and boundary conditions are complex and not easily measured. As a result, the equations are simplified to various forms, which are used to study specific processes. The two-dimensional vertically averaged model presented in this report has been developed to predict the horizontal variation in the mean flow, and works well for shallow tidal basins with little or no stratification. However, the model yields no information on the vertical velocity profile.

5.1.1 Classical Model

The typical approach to the vertical velocity profile is to relate the vertical Reynolds shear stress, using a mixing length model, to the vertical gradient of the horizontal velocity. This model is called an eddy viscosity model, and the coefficient of equality, called the eddy viscosity coefficient, is a product of a mixing velocity and length.

Ekman (1905) first used this type of model to investigate wind induced flow. In this work, the Navier-Stokes equations are simplified to a balance between the Coriolis term, and the vertical gradient of the vertical Reynolds shear stress or the equivalent Boussinesq approximation

$$fu = \frac{1}{\rho} \frac{\partial}{\partial z} (\tau_{yz}) = N_z \frac{\partial^2 v}{\partial z^2}$$

$$-fv = \frac{1}{\rho} \frac{\partial}{\partial z} (\tau_{xz}) = N_z \frac{\partial^2 u}{\partial z^2}$$

where u and v are the x - and y -components of velocity respectively, f the Coriolis parameter, ρ the density of water, z the vertical coordinate, τ_{yz} and τ_{xz} vertical Reynolds stress components and N_z the vertical eddy viscosity coefficient.

The surface boundary conditions are no surface stress in the x -direction

$$\rho N_z \frac{\partial u}{\partial z} \Big|_{z=0} = 0$$

and the surface stress in the y -direction is the wind stress

$$\tau_{sy} = -\rho N_z \frac{\partial v}{\partial z} \Big|_{z=0}$$

The bottom boundary condition is that of no velocity as the depth goes to infinity

$$u = v = 0 \Big|_{z=\infty}$$

The resulting profile has a velocity which decreases exponentially with depth, and the surface current direction is 45° to the right of the wind stress and the angle increases with depth. Changing the bottom boundary condition to a finite depth causes the magnitude of the current and deflection angle to decrease.

Similar, but more sophisticated models have recently been developed by many investigators. Unfortunately, the ability to make appropriate field measurements for evaluation, application and validation of these models has not developed as rapidly. Oil spill research has prompted study of surface currents, and in particular those produced by wind. The results of these field experiments indicate that the speed of the wind driven current is between 0 and 6 percent of the wind velocity, and the direction ranges from slightly to the left of wind direction to as much as 15° to the right (Stolzenbach, et al., 1977). As a result, for the purposes of modeling oil spill movements, the 3% rule is widely used.

This rule of thumb states that the surface current speed is 3% of the wind speed, and is in the same direction (Van Dorn, 1953).

Therefore, although there are several sophisticated models which may be employed in the scientific study of these processes, the effort and cost of correspondingly sophisticated field data limits the usefulness of these models for making predictions. In the case of Bristol Harbor, the simpler model applied here is adequate for producing predictions for the purposes required.

5.1.2 Analytical Model

For steady state flow in one direction, the Navier-Stokes equation (the equation of motion) simplifies to

$$\rho g \frac{\partial n}{\partial x} = \frac{\partial}{\partial z} \left(\rho N_z \frac{\partial u}{\partial z} \right) \quad (1)$$

where $\rho N_z \frac{\partial u}{\partial z}$ is a mixing length representation of the vertical Reynolds shear stress. Assuming the density, ρ , and eddy viscosity coefficient, N_z , to be constant over depth,

$$g \frac{\partial n}{\partial x} = N_z \frac{\partial^2 u}{\partial z^2} \quad (2)$$

Two boundary conditions must be specified to solve the above equations. Boundary conditions appropriate to the model are:

- (1) The surface stress is the wind stress τ_s

$$-\rho N_z \frac{\partial u}{\partial z} \Big|_{z=0} = \tau_s \quad (3a)$$

- (2) The current velocity is zero at the bottom

$$u \Big|_{z=H} = 0 \quad (3b)$$

Equation (2) is solved by integrating over depth twice and applying the boundary conditions (3).

$$u = \frac{gH^2}{N_z} \frac{\partial n}{\partial x} \left[\frac{1}{2} \left(1 - \frac{z}{H}\right)^2 - \left(1 - \frac{z}{H}\right) \right] + \frac{\tau_s H}{\rho N_z} \left(1 - \frac{z}{H}\right) \quad (4)$$

The solution for u contains a second unknown, the surface slope $\partial n / \partial x$, therefore a second equation must be written. As this is a steady-state model, the net flux through a cross-section of the channel must be zero.

$$\int_0^H u \, dz = 0 \quad (5)$$

Substituting equation (4) into (5) and integrating yields an expression which is solved for the surface slope to obtain:

$$\frac{n}{x} = \frac{3\tau_s}{2\rho gH} \quad (6)$$

This expression can now be substituted into equation 4 to obtain the wind-driven current velocity as a function of depth.

$$u = \frac{\tau_s H}{4\rho N_z} \left(1 - \frac{z}{H}\right) \left(1 - 3\frac{z}{H}\right) \quad (7)$$

At the surface ($z=0$) the velocity is:

$$u \Big|_{z=0} = \frac{\tau_s H}{4\rho N_z} \quad (8)$$

This can be replaced by the three percent rule, which states that the wind-induced surface current is approximately 3% of the wind velocity.

$$u \Big|_{z=0} = 0.03 V_w \quad (9)$$

and

$$u = 0.03 V_w \left(1 - \frac{z}{H}\right) \left(1 - 3\frac{z}{H}\right) \quad (10)$$

A non-dimensional plot of current velocity as a function of depth is presented in Figure 14. It can be seen that water flows in the direction of the wind near the surface, and in the opposite direction near the bottom, which results in a net circulation. The maximum current velocity in the direction of the wind occurs at the surface, and the maximum current velocity in the opposite direction occurs at $z = (2/3)H$. The mass flux due to this circulation can be evaluated. The depth at which the current velocity changes sign is

$$\left(1 - 3\frac{z}{H}\right) = 0 \text{ or } z = \frac{H}{3} \quad (11)$$

The net flux (per unit width of the basin) in this upper layer is

$$q = \int_0^{H/3} u \, dz \quad (12)$$

$$q = \frac{\tau_s H}{4\rho N_z} \left(\frac{4H}{27}\right) = 0.03 V_w \left(\frac{4H}{27}\right) = 0.00444 V_w H \quad (13)$$

For a basin of width W and length L , the total volume of water in the basin is WLH , and the length of time for the wind-driven circulation to flush the basin is

$$T = \frac{WLH}{Wq} = \frac{LH}{q} = \frac{LH}{0.0044 V_w H} = \frac{L}{0.0044 V_w}$$

Thus the flushing time depends only on the length of the estuary and the wind velocity. Table 2 presents maximum wind-generated currents and flushing times for basins of one and two nautical miles in length for several wind velocities, assuming that upper Bristol Harbor is one nautical mile long and the total harbor length is two nautical miles.

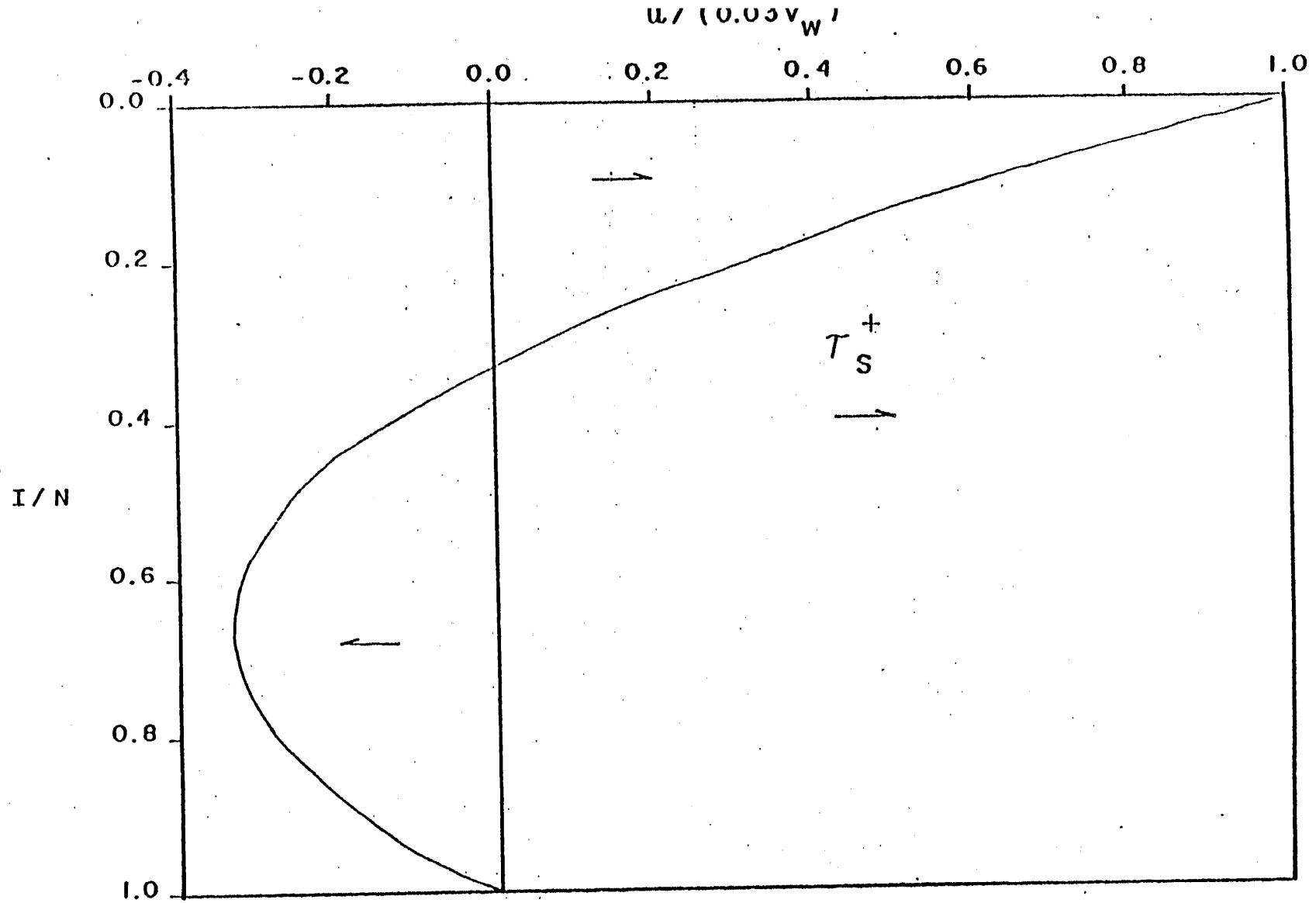


Figure 14. Normalized plot of current velocity vs depth. Bristol Harbor, Rhode Island.

TABLE 2. MAXIMUM WIND DRIVEN CURRENTS AND FLUSHING TIMES FOR BASIN LENGTHS OF 1 AND 2 NAUTICAL MILES AT VARIOUS WIND SPEEDS. BRISTOL HARBOR, RHODE ISLAND.

WIND SPEED		SURFACE CURRENT		MAXIMUM RETURN CURRENT		FLUSHING TIME (HOURS) BY LENGTH	
(knots)	cm/sec	(knots)	cm/sec	(knots)	cm/sec	1 n mi	2 n mi
5	257	0.15	7.7	0.05	2.6	45	90
10	514	0.30	15.4	0.1	5.1	23	45
15	772	0.45	23.2	0.15	7.7	15	30
20	1029	0.60	30.9	0.2	10.3	11	23

When interpreting these results, it must be remembered that this model is for an idealized situation, where the wind has been blowing steadily for a sufficient length of time to fully develop the circulation pattern. In addition, the flow is not one-dimensional, but in reality three dimensional, and effects such as tides and basin geometry are ignored. As such, these results should not be taken absolutely but rather interpreted as being indicative of the wind-driven circulation characteristics.

This analysis also has several hidden assumptions which require discussion. The derivation assumes the wind generates the only current within the system and waves are ignored. We naively assume that wind currents and tidal currents are linear systems whose combined effects can be superimposed, that is, the net current is simply the sum of the wind and tidal currents. By ignoring the existence of wind waves, we ignore the non-linear interaction between short-gravity waves generated by winds and long-gravity waves, which is the manifestation of tides and their associated velocity fields. This interaction called radiation stress appears as an additional term in the energy conservation relationship (Longuet-Higgins and Stewart, 1964). The effects of radiation stress have been measured both in the laboratory (Long and Huang, 1976) and the field (Vincent and Smith, 1976), but the emphasis has been more on wave effects. Thus, the existence of the interaction term means that superposition of the analytical model on tidal circulation would only

yield a lower limit estimation of current strength. In view of the short fetch that the harbor presents to the wind, effects generated by waves in the harbor can probably be ignored. One can not, however, make the same statement about high energy storm waves propagating into the harbor from Narragansett Bay with any surity.

A second hidden assumption in both the numerical and analytical models is that they are closed systems. In the analytical model, a result of this assumption is given by Equation 5 for zero-net flux through a channel cross-section. This means that there is no effect due to the wind on the vertically average tidal circulation of the numerical model. This result is unrealistic, since Equation 5 is invalid in an open system. However, the need for the closed system assumption must be recognized in spite of its unrealistic result. Defining a closed system makes both the numerical and analytical models tractable.

5.1.3 Velocity Profiles

The results of the depth-integrated numerical circulation model are the vertically-averaged velocities. These values can be approximately related to the surface velocity in the absence of wind stress by making several assumptions about the velocity distribution. Vanoni (1941) showed that the Prandtl universal log velocity-distribution law was applicable to two-dimensional (infinite-breadth) open channel flow

$$u(z) - u_{\max} = (u_* / \kappa) \ln (z/d)$$

where $u(z)$ is the velocity at a distance z from the channel bed, u_{\max} is the maximum (i.e. surface) velocity at distance d from the bed, u_* is the friction velocity and $\kappa \approx 0.40$ is von Kármán's constant for clear water. The friction velocity defined as

$$u_* \equiv \sqrt{\tau_0 / \rho}$$

where τ_0 is the bed shear stress, has the dimensions of a velocity, i.e., a length per unit time. Integrating the velocity profile over depth

yields the relationship

$$u(z) = V + (u_*/\kappa)(1+\ln(z/d))$$

where V is the mean velocity measured at a height $z = e^{-1}d \approx 0.368d$.

Assuming a stress relationship that is quadratic with respect to velocity

$$\tau = \rho C_D u^2$$

where the drag coefficient $C_D(z)$ and the velocity $u(z)$ are both functions of height above the bottom z (Schlichting, 1968). Substituting this relationship into the definition of u_* yields the expression

$$u_* = u(z) \sqrt{C_D(z)}$$

Using $z = 0.368d$ for u_* yields a relationship with respect to V ,

$u_* = V \sqrt{C_D(0.368d)}$ where V and $C_D(0.368d)$ are values used in the model.

The velocity relation becomes

$$u(z) = V + \frac{1}{\kappa} V \sqrt{C_D(0.368d)} (1+\ln(z/d))$$

or for the surface velocity $u_{\max} = u(0.368d)$,

$$u_{\max} = V(1 + \frac{1}{\kappa} \sqrt{C_D(0.368d)})$$

Assuming the model value for friction of $C_D = 0.020$, the surface current expression reduces to

$$u_{\max} = 1.354V$$

Thus, by knowing the mean velocity magnitude V , one can easily determine the appropriate surface speed u_{\max} .

5.1.4 Influence of Wind on Current Patterns in Harbor under Existing Conditions

Wind is significant in defining the water movement in Bristol Harbor. Wind blowing over the water in a semi-enclosed basin, such as Bristol Harbor, will cause a circulation pattern. The surface water moves in the direction of the wind stress at a speed typically 3.0% of the wind speed. In confined embayments such as Bristol Harbor conservation of mass must be maintained. For example, with wind blowing directly into the harbor, surface water will "pile up" on the inner shore of the harbor. To maintain the increased water level, a constant return flow must be established. This may manifest itself as either bottom or lateral flow against the wind. Conversely, if there is a wind with a component of the wind stress directed out of the harbor, surface waters will be pushed out of the harbor. To maintain a constant depressed water level, near-bottom flow must be into the harbor.

The wind-driven circulation increases the flushing rate over flushing due solely to tidal action. Because this circulation may vary with depth, the types of pollutants influence their flushing rates. For example, if the pollutant floats, i.e. "flotsam and jetsam" or oil, a southwest wind would cause it to collect in the inner confines of the harbor. If the pollutant is the type which disperses throughout the water column, i.e. fluid discharges, etc., then this pollutant would be flushed from the harbor under all wind conditions. If the wind is directed into the harbor, the pollutant would be flushed out in the near-bottom return flow. If the wind is directed out of the harbor, it will be flushed out in the near-surface flow.

Again consider Table 2 and the surface currents generated by various wind magnitudes. Since the maximum integrated, tidal current speed is about 3 cm/sec in the upper harbor, we can estimate surface currents of about 4 cm/sec. By the 3% rule, currents of this speed can be generated by a 2.6 kt wind. Surface current values of Table 2 tend to indicate that wind-induced circulation will dominate upper harbor circulation.

5.1.5 Influence of Various Breakwater Configurations on Non-tidal Circulation Effects

The various breakwater configurations will influence the wind driven circulation by decreasing the wind wave turbulence which may occur with a southwest wind. Waves can vertically mix pollutants in the water column, but will also tend to inhibit the development of a wind generated two layer circulation pattern. Increased current speeds through the passages around the breakwaters mean the stronger winds are needed to have an effect on the circulation. Southwest winds, however, are summer winds and, in general, tend to have lower magnitudes than the winter winds.

The stronger, winter winds come primarily from the northwest. Their strength, particularly during the passage of winter storms called extratropical cyclones, is most likely sufficient to have a substantial effect on upper harbor circulation. The net effect is probably an enhanced flushing of the upper harbor. However, wind circulation is dependent on duration rather than fetch. Remember the assumption on the wind-induced current speeds in Table 2 is that winds are steady, and of long-term duration. For strong, winter storm winds these assumptions do not hold. There is no doubt that these winds will have an effect on the current velocities and that wind-driven circulation will dominate the upper harbor flow pattern. When the circulatory pattern is significantly changed, this condition is only a temporary effect and the original pattern should be quickly restored within several tidal cycles.

Strong winds blowing on or off-shore also create conditions referred to as set-up and set-down. These are conditions relative to the tidal height. Set-up is the non-tidal increase in height of the water level, whereas set-down is the non-tidal decrease. Northwest winds will produce set-down. Since the tidal heights do not significantly change by building a breakwater (Appendix I), set-down will be no more severe with a breakwater than presently without one. In fact, a breakwater might even help reduce the magnitude of set-down.

5.2 WAVE EFFECTS

The most visible effects of wind blowing over water is the generation of wind waves. Wind waves on the sea surface are an extraordinarily complex phenomenon. All analytical descriptions are based on linear theory, which, surprisingly enough, can explain many features of surface waves. Non-linear wave theory is based on higher-order perturbations of first order models (Neuman and Pierson, 1966). In the following discussion, wind waves are considered independently of any non-linear interaction (such as with the tidal currents) called radiation stress (Longuet-Higgins and Stewart, 1964).

The wind waves of interest in coastal areas are called shallow-water or long waves. Characteristically, they have a depth-to-wavelength ratio (d/L) of less than one-half. Shallow water waves, like light waves, exhibit three important properties: reflection, diffraction and refraction (Bascom, 1964). In reflection, a portion of the wave energy is redirected in the interaction with a solid barrier. In diffraction, wave energy leaks into the geometric shadow of the wave train as it passes a solid barrier. In refraction, bottom friction and depth changes cause the wave direction to change with a roughly perpendicular orientation on the bottom contours. As the waves enter shallower water, the wave velocity decreases, the wave length shortens and the wave steepness increases. Finally at a depth equal to about 1.3 times the wave length, the wave becomes too steep to remain stable and breaks. All three properties are theoretically complex and analytically difficult to solve.

5.2.1 Limited Fetch

Waves along coastal regions have been extensively monitored and studied (TRIGOM, 1974). These observations were made of ocean waves with an effectively infinite fetch. However, the location of Bristol Harbor within Narragansett Bay dictates a finite fetch exists and should be used. Maximum fetch for Bristol Harbor appears to be about 3 nautical miles (5.6 km) from the southwest.

Darbyshire (1956) presented the following series of empirical results for fetch limited cases.

$$H_m \text{ (ft)} = 0.0076yU^2 \text{ (kt}^2\text{)}$$

$$T_s \text{ (s)} = 1.64yU^{1/2} \text{ (kt}^{1/2}\text{)}$$

for
$$y = x(x^2 + 3x + 65) / (x^3 + 12x^2 + 260x + 80)$$

where H_m is the maximum wave height, T_s the significant wave period U is 1.5 times the surface wind speed and x is the fetch in nautical miles. For an infinite fetch, $y = 1.0$. First, consider the average wind speed at Providence, RI. For a mean speed of 9.6 kn (4.9m/s) from TRIGOM (1974), the maximum wave height H_m is 0.4 ft (0.1 m) and the significant wave period is 1.6 seconds. Similarly, for the typical storm of 22 knots (11.3 m/s), given in TRIGOM (1974) the wave statistics are $H_m = 2.1$ feet (0.6 m) and $T_s = 2.4$ seconds.

5.2.2 Wave-Breakwater Interaction

Standard procedures to determine water wave properties have been established by the U. S. Army Coastal Engineering Research Center (1973). Comparing Plan A to the diffraction diagrams indicates that Town Pier may not be adequately protected from waves coming along the axis of maximum fetch. However, the dog-leg breakwater of Plan D_1 would ensure wave-height reduction in the Town Pier area of over 80%. No significant interaction of diffraction waves takes place between the two breakwaters of Plan D_2 . Each breakwater design will have significant reflection of waves away from the harbor. There is no problem of waves being reflected into the harbor. Using the rule of thumb that wave directions become orthogonal to the bottom contours. It appears that waves entering the harbor along the axis of maximum fetch may be directed through the eastern pass around Breakwater A into the Town Pier region. The dog-leg breakwater of Plan D_1 would effectively stop those waves.

6.0 CULVERT EFFECTS

6.1 CULVERT FLOW

There is the possibility of installing a 6-ft by 6-ft (1.8 m- by 1.8 m) culvert within the 700 ft (213 m) western breakwater of Plan D₂. The size of the culvert with respect to the breakwater make practical incorporation of this feature impossible with respect to the grids used for the CAFE and DISPER models. An analytic approach can be used to approximate the velocity or equivalently, the transport rate, through the culvert. To accomplish this, we use an empirical formulation based on the experimental work of Robert Manning (1890), a classic result found in any introductory fluid mechanics text.

6.1.1 The Manning Formula

The most widely used formulation used in open-channel flow problems is attributed to Manning (1890) from his work concerning friction factors. In metric units, the Manning formula, assuming steady uniform flow, is

$$V = \frac{1}{n} S^{\frac{1}{2}} R^{\frac{2}{3}}$$

where the velocity V is related to the Manning friction coefficient n , the hydraulic slope S and the hydraulic radius R . The Manning coefficient n is an empirically determined value for various surface materials. Precast concrete surfaces have n values of 0.011 to 0.013. Manning's n has the peculiar property of being a dimensional quantity, namely, $TL^{-1/3}$ (T is time and L is length). The values of n are metric; conversion to English units (ft - lb - sec) require dividing n by 1.486, which is the cube root of 3.281, the number of feet per meter.

The hydraulic slope (or the energy gradient) is defined as

$$S = h_L/L$$

where h_L is the head loss (change in height) and L is the length measured along the channel bottom, not the horizontal. If the horizontal is measured as l , then by the Pythagorean Theorem $L = (l^2 + h_L^2)^{1/2}$. The hydraulic radius is defined as

$$R = A/P$$

where A is the cross-sectional area and P is the wetted perimeter. R should not be confused with the circular radius r , since it can be shown by the above formulation that $R = r/2$ for a circular pipe filled with fluid.

6.1.2 Culvert Application

The flow rate, as previously mentioned, can be expressed as the product of the average velocity and the cross-sectional area or $Q = VA$. We assume that the culvert is precast concrete and that Manning's formula is applicable over the range of flows in this application. Since in the numerical model application, flow normal to the breakwater was defined as zero, the driving force of flow through the culvert is simply the tidal height differential across the breakwater. These are results produced in the CAFE output.

6.1.3 Culvert Results

Values for the head loss h_L from the CAFE results, and calculation results for the velocity V and flow rate Q_C of the culvert are listed in Table 3 for the two tidal cases of interest. Head loss values are height differentials measured at nodes on opposite sides of the short western breakwater. These two nodes are separated by a distance of 252.5 meters. The results of applying Manning's formula to calculate the velocity V and flow rate Q_C do not exhibit a regularity that parallels the tidal ebb and flood cycle. The reason for this lack of regularity

is not entirely clear. There are two possible explanations. First, the problem could be within the model itself. Secondly, the model is responding accurately and these results simply reflect the complex behavior of the simulated tidal dynamics. For lack of any evidence to place the blame on a model flaw, the more probable explanation appears to be the latter case.

In addition, other results from the CAFE model are also included in Table 3. Flow rates across the critical openings are listed. These flow rates are the product of the nodal distance and the mean of two nodal values of flow rate per unit width (CAFE results). The inter-breakwater flow rates Q_{mc} are the sums of contributions from three elements, whereas only a single element contributes to the flow rate between the dog-leg breakwater and the shore Q_{sc} .

These other flow rates are shown for the purpose of comparison with the culvert flow rates Q_c . These other flow rates, it should be noted, exhibit a regularity consistent with the tidal cycle. The culvert flow rates Q_c are one-to-two orders of magnitude smaller than the side channel flow rate Q_{sc} and two-to-three orders of magnitude less than the main channel flow rate Q_{mc} . These results, of course, assume that the top of the culvert is located below mean low water. If the culvert is positioned any higher, then it will not always flow full. The values of the hydraulic radius R decrease implying the results for the velocity V and the flow rate Q_c will also decrease.

The results of this analysis indicate that installing a submerged culvert through the western breakwater of Plan D₂ will have a minimal effect on the overall flow rate between the upper and lower harbor. Anomalies within the head losses tend to indicate the use of tidal height differentials to drive the culvert flow is unreliable. Since a land-connected breakwater appears to be a problem, then considerations should be made for detaching it, like the dog-leg breakwater on the eastern side. The overall circulation and dispersion patterns should remain the same; however, within the immediate vicinity of the breakwater,

TABLE 3. COMPARATIVE FLOW RATES FOR TWO TIDAL CASES ACROSS THE CULVERT Q_c , THE EASTERN SIDE CHANNEL Q_{sc} AND THE MAIN CENTRAL CHANNEL Q_{mc} (PLAN D₂). THE HEAD LOSSES h_L AND MEAN VELOCITIES V WERE USED FOR Q_c . BRISTOL HARBOR, RHODE ISLAND, 1980.

TIDAL STATE	n (m)	MODEL TIME (sec)	h_L (m)	V (cm/s)	Q_c (m ³ /s)	Q_{sc} (m ³ /s)	Q_{mc} (m ³ /s)
ME	0.02	22320	-.00234	-15.055	-.50353	10.579	140.14
	-.29	26040	0.00029	5.300	0.17726	19.386	431.37
	-.52	29760	0.01086	32.434	1.08476	17.796	517.39
LS	-.61	33480	-.00016	-3.937	-.13167	14.681	526.36
	-.63	37020	0.00610	24.308	0.81299	7.988	503.32
	-.32	40800	-.00198	-13.849	-.46318	8.843	409.79
MF	-.03	44520	-.00710	-26.225	-.87710	-9.797	2.35
	0.28	48240	-.00198	-13.849	-.46318	-26.961	-477.20
	0.51	51960	-.00160	-12.449	-.41637	-43.688	-691.87
HS	0.61	55680	0.00295	16.904	0.56537	-43.440	-751.34
	0.54	59280	-.01077	-32.299	-1.08025	-21.643	-678.79
	0.33	63000	-.00301	-17.075	-.57109	-3.185	-507.76
ME	0.02	22320	-.00121	-10.826	-.36208	7.555	-55.47
	-.36	26040	0.01684	40.388	1.35079	21.475	366.49
	-.64	29760	0.01177	33.766	1.12929	15.784	556.31
LS	-.76	33480	0.02634	50.512	1.68938	10.413	553.55
	-.67	37200	-.00473	-21.405	-.71589	11.244	525.80
	-.40	40920	0.01880	42.674	1.42724	7.263	448.64
MF	-.02	44640	-.07062	-82.708	-2.76619	0.683	1.86
	0.36	48360	-.10728	-101.940	-3.40940	-31.635	-559.72
	0.65	52080	-.05093	-70.238	-2.34912	-50.350	-791.04
HS	0.76	55800	0.04033	62.503	2.09041	-45.983	-868.65
	0.67	59520	-.01951	-43.472	-1.45394	-26.348	-778.76
	0.40	63240	0.03296	56.504	1.88978	-2.701	-551.79

substantial changes will exist. Intuitively, flows will pass between the breakwater and the western shore, similar to that of the eastern passage. Entrapment behind the breakwater is eliminated, and flushing is enhanced relative to the present configuration of Plan D₂. With flows on both sides of the breakwater, the eddies that develop north and south of the breakwater should increase somewhat in strength. The culvert would be unnecessary. These pattern changes will require the appropriate models be run.

1. Difference in velocities
around Hog Island between
existing & modified conditions
for low slack and high slack

2. It appears that most of the
conclusions were intuitive to
start with, plus the qualifier
in last paragraph on p. 82 places
the validity in question.

7.0 CONCLUSIONS AND RECOMMENDATIONS

The application of the CAFE model to Bristol Harbor as it presently exists (i.e. no breakwater) shows a very simple two-dimensional circulation pattern. During the ebb, currents flow counterclockwise around Hog Island in the lower harbor and seaward (south) in the upper harbor. On the flood, these currents reverse. The breakwaters each have the same general effect on upper harbor circulation while not affecting currents in the lower harbor. Eddies are formed north and south of each breakwater; their maximum speeds occur an hour before and after slack water with a relative minimum during slack water. During mid-ebb and mid-flood these eddies disorganize but soon after they reorganize in the reverse direction. Tidal heights are not significantly altered by the breakwater construction with an overall range difference of several centimeters.

Three source areas of pollution have been identified and dispersion within the harbor has been mapped by simulating the conservative mixing of dye released from the source points. Eighty-three percent of the input is assumed to originate from the Walker Cove outfall from the town's primary sewage treatment plant, sixteen percent from the industrial area adjacent to Town Pier and one percent from the yacht club. Concentrations within the upper harbor without a breakwater are maximum at high-slack and minimum at low-slack water. Dispersion patterns for breakwater Plans A and D₁ most resemble the ambient pattern since those plans are the least restrictive with respect to flow. The concentration maps for Plan D₂ indicate a tendency for a higher concentration build-up during certain tidal phases. This means that the flushing for Plan D₂ is not as efficient as the other two. This build-up may also have adverse effects on the biota, especially the benthic organisms.

Without any breakwater, analyses indicate that the upper harbor tends to be dominated by wind-driven circulation rather than tidal circulation. Northwest winds which predominate the winter will increase flushing. Southwest winds characteristic of summer will retard flushing, but, since they are generally weak, they are not a serious

problem. The restrictive nature of the breakwaters causes increased current speeds within and around the upper harbor. Although upper harbor circulation with the breakwaters will still be influenced by wind effects, the increased current speeds will help to insure harbor flushing.

Wind waves are expected to be fetch-limited and substantial generation is expected only from a southwest wind. The dog-leg breakwater of Plan D₁ seems adequate to protect the Town Pier area from the waves generated along the area of maximum fetch, whereas the single, straight breakwater of Plan A appears inadequate. Winds from other directions do not have as large a fetch, and wave production should be significantly reduced. In this respect, unless there is a problem with wave damage from south winds at the Bristol Yacht Club, the short western breakwater of Plan D₂ serves no purpose.

Culvert flows through the short eastern breakwater of Plan D₂ have a minimal on the overall flow rate between the upper and lower harbors. Flows did not exhibit a regularity in phase with the tide and this tends to indicate an unreliability in this method of flushing. To reduce the entrapment of material by this breakwater, the breakwater can be detached from the western shore. Eddies will still develop but flow around the detached flank will enhance flushing relative to the present configuration. Thus the need for the culvert is eliminated. In fact, questions on the usefulness of this breakwater indicate it should be eliminated entirely.

These conclusions have been made from results whose methods have their own particular assumptions. The assumptions place certain limitations on the situations when these results are valid. The lack of field data places additional limitations on the model results because of an uncertainty in the calibration. However, the successful use of these models in other areas and good agreement with field data indicates the results of those simulations have given us good insight into the hydrodynamic behavior of concern to this study.

On the basis of these conclusions, the following recommendations are made. Plan A should be dropped for consideration as a viable plan. Although adequate flushing is maintained in the upper harbor, there is a serious question concerning protection of the industrial area around Town Pier from waves generated from a southwest wind along the axis of maximum fetch. Plan D₂ should be retained only as an alternate choice. The short, western breakwater both restricts flushing relative to present conditions and may be unnecessary as a protection measure for the yacht club. If this protection is necessary due to damage suffered in the past, then the breakwater should be detached from the eastern shore to enhance flushing and eliminate entrapment. The use of a culvert through the breakwater in the present configuration is questionable, and the entrapment that the culvert is supposed to eliminate could better be reduced by detachment. The present arrangement Plan D₂ shows that the trade-off for more protection would be a decrease in the flushing rate of the upper harbor relative to the present situation of no breakwater and to the other two plans. Detachment to enhance flushing would decrease the amount of higher concentration water in the upper harbor, but without additional work, it is not clear how much of a reduction is possible. Plan D₁ appears to fit the criteria of good flushing and adequate protection, and these results support this configuration as first choice for construction.

In the context of this study area, there does not appear to be any particular reorientation which would enhance flushing. The length of the short western breakwater of Plan D₂ appears to be near minimum to serve as protection for the yacht club. If it is required, then the breakwater should be detached from the western shore to enhance flushing and eliminate entrapment. The length of the dog-leg breakwater (D₁) depends on how much protection should be afforded to industrial areas around Town Pier. If the need for protection is limited to the area between Town Pier and the U. S. Coast Guard Station, then the breakwater could probably be shortened by a few hundred feet. This dog-leg configuration seems to be better in terms of protection than on equivalent straight breakwater for this area.

The design storm is taken from the maximum winter winds as recorded at Providence, RI (TRIGOM, 1974). These winds were measured at 44 knots or 22.6 m/sec from the southwest which is along the axis of maximum fetch. Although these are maximum winds that are not sustained long enough to fully arouse the water, they do represent an upper limit that is useful as design criterion. Using the formulations of Darbyshire (1956) for fetch-limited waves one determines that the significant wave height H_s is 5.0 feet or 1.5 meters, and the significant wave period T_s is 3.3 seconds. Using the Shore Protection Manual (CERC, 1973), the equivalent wavelength L is 54.2 feet or 16.5 meters for a depth of 16 feet or 4.9 meters.

This wavelength becomes a unit of measure for the wave diffraction diagrams in the Shore Protection Manual (CERC, 1973). We assume here that the dominant wave property is diffraction and the approach of the wave crest is 75 degrees. Overlaying the dog-leg breakwater (1100 + 600 ft) of Figure 2 on an extrapolated wave diffraction diagram, two points are evident. First, the height outside the breakwater is reduced by 50% at the northern end of the industrial region. Second, along the southern half of the industrial area, which includes the Town Pier area, the wave height is reduced by 88% or more. The breakwater can be shortened by 400 feet or 122 meters (700 + 600 ft) which keeps the Town Pier area in the area of reduction of 88% or more. However, the northern end of the industrial region has a reduction in wave height by only 25%. The northern quarter has a reduction by 25 to 50% and the southern quarter by greater than 88%.

The present configuration of Plan D_1 allows for adequate flushing of the inner harbor which would be almost as good as harbor flushing without any breakwater(s). Although increasing the length of the breakwater by, say 400 feet, would mean more protection, flushing would be similarly retarded as in Plan D_2 . Shortening the breakwater would decrease protection, but would not necessarily provide a significant increase in flushing. The length in Plan D_1 is considered optimal given the present orientation of the breakwater. A change from the present

orientation is, likewise, rejected as a mechanism to significantly enhance flushing. If the orientation was significantly changed, then the breakwater would have to be lengthened to provide the same level of protection as Plan D₁. However, lengthening the breakwater would retard flushing which would negate the effect of changing the orientation. Considering the length and orientation of the breakwater with respect to flushing and protection, the present dimensions and orientation of Plan D₁ are considered optimal.

8.0 REFERENCES

- Ames, W.F., 1977. Numerical Methods for Partial Differential Equations. (2nd ed.) Academic Press, NY
- Bascom, W., 1964. Waves and Beaches: The Dynamics of the Ocean Surface. Doubleday, Garden City, NY 267 pp.
- Briggs, D.A. and O.S. Madsen. 1974. Mathematical Models of Massachusetts Bay. Part II. Analytical Models for One- and Two-Layer Systems in Rectangular Basins. Massachusetts Institute of Technology. Sea Grant Report No. MITSG 74-4.
- Celikkol, B. and R. Reichard. 1976. Hydrodynamic Model of the Great Bay Estuarine System. University of New Hampshire, Sea Grant Report No. UNH-SG-153.
- Connor, J.J. and J.D. Wang. 1974. Mathematical Models of the Massachusetts Bay. Part I. Finite Element Modeling of Two-Dimensional Hydrodynamic Circulation. Massachusetts Institute of Technology, Sea Grant Report No. MITSG 74-40.
- Darbyshire, J., 1956. An investigation into the generation of waves when the fetch of the wind is less than 100 miles. Quarterly Journal of the Royal Meteorological Society. 82:461-468.
- Ekman, V.W. 1905. On the influence of the earth's rotation on ocean currents. Ark. F. Mat., Astron. och Fysik, 2(11):1-53.
- Leinkukler, W.F., G. Christodoulou, J. J. Connor, S.L. Sundgren and J.D. Wang. 1975. A Two-dimension Finite Element Dispersion Model. Massachusetts Institute of Technology. Sea Grant Report No.
- Long, S.R. and N.E. Huany. 1976. Observations of Wind-Generated Waves on Variable Current. J. Physical Oceanography. 6:962-968.
- Longuet-Higgins, M.S. and R.W. Stewart. 1964. Radiation Stresses in Water Waves, a physical discussion, with applications. Deep-Sea Research, 11:529-562.
- Manning, R., 1890. Flow of water in open channels and pipes. Trans. Inst. Civil Engrs. (Ireland), Vol. 20.
- NOS; NOAA. 1980a. Tidal Current Tables, Atlantic Coast of North America. NOS. Rockville, Maryland.
- _____. 1980b. Tide Tables, High and Low Water Predictions, East Coast of North and South America. NOS, Richville, Maryland.
- Neumann, G. and W.J. Pierson, Jr., 1966. Principles of Physical Oceanography. Prentice-Hall, Inc. Englewood Cliffs, N.J.

- Normandeau Associates, Inc. 1979a. Hydrographic Analyses at Sakonnet, Harbor, Little Compton, Rhode Island for Small Navigation Project. Prepared for Department of the Army, New England Division Corps of Engineers. 53 pages.
- _____. 1979b. New Haven Harbor Hydrodynamic and Dispersion Model Summary Unpublished report prepared for Metcalf & Eddy, Inc.
- _____. 1980. Hydrodynamic Study for Tanker Terminal on Piscataqua River. Final Report for Dorchester Sea-3 Products, Inc. 26 pages and 8 appendices.
- Parsons, Brinckerhoff, Quade & Douglas, Inc., and Normandeau Associates, Inc. 1976. Dredging, Portsmouth Naval Shipyard, Portsmouth, New Hampshire. Prepared for the Navy Department, contract number NG2472-76-C-0243.
- Reichard R. and B. Celikkol, 1978. Application of a finite element hydrodynamic model to the Great Bay Estuary System, New Hampshire. USA in Hydrodynamics of Estuaries and Fjords. J.C.J. Nihoul (ed.) Elsevier Scientific Publishing Co., Amsterdam.
- Roache, P.J. 1976. Computational Fluid Dynamics. Hermosa Publishers, Albuquerque, New Mexico. 446 pages.
- Sayre, W.W. 1975. Dispersion of Mass in open-channel Flow. Hydrologic papers no. 75. Colorado State University, Fort Collins.
- Schlichting, H. 1968. Boundary Layer Theory (6th ed.) McGraw Hill, NY 748 pp.
- Spaulding, M. and C. Swanson. 1974. Tides and Tidal Currents of Narragansett Bay. University of Rhode Island, Marine Technical Report 35.
- Stolzenbach, K.D., O.S. Madsen, E.E. Adams, A.M. Pollack and C.K. Cooper. 1977. A review and Evaluation of Basic Techniques for Predicting the Behavior of Surface Oil Slicks. MIT Parsons Lab. Tech. Rept. No. 222.
- Swanson, C. and M. Spaulding. 1977. Generation of Tidal Current and Height Charts for Narragansett Bay Using a Numerical Model. University of Rhode Island, Marine Technical Report 61.
- Thacker, W.C. 1978a. Comparison of Finite-element and Finite-difference Schemes. Part I: One-dimensional gravity wave motion. Journal of Physical Oceanography, 8(4):676-679.
- _____. 1978b. Comparison of Finite-element and Finite-difference Schemes. Part II: Two-dimensional gravity wave motion. Journal of Physical Oceanography, 8(4):680-689.
- TRIGOM, PARC, 1974. A Socio-Economic and Environmental Inventory of the North Atlantic Region. Volume I, Books 1 and 2. The Research Institute of the Gulf of Maine, South Portland. 519 and 617 pp.

- U. S. Army Coastal Engineering Research Center, 1973. Shore Protection Manual, Vol. I, III. U. S. Army CERC, Fort Belvoir, VA. 496 and 141 pp.
- VanDorn, W.G. 1953. Wind stress of an artificial pond. J. Marine Research, 12(3):249-276.
- Vanoni, V.A. 1941. Velocity distribution in open channels, Civil Engineering. 11:356-357.
- Vincent, C.E. and D.J. Smith, 1976. Measurements of Waves in Southampton Water and their Variation with the Velocity of the Tidal Current. Estuarine and Coastal Marine Science. 4(6):641-652.



NORMANDEAU ASSOCIATES, INC.

25 Nashua Road • Bedford, New Hampshire 03102 • (603) 472-5191
ENVIRONMENTAL CONSULTING • RESEARCH • SERVICE

September 24, 1980

U.S. Army Corps of Engineers
424 Trapelo Road
Waltham, MA 02154

Attention: Mr. Gilbert Chase

Dear Gib:

Enclosed please find addendum to Bristol Harbor report. If you have any other questions or need further clarification give me or Ray a call.

Sincerely,

NORMANDEAU ASSOCIATES, INC.

Weldon S. Bosworth, Ph.D.
Executive Vice President

WSB/jgk
Enc.
cc: Ray Sosnowski, NAI



ADDENDUM TO SECTION 7.0 CONCLUSIONS AND RECOMMENDATIONS

The design storm is taken from the maximum winter winds as recorded at Providence, RI (TRIGOM, 1974). These winds were measured at 44 knots or 22.6 m/sec from the southwest which is along the axis of maximum fetch. Although these are maximum winds that are not sustained long enough to fully arouse the water, they do represent an upper limit that is useful as design criterion. Using the formulations of Darbyshire (1956) for fetchlimited waves on page 75, one determines that the maximum wave height H_m is 8.3 feet or 2.5 meters, and the significant wave period T_s is 3.3 seconds.

From the following formulation, the deep-water wavelength L_o can be determined from the wave period T ,

$$L_o = g T^2 / (2\pi)$$

where g is the acceleration due to gravity (32.2 ft/sec^2 or 9.81 m/sec^2). Using the value for T_s as T , the deep-water wavelength is 57.0 feet or 17.4 meters. From the nautical charts, the depth of water in the vicinity of the breakwater is 16 feet or 4.9 meters making the depth-to-deepwater-wavelength ratio 0.2808. Using the tables in Volume III of the Shore Protection Manual (CERC, 1973), the equivalent depth-to-wavelength ratio is 0.2950 so that the equivalent wavelength L for this depth is 54.2 feet or 16.5 meters.

This wavelength becomes a unit of measure for the wave diffraction diagrams in Volume I of the Shore Protection Manual (CERC, 1973). We assume here that the dominant wave property is diffraction and the approach of the wave crest is 75 degrees. Overlaying the dog-leg breakwater (1100 + 600 ft) of Figure 2 on an extrapolated wave diffraction diagram, two points are evident. First, the height outside the breakwater is reduced to 50% at the northern end of the industrial region. Second, along the southern half of the industrial area, which includes the Town Pier area, the wave height is reduced to less than 12%.

less. The breakwater can be shortened by 400 feet or 122 meters (700 + 600 ft) which keeps the Town Pier area in the area of reduction of 12% or less. However, the northern end of the industrial region has a reduction in wave height to only 75%. The northern quarter has a reduction to 50 to 75% and the southern quarter to less than 12%. Since the design storm is twice the strength of the mean storm, then this length reduction under the given assumptions is an acceptable result.

CORRECTIONS

In the following lines of text, the word "eastern" should be changed to "western".

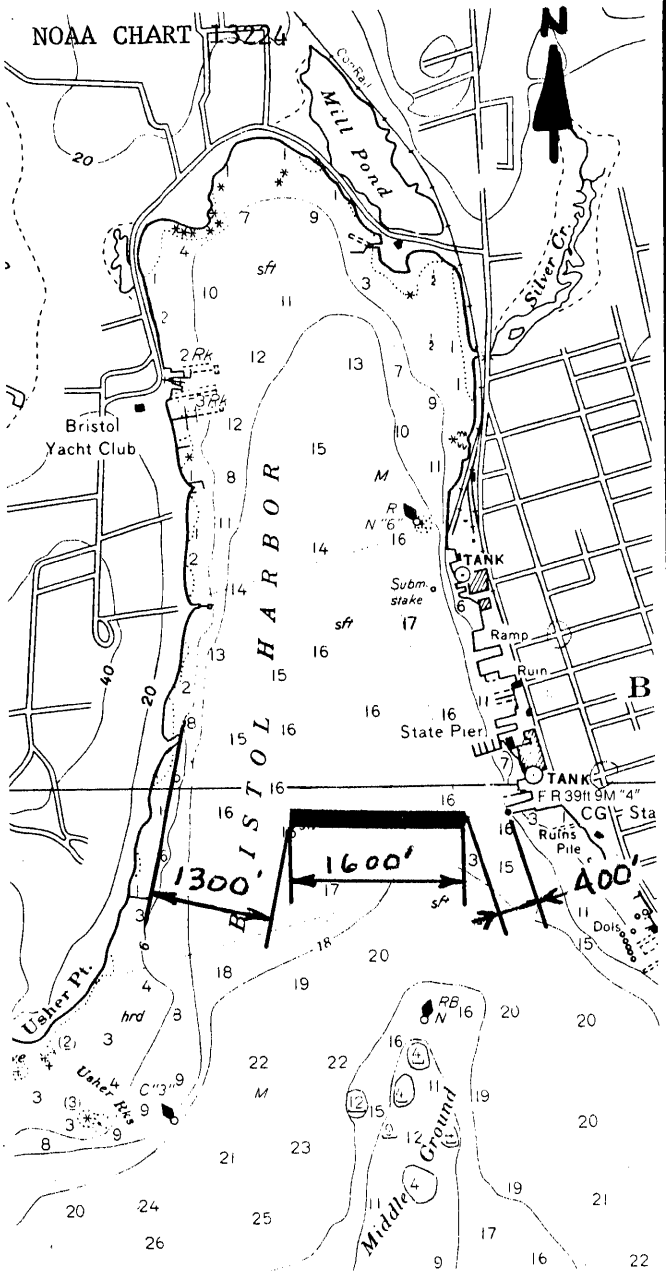
page 82, 1st paragraph, line 8

page 82, 2nd paragraph, line 6

page 83, 1st paragraph, line 7

page 83, 2nd paragraph, lines 3 and 5.

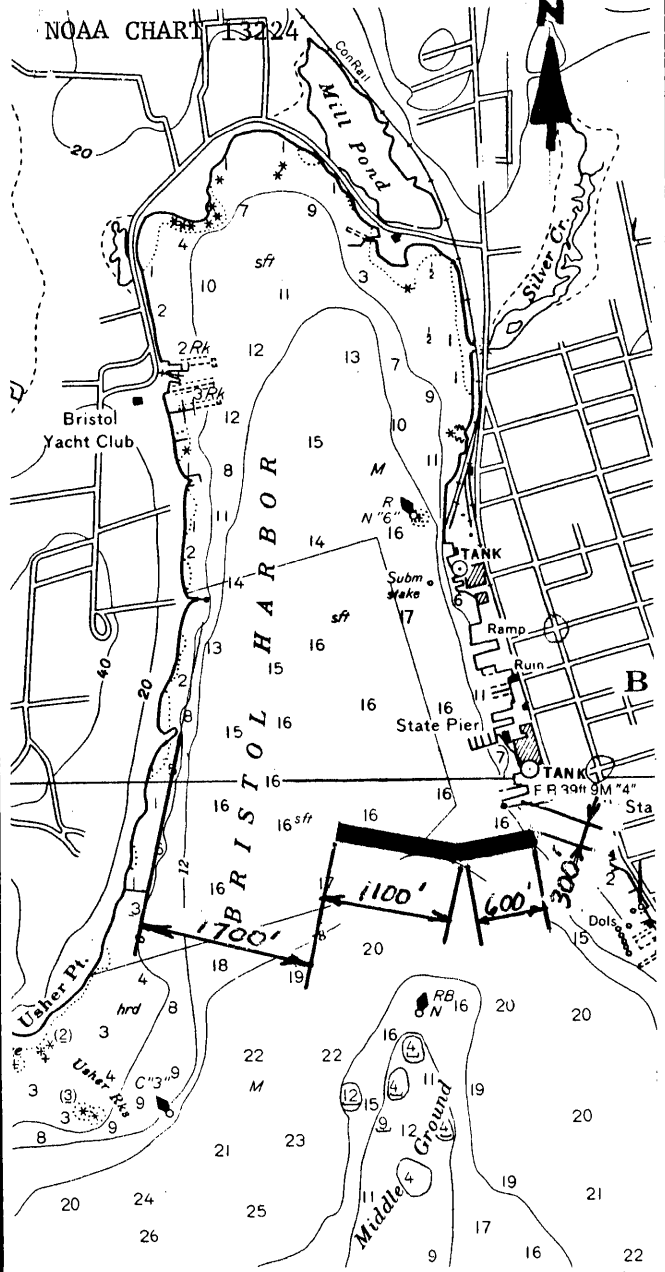
NOAA CHART 13224



PLAN A

1:20,000

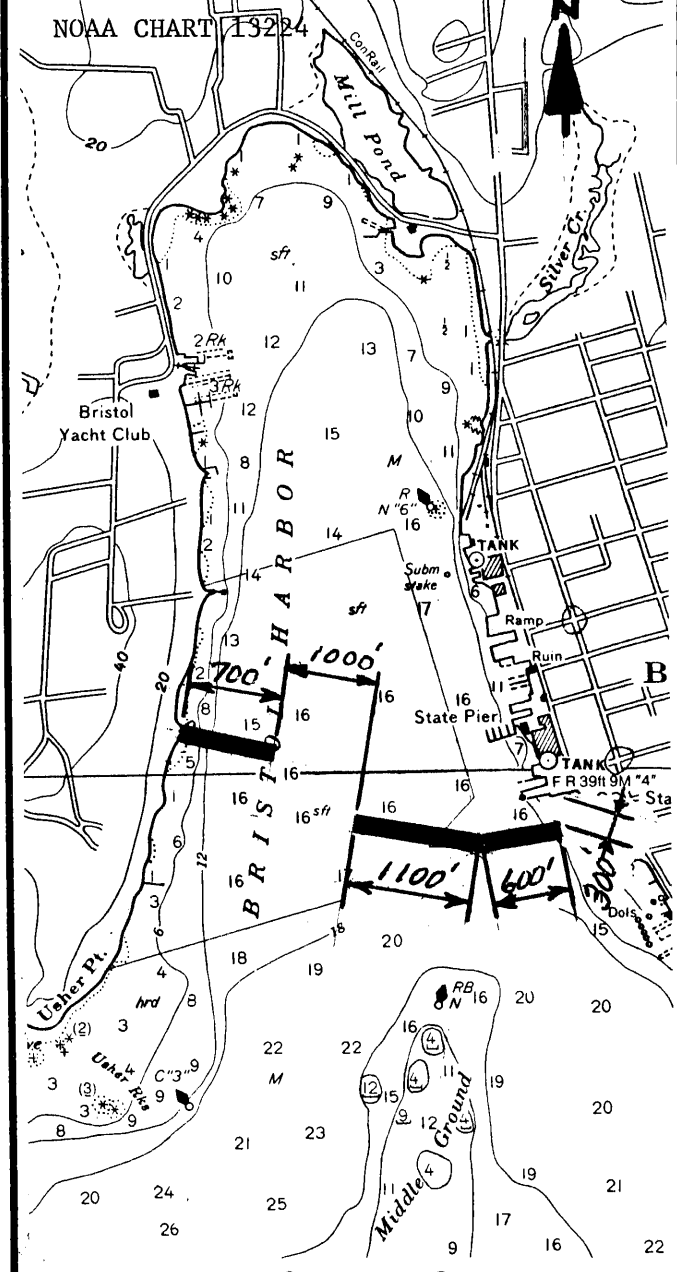
NOAA CHART 13224



PLAN B

1:20,000

NOAA CHART 13224



PLAN C

1:20,000